UNIVERSITÉ DE LORRAINE

Ecole Doctorale RP2E : Ressources, Procédés, Produits, Environnement
Laboratoire Réactions et Génie des Procédés – UMR 7274 CNRS – ENSIC

THÈSE

Présentée par

El Sayed Rabie El Sayed HASSAN

Pour l'obtention du grade de

Docteur de l'Université de Lorraine
en Génie des Procédés et des produits
Spécialité : Chimie-Physique

Use of Ionic Liquids for the Treatment of Biomass Materials and Biofuel Production

Soutenue publiquement le 10 Juin 2014 devant la commission d'examen :

Rapporteurs:

Prof. Micheline DRAYE
Dr. Mireille TURMINE

Examinateurs:

Prof. Amina NEGADI
Prof. Nicolas BROSSE
Dr. Fabrice MUTELET
Dr. Jean-Charles MOÏSE

Remerciements

Ce travail a été réalisé au Laboratoire Réactions et Génie des Procédés (LRGP-UMR 7274 CNRS) à Nancy. Je tiens tout d'abord à remercier Monsieur Gabriel WILD, (ancien directeur du LRGP) et Monsieur Laurent FALK (actuel directeur), pour m'avoir accueilli dans ce laboratoire.

Je tiens à exprimer mes sincères remerciements à mon directeur de thèse Mr. Fabrice MUTELET, pour la confiance qu'il m'a accordée durant ces trois années et pour avoir réuni les conditions nécessaires au bon déroulement de mes travaux. Je le remercie pour ses encouragements, sa compréhension, sa grande disponibilité et son aide indispensable qui ont rendu ce travail de thèse très enrichissant sur le plan scientifique.

J'adresse mes plus vifs remerciements à Mr. Jean-Charles MOÏSE qui m'a co-encadré tout au long de ce travail. J'ai apprécié sa gentillesse, son calme et ses conseils. Je lui exprime ma profonde reconnaissance.

Je tiens également à remercier Mr. Mohammed BOUROUKBA pour son aide préciseuse et pour les nombreuses discussions scientifiques que nous avons eu ensemble. Que Mr. Steve PONTVIANNE soit également assuré de ma gratitude pour sa grande disponibilité et son aide.

Que mesdames Micheline DRAYE et Mireille TURMINE trouvent ici l'expression de ma sincère reconnaissance pour avoir accepté la tâche de rapporteurs. Leur présence dans le jury m'honore. J'assure ma profonde gratitude à Mme Amina NEGADI et Mr. Nicolas BROSSE pour avoir accepté de juger ce travail.

Un grand merci à tous les membres de l'equipe ThermE : Jean-Noël JAUBERT (Responsable de l'équipe), Dominique ALONSO, Michel DIRAND, Nathalie HUBERT et Roland SOLIMANDO.

Je voudrais aussi remercier tous les étudiants qui ont su faire de ces trois ans une expérience agréable et enrichissante : Afef ATTIA, Niramol JUNTARACHAT, Yushu CHEN, El Shaimaa ABUMANDOUR, Imane HADDADOU, Amal AYAD, Zehor BENSAID ainsi que Vincent PLEE.

Pour terminer, le plus important, je voudrais remercier mes parents ainsi que ma femme Walaa et mes filles Haiaa et Joree, qui de près ou de loin, ont toujours su m'offrir leur soutien, leurs encouragements et leur affection.

Table of Contents

Nomenclature and Symbols

Abreviations

NRTL	Non-Random Two Liquid Model
UNIQUAC	Universal Quasi-Chemical Approach
PC-SAFT	Perturbed Chain Satatistical Associating Fluid Theory
PPR78	Predictive Peng-Robinson 1978
SLE	Solid-liquid equilibrium
ILs	Ionic liquids
OF	Objective function
RMSD	Root mean square deviation
DFT	Density functional theory
B3LYP	The hybrid Becke 3−Lee−Yang−Parr
BSSE	Basis set superposition error
ZPE	Zero point energy
ANOVA	Analysis of variance
NREL	National Renewable Energy Laboratory
H.B.	Hydrogen bond
FPU	Filter paper unit
MCC	Microcrystalline cellulose
AvC	Avicel cellulose

Symbols

i and j	Symbols represent the components i and j
M_w	Molecular weight
R	Gaz constant
T	Temperature
T_{fus}	Temperature of fusion
T^{SLE}	The saturated temperature
V	Molar volume
x	Molar/or mass fraction
$\Delta_{fus}H$	Melting enthalpy
r_i	Molecular van der Waals volume
q_i	Molecular surface area

Δg_{ij} or Δu_{ij}	Temperature dependent model parameters
z	Lattice coordination number
a_{12}, a_{21}, b_{12} and b_{21}	Adjustable parameters
α	Nonrandomness parameter
α, β and π*	The Kamlet–Taft solvatochromic parameters
r (Å)	bond length in angstrom
∠°	bond angle in degree
ΔE	Interaction energy
ΔE_{Corr}	Corrected interaction energy

Greek letters

γ	Activity coefficient
ρ	Molar density
θ	Surface fraction
ϕ	Volume fraction
τ_{ij}	Interaction parameter

Indices

att	Attraction
cal	Calculated
exp	Experimental
ex	Extracted
cell	Cellulose
diss	Dissolution
rec	Recovery
reg	Regenerated
hyd	Hydrolysis
effic	Efficiency

Introduction

Le pétrole est actuellement utilisé comme source majeure pour l'élaboration de produits chimiques et de carburants. Son utilisation pose néanmoins des questions importantes en raison de la diminution de ses ressources, de l'augmentation des coûts et de la protection de l'environnement. Une matière première alternative au pétrole est la biomasse lignocellulosique. Dans le passé, la biomasse a d'ailleurs été l'une des premières sources d'énergie à avoir été exploitée par l'homme mais elle a perdu de son importance suite à la révolution industrielle. Elle connaît néanmoins depuis quelques années un regain d'intérêt. Par exemple, les biocarburants dits "de seconde génération" pourront être produits à partir des matières cellulosiques que sont la paille et le bois après extraction et régénération de la cellulose. De plus, les dérivés de la cellulose ont de nombreuses applications dans l'industrie des peintures, des fibres et du papier. Cependant, il n'existe qu'un nombre limité de solvants dans lesquels la cellulose est soluble comme le disulfure de carbone, les sels inorganiques, les acides minéraux. Les solvants traditionnels actuellement utilisés pour l'extraction de la cellulose présentent de nombreux inconvénients tels qu'une forte volatilité et la génération de gaz toxiques. De plus, la cinétique de dissolution de la cellulose dans les solvants organiques traditionnels est particulierement lente.

Ces dernières années, une nouvelle classe de solvants nommée Liquides Ioniques (LIs) a attiré l'attention de la communité scientifiques. Des travaux récents ont d'ailleurs montré que l'utilisation de LIs pour dissoudre et régénérer la cellulose et les composés majoritaires du bois présentait un intérêt particulier. Les premiers résultats indiquent, en effet, que le prétraitement de la biomasse à l'aide de ces solvants augmente le taux de conversion de la cellulose en glucose, qui par fermentation se transforme en éthanol-biocarburant.

L'objectif de ce travail est donc d'étudier le comportement de ces solvants en présence de divers constituants présents dans la biomasse et de définir les conditions optimales d'extraction et de régénération de la cellulose.

Dans le chapitre 1, nous présenterons les liquides ioniques en insistant sur leurs définitions, leurs propriétés physico-chimiques et leurs différentes applications. Ensuite, les différents modèles thermodynamiques capables de représenter les propriétés thermodynamiques des liquides ioniques seront présentées.

Après ce premier chapitre de synthèse bibliographique, nous nous sommes intéressés à l'étude de la solubilité des sucres, les unités structurales qui forment la cellulose, dans des liquides ioniques de type imidazolium. Une fois ce travail effectué, nous avons évalué la possibilité d'extraire ces sucres en utilisant la méthode de l'antisolvant. Les résultats expérimentaux ont ensuite été corrélés avec les résultats obtenus par les modèles thermodynamiques de type NRTL et UNIQUAC.
Le chapitre 3, présente une étude théorique basée sur le calcul ab initio. Ce travail a permis de définir les structures géométriques des LIs étudiés ainsi que celles des sucres ou de la cellulose mais aussi de mieux comprendre les intercations mises en jeu dans les systèmes {sucres + LI} ou {cellulose + LI}.

Enfin, la dernière partie est consacrée à l'extraction et à la régénération de la cellulose issue du miscanthus à l'aide de liquides ioniques. Différentes techniques de fermentation et d'hydrolyse enzymatique ont ensuite été testées afin de convertir la cellulose extraite en biocarburant.

Chapitre I. Synthèse bibliographique

I.1. Généralités sur les liquides ioniques

Les liquides ioniques sont des sels liquides qui présentent une température de fusion inférieure à 100 °C. Dans la plupart des cas, ces sels sont liquides à température ambiante.[1] Ces composés ont reçu une attention particulière aussi bien dans le monde industriel qu'universitaire parce qu'ils ont le potentiel de révolutionner notre façon de penser et d'utiliser les solvants. En raison de leur très faible pression de vapeur, de leur facilité de recyclage et de leur non inflammabilité, ces solvants sont considérés par beaucoup comme solvants "verts". Les liquides ioniques sont des composés constitués d'un cation organique (imidazolium, pyridinium, tétraalkylammonium, phosphonium etc.) et d'un anion inorganique (PF_6^-, BF_4^-, Cl^-, Br^-) ou organique (alkylsulfate, alkylphosphate) (voir figure I.1). Les propriétés physico-chimiques peuvent être modifiées à souhait en remplaçant le cation, l'anion ou la chaîne greffée sur le cation.[2,3] Les liquides ioniques de type dialkylimidazolium sont les plus étudiés. En règle général, les chaînes R_1 et R_2 sont des chaînes alkyles, mais il est possible d'introduire des groupes fonctionnels particuliers tels que des groupements amines, alcools, acides carboxyliques afin de créer des liquides ioniques à tâche spécifique.[4-7]

Dans le cas des anions, certains sont d'origine inorganiques comme le tétrafluoroborate $[BF_4]^-$ et le hexafluorophosphate $[PF_6]^-$. Ces deux derniers, qui sont très utilisés en chimie organique, sont très présents dans de nombreux sels liquides. Comme dans le cas des cations, des anions à propriétés spécifiques ont été développés avec par exemple des anions chiraux ou des anions fonctionnalisés à base de nitriles ou de bases de Lewis.[8]

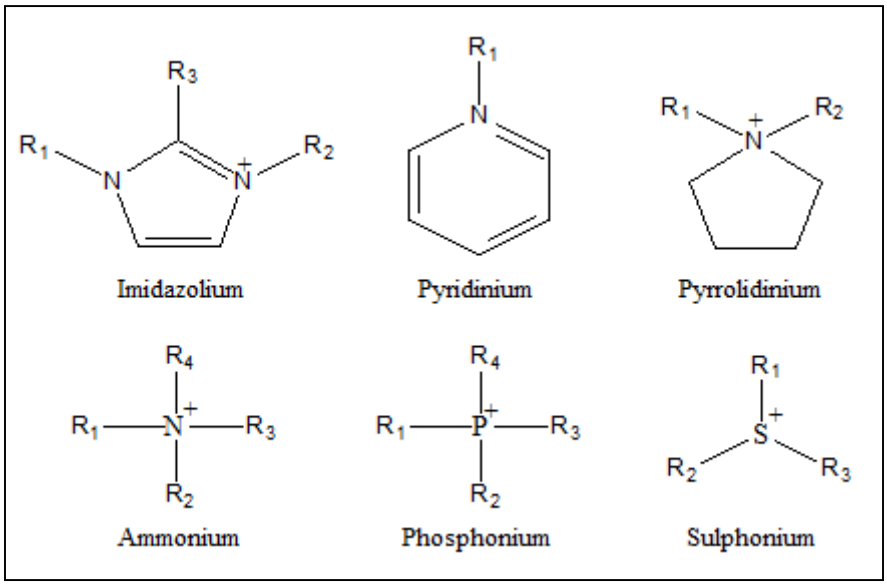

Figure I.1. Cations des liquides ioniques

La viscosité et la densité des LIs sont en général plus élevées que celles de l'eau ou des autres solvants organiques. Leur densité est en effet comprise entre 1 et 1.6 $g.cm^{-3}$. En ce qui concerne leur viscosité, elle est généralement dix fois supérieure à celle des solvants organiques classiques et s'explique principalement par la capacité qu'ont les LIs à former des liaisons hydrogène ou des forces d'interactions de Van der Waals.[9]

La stabilité thermique des LIs est fonction de leur température de décomposition. Dans le cas du cation imidazolium, la température de décomposition est relativement élevée ce qui permet de les utiliser à des températures allant jusqu'à 250 °C. Pour un liquide ionique constitué d'un cation imidazolium, la stabilité thermique dépend essentiellement de la structure de l'anion. Il a été en effet observé que les anions qui présentent les plus faibles interactions intermoléculaires permettent d'obtenir les températures de décomposition les plus élevées.[10]

Bien évidemment toutes les propriétés physico-chimiques des liquides ioniques dépendent également de la pureté du liquide ionique. Cette pureté joue un rôle très important dans le déroulement des réactions.

I.2. Applications des liquides ioniques

I.2.1. Utilisation des liquides ioniques dans les procédés de séparation : extraction liquide-liquide

Les procédés de séparation sont le cœur de l'industrie chimique dans des domaines variés tels que la pétrochimie, l'hydrométallurgie, les industries pharmaceutiques ou l'agroalimentaire. De part leurs propriétés, les liquides ioniques sont envisagés pour l'extraction liquide-liquide de solutés d'intérêt dans diverses applications. Un des principaux problèmes de l'industrie chimique est la séparation de systèmes azéotropiques. Les propriétés physico-chimiques ainsi que la remarquable capacité des LIs à casser les azéotropes les classent parmi les alternatives durables possibles aux solvants conventionnels utilisés dans l'industrie. De plus, leur faible corrosivité devrait permettre leur utilisation dans les procédés de séparation.

La désulfuration des carburants par l'extraction liquide-liquide utilisant les LIs est également de plus en plus étudiée. A titre d'exemple, l'extraction des composés organiques soufrés à l'aide des LIs a été proposée pour la première fois par Bössman et al.[11] et a été suivie par de nombreuses autres études.[12,13] Dans ces études, l'effet de la nature du liquide ionique sur la performance de l'extraction a été evalué. Les résultats de ces travaux montrent que le choix de l'anion semble être plus important que le choix du cation pour l'extraction. Les LIs constitués du cation alkylméthylpyridinium présentent des taux d'extraction supérieur à 70 % pour les composés organiques soufrés.[14] Ce résultat peut encore être amélioré en couplant ce cation avec des anions tels que le thiocyanate.

De nombreuses études expérimentales des équilibres de phases ont été réalisées afin d'évaluer la capacité des liquides ioniques à extraire divers solutés gazeux ou liquides. La majorité des données expérimentales est corrélée à l'aide de modèles thermodynamiques tels que : NRTL, UNIQUAC ou électrolyte-NRTL.[13, 15-16] L'étude de Simoni et al. a démontré que ces modèles peuvent être utilisés pour présenter les équilibres de phases moyennant quelques améliorations.[17]

I.2.2. Utilisation des liquides ioniques pour l'extraction de constituants issus de la biomasse

Depuis 2010, quelques études ont été menées sur la solubilité de différents constituants présent dans la biomasse dans les liquides. Ces études sont généralement consacrées aux sucres, à la cellulose ou bien la lignine.

En 2000, Sheldon et al. ont été les premiers à étudier le potentiel des LIs comme milieux réactionnels pour les transformations de sucres.[18] En 2001, deux équipes de recherche[19,20] ont présenté la solubilité du glucose dans divers LIs. Ces LIs contenant une chaine éther sont capables d'établir des liaisons hydrogène avec les groupes hydroxyle des sucres. Il a été démontré que la solubilité des sucres était influencée principalement par la nature de l'anion. La dissolution complète des sucres dans un solvant adéquat est un facteur important dans la chimie des sucres. Un point essentiel ensuite est l'extraction de ces composés et la suppression du solvant.[21] L'extraction de sucres dissous dans une solution aqueuse a été effectuée à l'aide de sels d'ammonium quaternaire et d'acide boronique.[21,22] Les liquides ioniques hydrophobes ont été récemment étudiés pour l'extraction de métaux[23] ou des composés organiques polaires,[24] tels que des alcools,[25] d'une phase aqueuse. De récentes études ont présentées une méthode simple pour l'extraction des sucres, où un LI hydrophobe peut directement extraire le composé dissous dans une solution aqueuse sans l'utilisation d'un tensioactif ou d'une solution tampon dans la phase aqueuse.

Ces dernières décennies, les solvants couramment utilisés pour dissoudre la cellulose sont des solvants organiques polaires tels que le dimethylformamide, le dimethylacetamide, le dimethylimidazolidinone ou bien le dimethyl sulfoxide en présence de composés chargés tels que [NBu4] [F] ou chlorure de lithium. Cependant, ces solvants souffrent de leur toxicité, de leur coût élevé, de leur faible capacité à dissoudre, d'un recyclage difficile et de leur instabilité thermique dans les conditions de procedé.[26] Par conséquent, le traitement de la cellulose est souvent complexe et très onéreux. La dissolution de la cellulose dans un liquide ionique a été présentée pour la première fois en 1934 dans un brevet américain. Le solvant utilisé était le N-éthylpyridinium chloride en présence d'une base azotée telle que la pyridine. Cependant, ce système présentait un point de fusion relativement élevé (mp: 118-120°C).[27] En 2002, Rogers et al. ont démontré que la cellulose pourrait être dissous dans les liquides ioniques.[28] Cette équipe a demontré que dans le meilleur des cas, 8 à 12% de la cellulose est soluble dans le 1-butyl-3-méthylimidazolium chloride (BMIMCl). Par activation par micro-ondes, ce résulat peut atteindre jusqu'à 25%. Cependant, on observe une dégradation plus importante lors d'utilisation des micro-ondes que dans des conditions classiques.[29]

Ces résultats ont permis de développer une classe de solvants pour l'extraction de la cellulose et d'initier une recherche approfondie dans ce domaine. En général, la capacité des LIs à dissoudre la cellulose dépend de la nature de la cellulose (son degré de polymérisation et sa cristallinité), des conditions opératoires (température, temps de réaction, concentration

initiale de la cellulose, activation avec des micro-ondes) et de la présence d'impuretés, principalement de l'eau qui peut modifier considérablement les résultats.

Quelques liquides ioniques sont connus pour bien dissoudre la cellulose. Les plus étudiés sont le 1-butyl-3-methylimidazolium chloride et le 1-butyl-3-methylimidazolium acetate. Un grand nombre de LIs avec différents anions a été étudié pour la dissolution des sucres. Les anions $[BF_4]^-$ et $[PF_6]^-$ ont été rapidement éliminés en raison de leur faible capacité à dissoudre tout type de cellulose.[30] Pour la même raison, le bis(trifluoromethylsulfonyl)imide $[Tf_2N]$ et $[N(CN)_2]$ ont été écartés. Pour des raisons pratiques, il est nécessaire de trouver une nouvelle classe de liquides ioniques possédant des viscosités et des points de fusion plus faibles que ceux des sels de chloride utilisés actuellement.[31] Les LIs à base de formiate, d'acétate ou de phosphate ont montré un potentiel intéressant pour dissoudre la cellulose dans des conditions douces.

I.3. Modèles thermodynamiques pour présenter les propriétés thermodynamiques des liquides ioniques

L'étude des opérations unitaires des procédés industriels telles que la distillation, l'absorption, l'extraction liquide-liquide, etc. nécessite la prédiction et la corrélation des propriétés thermodynamiques des fluides. Les équations d'état restent l'outil de choix à cet effet car elles permettent le calcul des propriétés thermodynamiques mais aussi des équilibres de phases. De nombreuses équations d'état sont dérivées du modèle cubique basé sur la théorie de Van Der Waals.

En 1873, Van der Waals[32] a proposé la première équation d'état cubique capable de prédire et représenter aussi bien les phases liquides que gazeuses. Cependant, l'équation de Van Der Waals est d'une précision insuffisante et uniquement applicable à des fluides simples, ce qui a conduit à de nombreuses modifications.

Actuellement le défi réside dans la modélisation de procédés complexes, de propriétés de fluides eux-mêmes complexes, tels que les systèmes polaires, les systèmes de macromolécules biologiques, les liquides ioniques, parfois en conditions supercritiques. Contrairement aux fluides simples, les fluides complexes contiennent des molécules qui interagissent les unes avec les autres au moyen d'interactions spécifiques comme les interactions polaires ou associatives. C'est le cas des LIs, qui sont considérés comme des composés associatifs ou polaires.[33,34] L'estimation de leurs propriétés par différents modèles thermodynamiques tels que les modèles

de coefficient d'activité (NTRL et UNIQUAC), Cubique et SAFT seront présentés dans ce chapitre.

I.3.1. Equation d'état cubique et de type SAFT

Les équations d'état cubiques sont très utilisées dans le domaine de la thermodynamique des fluides. Parmi les plus connues, nous allons citer celle de Van der Waals, Peng-Robinson, Soave-Redlich-Kwong ou bien PPR78.[35] Le modèle PPR78 dévelopé au sein de notre équipe utilise l'équation d'état de Peng-Robinson dans sa version de 1978, les règles de mélange de Van der Waals, et suppose que le coefficient d'interaction binaire k_{ij} est uniquement fonction de la température T. La méthode est rendue prédictive par le calcul de k_{ij} à partir d'une méthode de contributions de groupes.[36,37]

Dans les travaux de thèse de Revelli, le modèle PPR78 a été appliqué à la représentation des propriétés des LIs purs et en mélanges avec du CO_2. Ce modèle nécessite la connaissance de trois paramètres des corps purs: la température critique Tc, la pression critique Pc et le facteur acentrique ω_i de chaque constituant. Malheureusement, il est impossible de mesurer expérimentalement les propriétés critiques des LIs car la plupart d'entre eux se décomposent avant d'atteindre le point critique. Ces propriétés critiques sont généralement calculées à partir d'une méthode de contributions de groupes proposée par Valderrama et al..[38] Les résultats obtenus par Revelli indiquent que ce modèle est capable de décrire les diagrammes de phases des systèmes {CO_2+LIs} à condition que les propriétés critiques soient connues. Marina et al.[39] ont présenté l'importance de l'association intermoléculaire lors de leur étude de la solubilité du dioxyde de carbone dans les LIs. Cette étude a évalué trois équations d'état Peng-Robinson, Soave-Redilich-Kwong et l'équation cubique plus association (CPA) avec un paramètre d'interaction dépendant de la température. Les auteurs ont démontré que l'utilisation d'un terme associatif n'apportait pas d'avantage majeur pour l'étude des systèmes binaires {LIs+CO_2}.

Les équations d'état de type SAFT[40] (Statistical Associating Fluid Theory), en particulier PC-SAFT[41] et Soft-SAFT sont de plus en plus utilisées pour représenter les propriétés des LIs purs et en mélange. Llovell et Vega[42] ont utilisé l'équation Soft-SAFT pour estimer les propriétés thermodynamiques des LIs purs et en mélanges. Les LIs purs ont d'abord servi à paramétrer le modèle et à évaluer sa fiabilité. Le comportement des LIs dans les mélanges binaires avec des autres composés associatifs ont alors été prédits. Llovell et Vega ont conclu que le comportement thermodynamique des LIs purs mais aussi des mélanges binaires peut être représenté avec une grande précision à l'aide de l'équation Soft-SAFT. En 2012, Domanska et

al.[43] et Chen et al.[44] ont appliqué le modèle PC-SAFT à l'étude de systèmes contenant des liquides ioniques. Les auteurs ont démontré que le modèle PC-SAFT permettait de représenter des équilibres liquide-vapeur ainsi que des équilibres liquide-liquide de systèmes constitués d'aromatiques et de liquides ioniques à base d'isoquinolium.

I.3.2. Modèle d'énergie de Gibbs molaire totale d'excès g^E

Les modèles d'énergie de Gibbs d'excès g^E, appelés modèles de coefficient d'activité sont essentiels pour calculer les équilibres de phases dans les régions sub-critiques. De nombreux travaux ont montré que les modèles de g^E tels que NRTL[45] et UNIQUAC[46] sont capables de représenter les propriétés des LIs en mélange et de simuler l'extraction liquide-liquide des systèmes ternaires.

A l'heure actuelle, la majorité des données d'équilibre liquide-liquide (ELL) de systèmes ternaires contenants un LI est corrélée à l'aide de modèles de g^E tels que NRTL et UNIQUAC. [47,48] Ces modèles donnent des résultats très satisfaisants pour la représentation des données expérimentales. Cependant, en 2008, les travaux de Simoni et al. ont montré que les modèles NRTL et UNIQUAC n'étaient pas complètement satisfaisants pour représenter simultanément des données d'équilibre liquide-vapeur et d'équilibre liquide-liquide.

I.4. Conclusion

En conclusion, les récents travaux montrent que les liquides ioniques peuvent être utilisés pour extraire ou améliorer l'extraction de divers constituants de la biomasse. Le développement de procédés de valorisation de ressources naturelles nécessite une bonne connaissance des propriétés physico-chimiques de ces systèmes. Cependant, la synthèse bibiographique indique qu'il y a un manque de données sur ces systèmes complexes. De plus, peu de travaux présentent une étude complète sur l'extraction de la cellulose à l'aide de liquides ioniques. Ce travail propose donc d'apporter de nouvelles données expérimentales sur des systèmes contenant des liquides ioniques et des constituants de la biomasse (sucres, cellulose, lignine). Dans ce cadre, les modèles NRTL et UNIQUAC ont été choisis afin d'évaluer leur capacité à reproduire le comportement de ces systèmes. La seconde partie de ce travail propose d'évaluer la performance de quelques LIs pour l'extraction de la cellulose du Miscanthus et de déterminer les conditions optimales.

Références bibliographiques

[1] M. Earle, K. Seddon, Ionic liquids, Green solvents for the future, Pure Appl. Chem., 72 (2000) 1391-1398.

[2] J. G. Huddleston, A. E. Visser, W. M. Reichert, H. D. Willauer, G. A. Broker, R. D. Rogers, Characterization and comparison of hydrophilic and hydrophobic room temperature ionic liquids incorporating the imidazolium cation, Green Chem., 3 (2001) 156-164.

[3] K. R. Seddon, A. Stark, M. J. Torres, Influence of chloride, water, and organic solvents on the physical properties of ionic liquids, Pure Appl. Chem., 72 (2000) 2275-2287.

[4] L. C. Branco, J. N. Rosa, J. J. M. Ramos, C. A. M. Afonso, Preparation and characterization of new room temperature ionic liquids, Chem. Eur. J., 8 (2002) 3671-3677.

[5] H. S. Schrekker, M. P. Stracke, C. M. L. Schrekker, J. Dupont, Ether-functionalized imidazolium hexaflurophosphate ionic liquids for improved water miscibilities, Ind. Eng. Chem. Res., 46 (2007) 7389-7392.

[6] Y. Fukaya, K. Hayashi, M. Wada, H. Ohno, Cellulose dissolution with polar ionic liquids under mild conditions: required factors for anions, Green Chem., 10 (2008) 44-46.

[7] Z. F. Fei, D. B. Zhao, R. Scopelliti, P. J. Dyson, Organometallic complexes derived from alkyne-functionalized imidazolium salts, Organometallics, 23 (2004) 1622-1628.

[8] D. R. MacFarlane, J. M. Pringle, K. M. Johansson, S. A. Forsyth, M. Forsyth, Lewis base ionic liquids, Chem. Commun., 18 (2006) 1905-1917.

[9] T. L. Greaves, C. J. Drummond, Protic ionic liquids: properties and applications, Chem. Rev., 108 (2008) 206-237.

[10] P. Bonhôte, A. P. Dias, N. Papageorgiou, K. Kalyanasundaram, M. Grätzel, Hydrophobic, highly conductive ambient-temperature molten salts, Inorg. Chem., 35 (1996) 1168-1178.

[11] A. Bosmann, L. Datsevich, A. Jess, A. Lauter, C. Schmitz, P. Wasserscheid, Deep desulfurization of diesel fuel by extraction with ionic liquids, Chem. Commun., (2001) 2494-2495.

[12] J. Esser, P. Wasserscheid, A. Jess, Deep desulfurization of oil refinery streams by extraction with ionic liquids, Green Chem., 6 (2004) 316-322.

[13] L. Alonso, A. Arce, M. Francisco, O. Rodríguez, A. Soto, Gasoline desulfurization using extraction with [C_8mim][BF_4] ionic liquid, AIChE J., 53 (2007) 3108-3115.

[14] J. D. Holbrey, I. Lopez-Martin, G. Rothenberg, K. R. Seddon, G. Silvero, X. Zheng, Desulfurization of oils using ionic liquids: selection of cationic and anionic components to enhance extraction efficiency, Green Chem., 10 (2008) 87-92.

[15] L. D. Simoni, A. Chapeaux, J. F. Brennecke, M. A. Stadtherr, Extraction of biofuels and biofeedstocks from aqueous solutions using Ionic liquids, Comput. Chem. Eng., 34 (2010) 1406-1412.

[16] G. W. Meindersma, A. J. G. Podt, A. B. de Haan, Ternary liquid–liquid equilibria for mixtures of toluene+< i> n</i>-heptane+ an ionic liquid, Fluid Phase Equilib., 247 (2006) 158-168.

[17] L. D. Simoni, Y. Lin, J. F. Brennecke, M. A. Stadtherr, Modeling liquid-liquid equilibrium of ionic liquid systems with NRTL, electrolyte-NRTL, and UNIQUAC, Ind. Eng. Chem. Res., 47 (2008) 256-272.

[18] R. M. Lau, F. van Rantwijk, K. R. Seddon, R. A. Sheldon, Lipase-catalyzed reactions in ionic liquids, Org. Lett., 2 (2000) 4189-4191.

[19] S. Park, R. J. Kazlauskas, Improved preparation and use of room-temperature ionic liquids in lipase-catalyzed enantio-and regioselective acylations, J. Org. Chem., 66 (2001) 8395-8401.

[20] N. Kimizuka, T. Nakashima, Spontaneous self-assembly of glycolipid bilayer membranes in sugar-philic ionic liquids and formation of ionogels, Langmuir, 17 (2001) 6759-6761.

[21] M. Matsumoto, K. Ueba, K. Kondo, Sep. Purif. Technol., Separation of sugar by solvent extraction with phenylboronic acid and trioctylmethylammonium chloride, 43 (2005) 269-274.

[22] H. A. Aziz, A. H. Kamaruddin, M. Z. Abu Bakar, Process optimization studies on solvent extraction with naphthalene-2-boronic acid ion-pairing with trioctylmethylammonium chloride in sugar purification using design of experiments, Sep. Purif. Technol., 60 (2008) 190-197.

[23] D. Kogelnig, A. Stojanovic, M. Galanski, M. Groessl, F. Iirsa, R. Krachler, B. K. Keppler, Greener synthesis of new ammonium ionic liquids and their potential as extracting agents, Tetrahedron Lett., 49 (2008) 2782-2785.

[24] J. McFarlane, W. B. Ridenour, H. Luo, R. D. Hunt, D. W. DePaoli, R. X. Ren, Room temperature ionic liquids for separating organics from produced water, Sep. Sci. Technol., 40 (2005) 1245-1265.

[25] A. Chapeaux, L. D. Simoni, T. S. Ronan, M. A. Stadtherr, J. F. Brennecke, Extraction of alcohols from water with 1-hexyl-3-methylimidazolium bis(trifluromethylsulfonyl)imide Green Chem., 10 (2008) 1301-1306.

[26] L. Feng, Z.Chen, Research progress on dissolution and functional modification of cellulose in ionic liquids, J. Mol. Liquids, 142 (2008)1-5.

[27] C. Graenacher, cellulose solution, US Patent 1, 943,176. (1934).

[28] R. P. Swatloski, S. K. Spear, J. D. Holbrey, R. D. Rogers, Dissolution of cellulose with ionic liquids, J. Am. Chem. Soc., 124 (2002) 4974-4975.

[29] J. Vitz, T. Erdmenger, C. Haensch, U. S. Schubert, Extended dissolution studies of cellulose in imidazolium based ionic liquids, Green Chem., 11 (2009) 417-424.

[30] K. E. Gutowski, G. A. Broker, H. D. Willauer, J. G. Huddleston, R. P. Swatloski, J. D. Holbrey, R. D.Rogers, Controlling the aqueous miscibility of ionic liquids: aqueous biphasic systems of water-miscibile ionic liquids and water-stucturing salts of recycle, metathesis and separations, J. Am. Chem. Soc. 125 (2003) 6632-6633.

[31] Y. Cao, J. Wu, J. Zhang, H. Li, Y. Zhang, J. He, Room temperature ionic liquids (RTILs): a new and versatile platform for cellulose processing and derivatization, Chem. Eng. J. 147(2009)13-21.

[32] Van der Waals, Over de Continuiteit van den Gas- en Vloeistoftoestand (on the continuity of the gas and liquid state, J. D. Ph.D. thesis, Leiden (1873).

[33] M. C. Kroon, E. K. Karakatsani, I. G. Economou, G. J. Witkamp, C. J. Peters, Modeling of the carbon dioxide solubility in imidazolium-based ionic liquids with the tPC-PSAFT equation of state J. Phys. Chem. B, 110 (2006) 9262-9269.

[34] L. F. Vega, J. S. Andreu, The Solubility Behavior of CO_2 in Ionic Liquids by a Simple Model, J. Phys. Chem. C, 111 (2007) 16028-16034.

[35] D. Y. Peng, D. B. Robinson, A new two-constant equation of state, Ind. Eng. Chem. Fundam., 15 (1976) 59-64.

[36] J. N. Jaubert, F. Mutelet, VLE predictions with the Peng–Robinson equation of state and temperature dependent k_{ij} calculated through a group contribution method, Fluid Phase Equilib., 224 (2004) 285-304.

[37] S. Vitu, R. Privat, J. N. Jaubert, F. Mutelet, Predicting the phase equilibria of CO_2 + hydrocarbon systems with the PPR78 model (PR EOS and k_{ij} calculated through a group contribution method, J. Supercrit. Fluids, 45 (2008) 1-26.

[38] J. O. Valderrama, R. E. Rojas, Critical properties of ionic liquids revisited, Ind. Eng. Chem. Res., 48 (2009) 6890-6900.

[39] M. S. Manic, A. J. Queimada, E. A. Macedo, V. J. Najdanovic-Visak, High-pressure solubilities of carbon dioxide in ionic liquids based on bis(trifluoromethylsulfonyl)imide and chloride, Supercrit. Fluids, 65 (2012) 1-10.

[40] S. H. Huang, M. Radosz, Equation of state for small, large, polydisperse, and associating molecules, Ind. Eng. Chem. Res., 29 (1990) 2284-2294.

[41] J. Gross, G. Sadowski, Perturbed-chain SAFT: An equation of state based on a perturbation theory for chain molecules, Ind. Eng. Chem. Res., 40 (2001) 1244-1260.

[42] F. Llovell, E. Valente, O. Vilaseca, L. F. Vega, Modeling complex associating mixtures with [C_n-mim][Tf_2N] ionic liquids: predictions from the soft-SAFT equation, J. Phys. Chem. B, 115 (2011) 4387-4398.

[43] K. Paduszynski, U. Domanska, Thermodynamic modeling of ionic liquid systems: Development and detailed overview of novel methodology based on the PC-SAFTJ. Phys. Chem. B, 116 (2012) 5002-5018.

[44] Y. Chen, F. Mutelet, J. N. Jaubert, Modeling the Solubility of Carbon Dioxide in Imidazolium-Based Ionic Liquids with the PC-SAFT Equation of State, J. Phys. Chem. B, 116 (2012) 14375-14388.

[45] H. Renon, J. M. Prausnitz, Local compositions in thermodynamic excess functions for liquid mixtures, AIChE J., 14 (1968) 135-144.

[46] D. S. Abrams, J. M. Prausnitz, Statistical thermodynamics of liquid mixtures: A new expression for the excess gibbs energy of partly or completely miscible systems, AIChE J., 21 (1975) 116-128.

[47] U. Domanska, A. Pobudkowska, Z. Zolek-Tryznowska, Effect of an Ionic Liquid (IL) Cation on Ternary System (UL + p-Xylene + Hexane) at T = 298.15 K, J. Chem. Eng. Data., 52 (2007) 2345-2349.

[48] L. Alonso, A. Arce, M. Francisco, A. Soto, Thiophene separation from aliphatic hydrocarbons using the 1-ethyl-3-methylimidazolium ethylsulfate ionic liquid, Fluid Phase Equilib., 270 (2008) 97-102.

Chapter II. Study of the behavior of systems containing (Carbohydrate-ILs)

The aim of this chapter is to overcome the lack of experimental data on phase equilibria of biomass carbohydrates in ionic liquids. The solubility of glucose, fructose, sucrose and lactose in ionic liquids was measured within a temperature range from 283 K to 383 K. Solubility data were successfully correlated with local composition thermodynamic models such as NRTL and UNIQUAC. In this work, the possibility of extracting glucose from these ionic liquids using the antisolvent method has been also evaluated. The parameters affecting the extraction process are the ionic liquid type, ethanol / ionic liquid ratio, temperature, water content, and time. Results indicate that ethanol can be successfully used as an antisolvent to separate sugars from ionic liquids.

II.1. Introduction

The search for sustainable and alternative energy is of critical importance with the ever-growing energy demands and environmental concerns, together with the decrease of fossil fuel reserves.[1,2] Development of a technology platform, which could facilitate the access to natural biopolymers and enable the production of biofuels based on renewable sources, is a major step towards sustainability. Biomass is regarded as a permanent source of renewable feedstock on the planet for both material and energy. Lignocellulosic materials, such as agricultural residues (corn stover and wheat straw), waste paper, wood wastes, and energy crops, have been recognized as a potential sustainable source of sugars for biotransformation into bioethanol and value-added bio-based products.[3] Bioethanol production from cellulosic materials usually consists of three steps: (1) pretreatment of lignocellulose to enhance the enzymatic or microbial digestibility of polysaccharide components; (2) hydrolysis of cellulose and hemicellulose to fermentable sugars; and (3) fermentation of the sugars to liquid fuels.[4-6] Lignocellulosic biomass primarily consists of a complex mixture of lignin, hemicellulose, and semi crystalline cellulose. This complicated structure makes the production of fermentable sugars from lignocellulosic biomass expensive and inefficient when compared with the production of sugars from starch-based feedstocks. Pretreatment of lignocellulosic biomass is required to disrupt the lignin-carbohydrate complex, decrease cellulose crystallinity and partially remove lignin and hemicelluloses. The pretreated cellulose becomes more accessible to the enzymes that convert the carbohydrate polymers into fermentable sugars.[7-9] Ionic liquids (ILs) have recently emerged as promising new solvents capable of disrupting the native cellulose crystalline structure, possibly also breaking structurally important chemical linkages, in a wide range of biomass feedstocks.[10-13] Ionic liquids are salts in the liquid state having melting point below some arbitrary temperature, such as 100°C (373 K). They are solvents that facilitate more ecological applications in reactions and separations because of their unique properties, such as negligible vapor pressure[14] and high thermal stability.[15] Their very low vapor pressure reduces the risk of exposure that is a clear advantage over the use of the classical volatile solvents. They are considered as more environmentally-friendly than their volatile, toxic, and organic counterparts. ILs that are regarded as ‘‘green’’ solvents, have received worldwide attention in various fields including catalysis[16-17], electrochemistry[18-19], separation[20-21], chemical synthesis, polymer chemistry and nanotechnology. [22-23] Swatloski *et al.* (2000) reported the use of an ionic liquid as a solvent for cellulose both for the regeneration of cellulose and for the chemical modification of polysaccharide.[24] 1-butyl-3-methylimidazolium chloride (BMIMCl), was found

to be capable of dissolving up to 25% cellulose (by weight).[24] This provided a new platform for the ‘‘green’’ comprehensive utilization of cellulose resources. Although the fact that most of carbohydrates are soluble only in protic solvents, such as water, and insoluble in most organic aprotic solvents as they contain a high number of hydroxyl groups which hinder their dissolution, ionic liquids have been reported as new potential media to dissolve carbohydrates.[25-27] The solubility data of carbohydrates in ionic liquids is an important issue in order to develop chemical or bio-process involving these compounds. Nevertheless, the literature mainly concerns the application of ILs in the modification of cellulose trapped in the lignocellulosic biomass.[28] Studies on the dissolution and on the extraction of carbohydrates other than cellulose in ILs are limited.[29-30] The data reported in the literature concerning the solubility of biomass-derived compounds such as carbohydrates in ionic liquids is far from being enough to have a good knowledge on phase equilibria. In most cases, these data are not available in a sufficiently large range of temperature which turns the modeling process into a very difficult task.[31] Some ILs have been demonstrated to be excellent solvents for carbohydrates, Sheldon et al. were the first to connect ILs and carbohydrates by exploring their potential as media for carbohydrates transformations.[32] Park *et al*. and Kimizuka *et al*. reported the solubility of glucose in imidazolium based ILs.[30,33,34] These ILs containing an ether pendant substituent are currently named “sugar-philic” ILs due to their capacity to establish hydrogen bonds with the hydroxyl groups of the carbohydrate. MacFarlane *et al*.[35,36] and Sheldon *et al.* [37] described the dicyanamide as an attractive anion to dissolve carbohydrates due to its hydrogen bond acceptor properties. V. M. Egorov *et al*. found that BMIMCl is capable of dissolving until 56% fructose at 110°C. Many antisolvents have been used to separate carbohydrates from ionic liquids. The performance of dichloromethane for the extraction of carbohydrates from ionic liquids was studied by Rosatella *et al*. while Liu *et al*. studied the solubility of glucose in a binary mixture containing an IL and ethanol.[38] Ethanol precipitation is a separation technology with many advantages, such as safe solvent, easy operation, and high removal for high polarity components, such as saccharides, proteins, and inorganic salts. The correlation of carbohydrates solubility data in ionic liquids could be achieved using local composition thermodynamic models. Carneiro *et al*. measured the solubility of monosaccharides in ILs and these solubility data were correlated using the NRTL and UNIQUAC thermodynamic models.[31]

This work is focused on the dissolution of carbohydrates in ionic liquids and the extraction using the antisolvent method. This work is mainly divided into three parts, the first part aims to study the influence solubility of carbohydrates in ionic liquids in a temperature range from 280 K to 390 K. Solubility data have been successfully correlated with local composition

thermodynamic models such as NRTL and UNIQUAC and compared with solubility data in the literature. The second part of the article is devoted to the solubility of carbohydrates in binary mixtures {ethanol + ionic liquids} in order to evaluate the possible use of the anti solvent method for the extraction of carbohydrates from ionic liquids. The influence of different parameters such as temperature, ionic liquid/ethanol ratio, water content but also the structure of the IL on the performance of the extraction is evaluated. Then, in the third part the anti solvent method is tested for the extraction of carbohydrates from 1-butyl-3-methylimidazolium chloride.

II.2. Experimental techniques

II.2.1. Materials

D-(+)-Glucose anhydrous was purchased from Merck. D-(-)-Fructose, Sucrose and α-Lactose monohydrate were purchased from Sigma Aldrich. Ethyl alcohol absolute with a mass fraction purity of 0.999 was from Carlo Erba. Acetonitrile with a mass fraction purity of 0.999 was from Sigma-Aldrich.

The ionic liquids used in this work, 1-butyl-3-methylimidazolium chloride (BMIMCl), 1-ethanol-3- methylimidazolium chloride (EtOHMIMCl), 1-butyl-1-methylpyrrolidinium chloride (BMPyrCl), and 1,3-dimethyl-imidazolium methyl phosphonate (DMIMMPh), with purity 98%, were from Solvionic, and 1-ethyl-3-methylimidazolium thiocyanate (EMIMSCN) with purity 95% was from Sigma Aldrich. The physical properties of the selected ionic liquids are shown in table II.1. These ionic liquids were dried under vacuum for 3 hours at 363 K before use.

Table II.1. Physical properties of studied ionic liquids

Physical properties	BMIMCl	EtOHMIMCl	BMPyCl	EMIMSCN	DMIMMPh
Color and shape at 25°C	White powder	Yellow solid	White Powder	Red liquid	Colorless liquid
Molecular formula	$C_8H_{15}ClN_2$	$C_6H_{11}ClON_2$	$C_9H_{20}ClN$	$C_7H_{11}N_3S$	$C_6H_{13}N_2PO_3$
Purity (%)	98	98	98	95	98
Molecular weight	174.7	162.61	177.71	162.25	192.15
Melting point (°C)	65	80	114	-6	-20
Density (g/cm^3)	1.0528 at 80°C	n.d	n.d	1.114 at 25°C	1.18 at 25°C
Viscosity (cP)	142 at 80 °C	n.d	n.d	20 at 25°C	50.3 at 25°C
Decomposition temp. (°C)	250	>200	210	>200	>200
Water Content (ppm)	<1000	<1000	<1000	<1000	450
Solubility in water	Miscible	Miscible	Miscible	Miscible	Miscible
Solubility in ethanol	Miscible	Miscible	Miscible	Miscible	Miscible

II.2.2. Apparatus and procedures

Solid-liquid equilibrium phase diagrams of the studied systems were obtained at atmospheric pressure and at temperature ranges starting from 283 to 373 K. The solubility experiments of carbohydrates in pure ILs and in a binary mixture of IL with ethanol have been performed in jacketed glass cells using a dynamic method described in the literature. [39] The experimental set up consists of a cell with an internal volume of about 50 cm^3. The temperature of the cell was maintained constant using a thermostatic bath (polystat 5D +37, Fisher scientific.) with a precision of ±0.1 K. The internal temperature of the cell was also measured with a calibrated platinum probes Pt100 with an accuracy of ± 0.1 K. The mixtures, with compositions inside the immiscible region of the system, are weighed using a METTLER analytical balance with a precision of ± 0.0001 g.

For the solubility of carbohydrates in pure ILs, desired amounts of pure IL and sugar were loaded into a prepared cell. The cell was sealed and connected to the temperature controller. The mixture was rigorously stirred for 6 hours and was then heated very slowly (about $1K.h^{-1}$) until complete dissolution of the sugar in the ionic liquid. The solubility measurements were confirmed by the visual observation of the solution under microscope.

For the experiments of solubility of carbohydrates in a binary mixture (IL + EtOH), a desired amount of ethanol was loaded into a prepared cell, and then, a desired amount of IL with a given mass ratio of ethanol to IL was added quickly into the above ethanol solution. The cell was sealed and connected to the temperature controller until a transparent solution was formed. When the temperature of the system attained a desired value, an excessive amount of sugar was added to the mixture. At different time intervals, samples were withdrawn, filtrated with 0.45 μm film, and analyzed by a high performance liquid chromatography (HPLC) to determine the carbohydrate concentration.

An HPLC (SHIMADZU, USA) with a SHODEX Asahipak NH2-50 4E column (Shodex, Japan) and a differential refractive index detector (SHIMADZU, USA) was employed for analyzing concentrations of carbohydrates in the mixtures. The column oven temperature was 308 K, the mobile phase was a mixture of acetonitrile and water with a ratio (75:25), and the flow rate was 1 ml/min. The correlation coefficient of the sugars standard curve by the HPLC reached a value of 0.999. The expanded relative uncertainty of carbohydrate solubility in IL and antisolvent mixtures was estimated at 1.0%. The equilibration temperature was measured with an uncertainty of 0.2 K.

II.3. Results and discussion

Only a limited number of ionic liquids available have been studied until now in the various applications including the solubility studies. In this work, three ionic liquids, 1-ethanol-3-methylimidazolium chloride, 1-butyl-1-methylpyrrolidinium chloride, and 1,3-dimethyl-imidazolium methyl phosphonate, were investigated in order to increase the number of the potentially interesting solvents for carbohydrates. Two other classical ILs, BMIMCl and EMIMSCN used in the biomass conversion process were also studied to evaluate their behavior in the presence of carbohydrates.

II.3.1. Solubility of carbohydrates in pure ionic liquids

Solid-liquid equilibria (SLE) of binary systems {IL + sugar} were carried out in a large range of temperatures 280-390 K and compositions up to 60 % of sugar, table II.2. To our knowledge, the measurements of solubility of sugars in 1-ethanol-3-methylimidazolium chloride, 1,3-dimethyl-imidazolium methyl phosphonate are the first published in the literature. It is clearly obvious that the solubility of carbohydrates increases in the following order lactose < sucrose < glucose < fructose for ILs used in this study. The solubility increases at high temperature in the following order EMIMSCN < EtOHMIMCl ≤ BMIMCl < DMIMMPh. The Kamlet–Taft solvatochromic parameters are the most comprehensive and frequently used quantitative measure of solvent properties. The Kamlet–Taft solvatochromic parameters (α: hydrogen bond donating ability (acidity); β: hydrogen bond accepting ability (basicity) and π*: polarity/polarizability) can be used to explain the solubility of carbohydrates in Ils (see table II.3).[40-46] Studies on the dissolution of cellulose in BMIMCl indicate that the anion of the IL acts as a hydrogen bond acceptor which interacts with the hydroxyl groups of the cellulose.[24] It is found that the phosphonate and chloride imidazolium based ionic liquids displayed higher β and π* values if compared to other ionic liquids. Generally, the solvatochromic parameters α, β and π* affected by the alkyl chain length of the imidazolium cation. An increase of the alkyl chain of the imidazolium cation decreases the values α and π* while the β value increases. In this work, the solubility of sugars in ionic liquids increases with increasing the order of both hydrogen bond basicity and polarizability of the ionic liquids.

The solubility curves of glucose in EMIMSCN and in DMIMMPh presented in figure II.1 indicate that glucose is more soluble in EMIMSCN than in DMIMMPh at low temperature. This tendency is reversed for temperatures higher than 310 K. This behavior may be related to

different physico-chemical properties of ILs. ILs viscosity may play a role in carbohydrates dissolution. Indeed, it is generally considered that ILs with low viscosity are more efficient in dissolving carbohydrates or cellulose. Nevertheless, viscosity is not the key factor of the solubility of glucose in ILs. Basicity and polarity of ILs are also excellent indicators to estimate their ability to dissolve glucose. The compilation of our data on the solubility of glucose in EMIMSCN and the data in BMIMSCN published in the literature [47] proved that the solubility of glucose increases with a decrease of the alkyl chain length. Results obtained on the solubility of glucose in BMIMCl correspond well to those published in the literature. [48] At 343.15 K, the solubility of glucose was found to be 0.059 wt% in this work and 0.05 wt % in the literature. The solubility curves of glucose in BMIMCl and EtOHMIMCl follow the same trend. The glucose solubility is higher in BMIMCl than in EtOHMIMCl. The influence of a functional group grafted on the cation on the dissolution of the glucose is not neglected. Similar behavior was observed concerning the solubility of cellulose in ILs.[49] The presence of a hydroxyl end-group in the cation decreases the solubility of the glucose in the corresponding ILs, presumably by competing with glucose for hydrogen bond donation to the anion.

The compilation of our data on the solubility of fructose and sucrose in ionic liquids and the data published in the literature proved that the solubility of carbohydrates increases with an increase of the basicity and polarity of ILs and a decrease of the alkyl chain length, table II.4. The solubility of sucrose increases with increasing the hydrogen bond basicity and polarity of the anion of the ionic liquid in the following order: $C(CN)_3 < BF_4 < CF_3SO_3 < CH_3SO_3 < SCN < HSO_4 < Cl < CH_3HPO_3$.[29-31,37,47] Moreover, the solubility data of sucrose in dialkylimidazolium thiocyanate measured in this work and found in the literature[47] confirmed that the solubility of carbohydrates decreases with an increase of the alkyl chain length grafted in the cation.

At low temperature, the solubility of sucrose in BMIMCl measured in this work corrolates well to those published in the literature. Indeed, the solubility of sucrose at 343.15 K equals to 0.05 wt % is identical to the value found in the literature. Nevertheless, at 383.15 K, sucrose solubility is found to be two times bigger (0.413 wt %) than those published (0.18 wt %) by V. M. Egorov et al.[50] In our opinion, the published data is quite small while the solubility of sucrose in some moderate ionic liquids such as BMIMSCN and $BMIMHSO_4$ exceeds 0.25 wt %.[47] Moreover, Rogers et al. found that BMIMCl is capable of dissolving up to 0.25 wt% cellulose[24], a compound with structurally more complicated carbohydrate than sucrose.

Table II.2. Solid-Liquid equilibria (SLE) of the binary system (Sugar+IL), where X_2 is the sugar mass fraction, T_2 is the temperature (K), γ_2 is the activity coefficient calculated with NRTL equation

Glucose											
EMIMSCN			DMIMMPh			BMIMCl			EtOHMIMCl		
X_2	T_2 SLE/K	γ_2	X_2	T_2 SLE/K	γ_2	X_2	T_2 SLE/K	γ_2	X_2	T_2 SLE/K	γ_2
0.06	283.15	0.74	0.05	285.15	0.81	0.059	343.15	2.52	0.12	355.15	1.87
0.12	290.15	0.40	0.12	298.15	0.44	0.12	345.95	1.51	0.18	356.75	1.36
0.18	298.15	0.33	0.18	305.65	0.35	0.23	349.95	0.88	0.24	358.55	1.03
0.23	305.65	0.33	0.24	311.55	0.31	0.29	352.05	0.74	0.30	360.05	0.87
0.30	317.65	0.37	0.30	315.45	0.30	0.35	354.85	0.61	0.35	361.65	0.75
0.35	331.85	0.41	0.35	321.65	0.28	0.40	356.55	0.58	0.45	365.15	0.62
0.40	345.95	0.47	0.44	331.85	0.29	0.45	357.95	0.57	0.50	367.25	0.59
			0.53	346.45	0.30	0.50	360.45	0.55	0.55	369.35	0.57
			0.60	360.25	0.33				0.58	370.35	0.56
Fructose											
EMIMSCN			DMIMMPh			BMIMCl			EtOHMIMCl		
X_2	T_2 SLE/K	γ_2	X_2	T_2 SLE/K	γ_2	X_2	T_2 SLE/K	γ_2	X_2	T_2 SLE/K	γ_2
0.05	281.15	1.60	0.05	284.95	1.32	0.05	343.15	8.30	0.10	355.05	5.13
0.10	288.55	1.39	0.10	296.65	0.87	0.10	345.25	5.33	0.15	356.25	4.29
0.15	293.75	1.31	0.15	302.65	0.75	0.20	348.15	2.98	0.20	357.95	3.47
0.20	300.15	1.19	0.20	307.55	0.69	0.25	350.45	2.34	0.25	358.65	3.14
0.25	311.25	1.05	0.25	310.15	0.68	0.30	351.85	1.97	0.30	360.15	2.67
0.30	322.45	0.93	0.30	313.45	0.67	0.35	354.75	1.66	0.45	365.15	2.12
0.40	332.85	0.87	0.40	323.85	0.64	0.40	356.15	1.48	0.50	366.55	1.69
0.45	358.15	0.85	0.50	336.75	0.63	0.45	357.95	1.34	0.55	367.85	1.52
			0.60	344.15	0.69	0.50	359.25	1.25	0.6	369.15	1.38
Sucrose											
EMIMSCN			DMIMMPh			BMIMCl			EtOHMIMCl		
X_2	T_2 SLE/K	γ_2	X_2	T_2 SLE/K	γ_2	X_2	T_2 SLE/K	γ_2	X_2	T_2 SLE/K	γ_2
0.025	284.25	0.039	0.05	286.15	0.017	0.05	343.95	0.442	0.05	356.15	0.775
0.05	301.15	0.061	0.10	295.65	0.019	0.10	347.95	0.241	0.10	357.65	0.433
0.08	318.85	0.094	0.15	307.8	0.023	0.15	351.45	0.182	0.15	359.95	0.297
0.10	330.9	0.123	0.20	316.05	0.029	0.20	354.15	0.169	0.20	363.35	0.240
0.15	348.15	0.180	0.25	329.4	0.036	0.22	356.82	0.162	0.25	366.20	0.226
0.20	362.25	0.241	0.30	343.35	0.046	0.25	359.7	0.163	0.28	369.15	0.224
0.25	371.25	0.292	0.40	359.85	0.084	0.30	367.05	0.168	0.30	372.75	0.222
0.30	383.15	0.362	0.50	376.45	0.146	0.35	373.45	0.188	0.35	377.05	0.243
						0.40	380.3	0.219	0.40	384.15	0.271
Lactose											
EMIMSCN			DMIMMPh			BMIMCl			EtOHMIMCl		
X_2	T_2 SLE/K	γ_2	X_2	T_2 SLE/K	γ_2	X_2	T_2 SLE/K	γ_2	X_2	T_2 SLE/K	γ_2
0.025	288.05	0.0002	0.05	290.55	0.004	0.025	344.15	0.143	0.025	355.75	0.063
0.05	309.65	0.0007	0.10	299.25	0.003	0.05	351.95	0.088	0.05	360.5	0.042
0.08	326.75	0.0022	0.16	308.95	0.003	0.10	359.05	0.067	0.10	366.35	0.032
0.10	339.6	0.0056	0.23	319.05	0.004	0.15	366.85	0.059	0.15	372.55	0.029
0.125	362.25	0.0159	0.30	333.15	0.005	0.20	371.35	0.056	0.20	378.65	0.031
0.155	373.25	0.0320	0.32	338.85	0.006	0.28	381.55	0.058	0.25	384.15	0.039
0.18	382.55	0.0512	0.35	344.45	0.008						
			0.393	356.25	0.011						

Table II.3. Kamlet-Taft parameters of some ionic liquids and organic compounds, where α the hydrogen bond acidity, β is the hydrogen bond basicity and π* is the dipolarity[40-46]

ILs and organic compounds	α	β	π*
Water	1.17	0.47	1.09
Ethanol (EtOH)	0.86	0.75	0.51
Methanol (MeOH)	0.98	0.66	0.60
2-propanol	0.76	0.93	0.48
Acetonitrile	0.19	0.40	0.66
Dimethyl sulfoxide (DMSO)	0.00	0.76	1.00
1-butyl-1-methylpyrrolidinium bis(trifluoromethylsulfonyl)imide ($BMPyTf_2N$)	0.52	0.37	0.93
1-butyl-3-methylimidazolium tetrafluorophosphate ($BMIMPF_4$)	0.63	0.38	1.05
1-butyl-3-methylimidazolium tricyanomethanide ($BMIMC(CN)_3$)	0.51	0.54	0.94
1-butyl-3-methylimidazolium dicyanamide ($BMIMN(CN)_2$)	0.54	0.71	1.05
1-ethyl-3-methylimidazolium dicyanamide ($EMIM\ N(CN)_2$)	0.54	0.64	1.07
1-methanol-3-methylimidazolium dicyanamide ($HOMMIMN(CN)_2$)	0.80	0.51	1.11
1-butyl-3-methylimidazolium hydrogensulfate ($BMIMHSO_4$)	-	0.67	1.09
1-ethyl-3-methylimidazolium methylsulfate ($EMIMMSO_4$)	0.57	0.61	1.09
1-butyl-3-methylimidazolium methylsulfonate ($BMIMCH_3SO_3$)	0.44	0.77	1.02
1-ethyl-3-methylimidazolium ethylsulfate ($EMIMEtSO_4$)	n.a.	0.710	n.a.
1-butyl-3-methylimidazolium trifluoromethylsulfonate ($BMIMCF_3SO_3$)	0.50	0.57	0.90
1-butyl-3-methylimidazolium thiocyanate (BMIMSCN)	-	0.71	1.06
1-ethanol-3-methylimidazolium chloride (EtOHMIMCl)	0.73	0.68	1.16
1-butyl-3-methylimidazolium chloride (BMIMCl)	0.48	0.94	1.03
1-ethyl-3-methylimidazolium methyl phosphonate (EMIMMPh)	0.51	1.00	1.06

Table II.4. Solubility of carbohydrates in ILs in the literature[29-31, 37, 47]

Sucrose					
BMIMSCN		$BMIMHSO_4$		$BMIMC(CN)_3$	
S. (Wt%)	T/K	S. (Wt%)	T/K	S. (Wt%)	T/K
2.0	315.20	2.0	358.74	1.0	381.20
5.2	325.01	5.0	363.05	2.1	391.38
10.0	339.78	10.1	368.27	5.3	406.64
20.0	369.20	15.1	372.45	$BMIMCF_3SO_3$	
30.0	399.92	25.9	380.13	S. (g/l)	T/K
35.3	411.67	35.0	388.50	2.0	298.15
$BMIMBF_4$		$EMIMBF_4$		5.3	333.15
S. (g/l)	T/K	S. (g/l)	T/K	$EMIMCH_3SO_3$	
0.5	298.15	0.6	298.15	S. (g/l)	T/K
0.6	333.15	0.6	333.15	12.4	298.15
				80.0	348.15
Fructose					
$EMIMEtSO_4$		$BMIMCF_3SO_3$		$EMIMCF_3SO_3$	
S. (Wt%)	T/K	S. (g/l)	T/K	S. (g/l)	T/K
25.7	288.20	27.0	298.15	32.8	298.15
29.0	298.20	87.5	333.15	123.9	333.15
37.4	318.40				
Lactose					
$Bt_{14}CH_3SO_3$		$Bt_{14}N(CN)_2$		MOEOEMIMCl	
S. (Wt%)	T/K	S. (Wt%)	T/K	S. (Wt%)	T/K
8.0	348.15	8.0	348.15	10.69	308.15

Where, 1-butyl-3-methylimidazolium tetrafluroborate ($BMIMBF_4$), 1-ethyl-3-methylimidazolium tetrafluroborate ($EMIMBF_4$), 1-ethyl-3-methylimidazolium methylsulfonate ($EMIMCH_3SO_3$), 1-ethyl-3-methylimidazolium trifluoromethylsulfonate ($EMIMCF_3SO_3$), 1-butyl-3-methylbenzotriazonium methylsulfonate ($Bt_{14}CH_3SO_3$), 1-butyl-3-methylbenzotriazonium dicyanamide ($Bt_{14}N(CN)_2$), 1-(2-(2-methoxyethoxy)ethyl)-3-methylimidazolium chloride (MOEOEMIMCl).

II.3.2. Computational theory

In the present work, the NonRandom Two-Liquid equation (NRTL) proposed by Renon and Prausnitz[51] and the UNIversal QUAsi-Chemical (UNIQUAC) theory developed by Abrams and Prausnitz[52] were used for the correlation of the (solid + liquid) phase equilibrium at atmospheric pressure. The solubility of the carbohydrates in the ILs, was determined from an expression based on the symmetric convention for the calculation of the activity coefficients, i.e., the pure liquid at the solution temperature as a standard state for the carbohydrate, together with their

fusion enthalpy, $\Delta_{fus}H$ and melting temperature, T_{fus}, For a general case, this equation can be derived through an idealized thermodynamic cycle between the solid and liquid carbohydrate phase states, under this assumption: The solvent does not appear in the solid phase. Thus, the resulting expression to the calculation of the solubilities is: [53]

$$\ln(x_2\gamma_2) = \frac{-\Delta_{fus}H_2}{R} \cdot \left(\frac{1}{T^{SLE}} - \frac{1}{T_{fus,2}} \right) \tag{II.1}$$

where $\Delta_{fus}H_2$ and T_{fus2} denote melting enthalpy and temperature of the sugar, and x_2 stands for the solubility of the sugar at the saturated temperature T^{SLE}.

NRTL Model

For the NRTL model, the activity coefficient γ_i , for any component *i* of the ternary system is given by:

$$\ln \gamma_i = \frac{\sum_{j=1}^{m} \tau_{ji} G_{ji} x_j}{\sum_{l=1}^{m} G_{li} x_l} + \sum_{j=1}^{m} \frac{x_j G_{ij}}{\sum_{l=1}^{m} G_{lj} x_l} \left(\tau_{ij} - \frac{\sum_{r=1}^{m} x_r \tau_{rj} G_{rj}}{\sum_{l=1}^{m} G_{lj} x_l} \right) \tag{II.2}$$

with $G_{ji} = \exp(-\alpha_{ji}\tau_{ji})$, $\tau_{ji} = \frac{g_{ji} - g_{ii}}{RT} = \frac{\Delta g_{ji}}{RT}$ and $\alpha_{ji} = \alpha_{ij} = \alpha$

where *g* is an energy parameter characterizing the interaction of species *i* and *j*, x_i is the mole fraction of component *i*, α the nonrandomness parameter. Although α can be treated as an adjustable parameter, in this study α was set equal to 0.2 according to the literature.[54]

UNIQUAC Model

For the UNIQUAC model, the activity coefficient γ_i , for any component *i* of the binary system is given by:

$$\ln \gamma_i = \ln \frac{\Phi_i}{x_i} + \frac{z}{2} q_i \ln \frac{\theta_i}{\Phi_i} + l_i - \frac{\Phi_i}{x_i} \sum_{j=1}^{m} x_j l_j - q_i \ln(\theta_j \tau_{ji}) + q_i - q_i \sum_{j=1}^{m} \frac{\theta_j \tau_{ji}}{\sum_{k=1}^{m} \theta_k \tau_{kj}} \tag{II.3}$$

Where $\Phi_i = \frac{r_i x_i}{\sum_{j=1}^{m} r_j x_j}$, $\theta_i = \frac{q_i x_i}{\sum_{j=1}^{m} q_j x_j}$, $l_j = \frac{z}{2}(r_j - q_j) - (r_j - 1)$ and $\tau_{ji} = \exp\left(\frac{-\Delta u_{ij}}{RT}\right)$

Here, the lattice coordination number z is assumed to be equal to 10. Parameters r_i and q_i are respectively relative to molecular van der Waals volumes and molecular surface areas of the pure component i. The binary parameters for sugars were taken from the literature.[31] The required van der Waals parameters r_i and q_i of the UNIQUAC model for the ionic liquids were estimated with the correlation proposed by Domanska.[55]

$$r_i = 0.029281 \times V_i\left(cm^3.mol^{-1}\right)$$
$$q_i = \frac{(z-2)\times r_i}{z} + \frac{2}{z} \qquad \text{(II.4)}$$

where V_i is the molar volume of the ionic liquid at T = 298.15 K and z is the coordination number assumed to be equal to 10. Parameters of all pure components are given in table II.5.

To obtain a better description of the (solid + liquid) phase equilibrium simultaneously, temperature dependent model parameters (Δg_{ij} or Δu_{ij}) were assumed:

$$\Delta g_{12}\left(J.mol^{-1}\right) = g_{12} - g_{11} = a_{12} + b_{12} \cdot T(K)$$
$$\Delta g_{21}\left(J.mol^{-1}\right) = g_{21} - g_{22} = a_{21} + b_{21} \cdot T(K) \qquad \text{(II.5)}$$

A total of four adjustable parameters per binary Δg_{ji} or Δu_{ji} have to be set for each model. The model adjustable parameters of both models were found by minimization of the following objective function (OF):

$$OF = \sum_{i=1}^{n} \left(T_{\exp,i} - T_{calc,i}\right)^2 \qquad \text{(II.6)}$$

The root-mean-square deviation (RMSD) of temperature, σ_T, was calculated according to the following definition:

$$\sigma_T = \left(\sum_{i=1}^{n} \frac{\left(T_{\exp,i} - T_{calc,i}\right)^2}{n-2} \right)^{1/2} \qquad \text{(II.7)}$$

The NRTL and UNIQUAC parameters obtained after the regression of the experimental data are listed in table II.6. As can be seen in the results depicted in figure II.1, Both thermodynamic models correlate well with the experimental data.

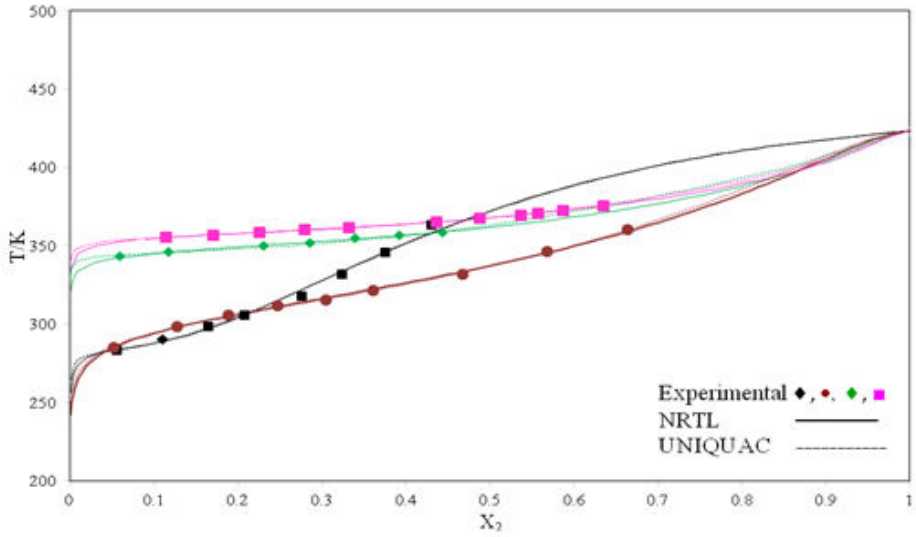

(a) Glucose

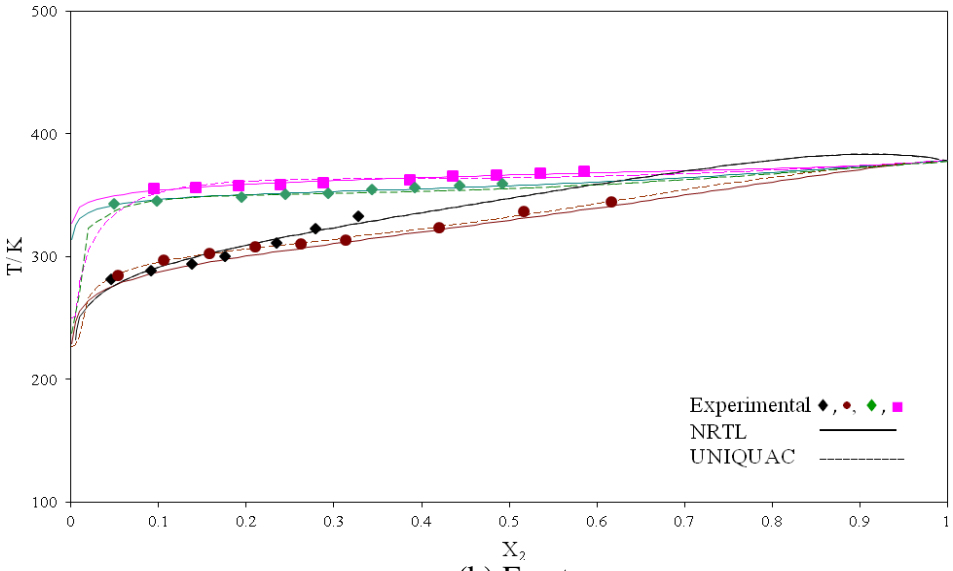

(b) Fructose

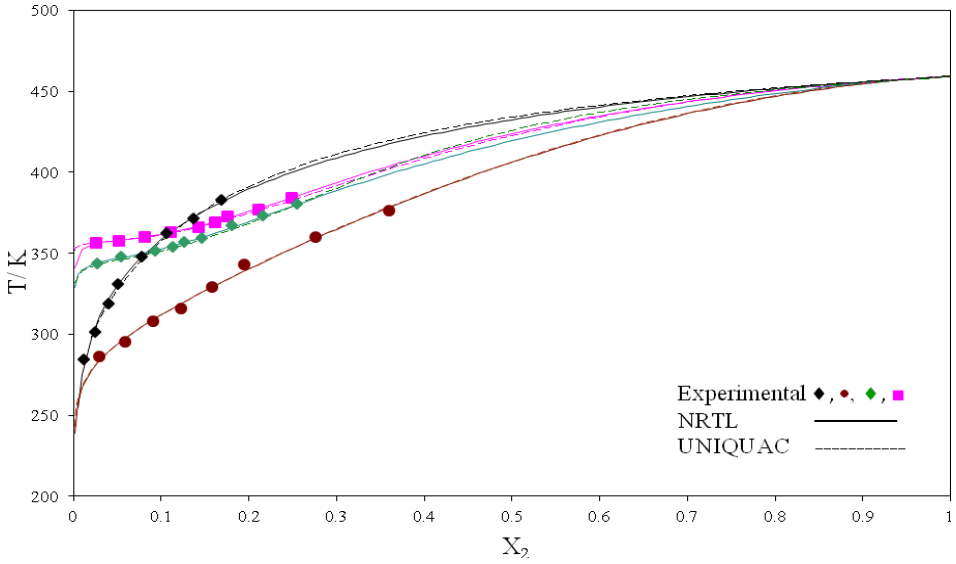

(c) Sucrose

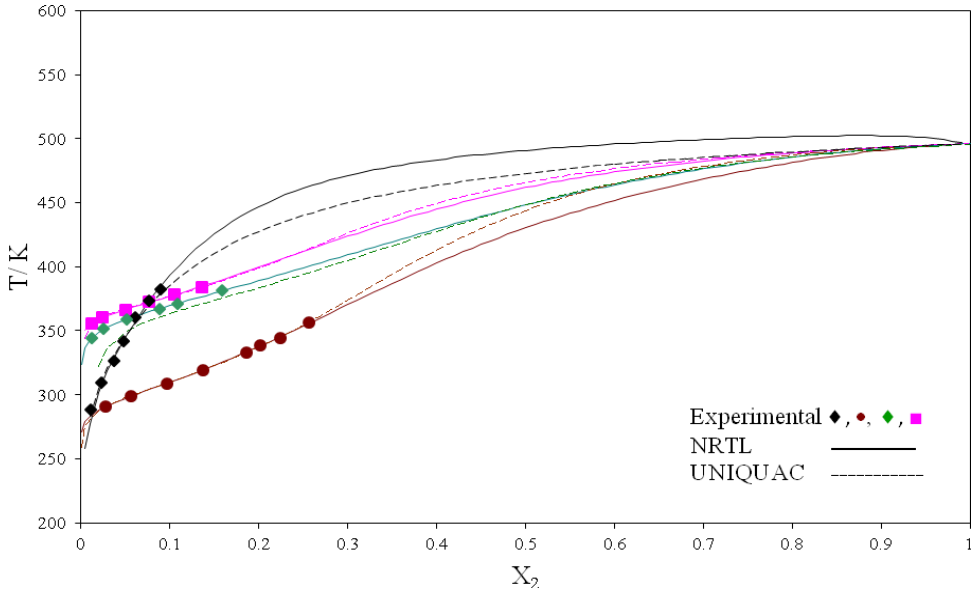

(d) Lactose

Figure II.1. Plot of the experimental and calculated SLE of {IL + sugar} binary systems: ♦ EMIMSCN; • DMIMMPh; ♦ BMIMCl; ■ EtOHMIMCl. The solid lines have been calculated using NRTL and UNIQUAC models with (a) Glucose, (b) Fructose, (c) Sucrose and (d) Lactose, where X_2 is the sugar mole fraction.

Table II.5. Van der waals volume and surface parameters for UNIQUAC model.

ILs/ Sugar	r_i	q_i
BMIMCl	4.709	3.967
EtOHMIMCl	4.487	3.790
DMIMMPh	6.017	4.756
EMIMSCN	4.437	3.75
Glucose	5.8	4.84
Fructose	5.8	4.92
Sucrose	14.5496	13.764
Lactose	12.5265	12.228

Table II.6. Correlation of the solid-liquid equilibria data by means of the NRTL and UNIQUAC equations, σ_T the temperature deviation

	Glucose				
Solvent	NRTL parameters				rmsd
Ionic liquid	a_{12}/(J.mol^{-1})	a_{21}/(J.mol^{-1})	b_{12}/(J.mol^{-1} .K^{-1})	b_{21}/(J.mol^{-1}.K^{-1})	σ_T
BMIMCl	110290.7	76188.6	-316.3	-218.5	0.51
DMIMMPh	34164.2	8957.3	-126.6	-25.9	1.04
EMIMSCN	33568.6	6678.3	-64	-49.5	2.84
EtOHMIMCl	147202	90547.2	-409.2	-253.3	0.12
Solvent	UNIQUAC parameters				rmsd
Ionic liquid	a_{12}/(J.mol^{-1})	a_{21}/(J.mol^{-1})	b_{12}/(J.mol^{-1} .K^{-1})	b_{21}/(J.mol^{-1}.K^{-1})	σ_T
BMIMCl	45000.0	19999.9	-122.6	-62.4	1.00
DMIMMPh	7434.9	3355.3	-29.4	-8.0	0.83
EMIMSCN	7434.9	3354.9	-9.1	-20.6	0.74
EtOHMIMCl	45000.0	20000.0	-124.4	-56.8	0.34
	Fructose				
Solvent	NRTL parameters				rmsd
Ionic liquid	a_{12}/(J.mol^{-1})	a_{21}/(J.mol^{-1})	b_{12}/(J.mol^{-1} .K^{-1})	b_{21}/(J.mol^{-1}.K^{-1})	σ_T
BMIMCl	89998.38	9998.16	-241.59	-1226.26	1.65
DMIMMPh	28596.29	524.41	-96.48	-3.09	2.54
EMIMSCN	100001.28	5002.78	151.19	856.42	6.08
EtOHMIMCl	147201.97	90547.33	-415.29	-206.45	1.17
Solvent	UNIQUAC parameters				rmsd
Ionic liquid	a_{12}/(J.mol^{-1})	a_{21}/(J.mol^{-1})	b_{12}/(J.mol^{-1} .K^{-1})	b_{21}/(J.mol^{-1}.K^{-1})	σ_T
BMIMCl	-4296.64	13303.32	17.67	-39.54	2.64
DMIMMPh	-4296.65	13303.31	13.67	-43.35	1.43
EMIMSCN	4009.51	10979.11	-21.81	111.23	5.39
EtOHMIMCl	9.98	9.97	3.17	0.83	3.40
	Sucrose				
Solvent	NRTL parameters				rmsd
Ionic liquid	a_{12}/(J.mol^{-1})	a_{21}/(J.mol^{-1})	b_{12}/(J.mol^{-1} .K^{-1})	b_{21}/(J.mol^{-1}.K^{-1})	σ_T
BMIMCl	93902.37	10365.21	-215.09	-59.64	0.65
DMIMMPh	-1993.92	5922.61	-9.37	-34.90	2.84
EMIMSCN	-18249.49	16869.27	36.39	4925.43	2.34
EtOHMIMCl	93902.41	10364.49	-202.85	-57.62	0.62
Solvent	UNIQUAC parameters				rmsd
Ionic liquid	a_{12}/(J.mol^{-1})	a_{21}/(J.mol^{-1})	b_{12}/(J.mol^{-1} .K^{-1})	b_{21}/(J.mol^{-1}.K^{-1})	σ_T
BMIMCl	-19791.44	17061.38	66.95	-55.81	0.89
DMIMMPh	912.18	322.39	-10.56	5.07	2.76
EMIMSCN	0.86	0.82	4.76	-4.79	2.25
EtOHMIMCl	18108.31	11535.19	-41.56	-38.23	0.99
	Lactose				
Solvent	NRTL parameters				rmsd
Ionic liquid	a_{12}/(J.mol^{-1})	a_{21}/(J.mol^{-1})	b_{12}/(J.mol^{-1} .K^{-1})	b_{21}/(J.mol^{-1}.K^{-1})	σ_T
BMIMCl	16672.21	30671.24	-44.28	-103.84	0.60
DMIMMPh	18055.20	26076.84	-59.27	-117.40	0.58
EMIMSCN	-58208.87	-32291.41	118.89	212.59	3.59
EtOHMIMCl	21787.11	21399.52	-10.25	-93.37	0.48
Solvent	UNIQUAC parameters				rmsd
Ionic liquid	a_{12}/(J.mol^{-1})	a_{21}/(J.mol^{-1})	b_{12}/(J.mol^{-1} .K^{-1})	b_{21}/(J.mol^{-1}.K^{-1})	σ_T
BMIMCl	-1550.39	14159.91	-0.63	-36.09	0.54
DMIMMPh	-3377.67	12309.61	4.55	-39.55	0.61
EMIMSCN	0.00	0.00	6.71	-6.71	3.78
EtOHMIMCl	-19451.16	30000.08	52.87	-83.45	0.92

II.3.3. Solubility of carbohydrates in a binary mixture of (IL + EtOH)

The dissolution of glucose, fructose, sucrose and lactose monohydrate in binary mixtures {ionic liquid + ethanol as an antisolvent} was evaluated in five ionic liquids: 1-butyl-3-methylimidazolium chloride (BMIMCl), 1-ethanol-3-methylimidazolium chloride (EtOHMIMCl), 1,3-dimethyl-imidazolium methyl phosphonate (DMIMMPh), 1-ethyl-3-methylimidazolium thiocyanate (EMIMSCN) and 1-butyl-1-methylpyrrolidinium chloride (BMPyrCl).

II.3.3.1. Effect of the structure of the ionic liquid

Figures II.2 - II.6 indicate that the solubility of sugars in a binary mixture of (IL+ EtOH) increases in the following order, BMPyrCl < EMIMSCN < BMIMCl < EtOHMIMCl < DMIMMPh, (except for the solubility of fructose and sucrose in BMIMCl which is higher than its solubility in EtOHMIMCl at high temperature). Compared with other ionic liquids, the methyl phosphonate based ionic liquids have high dissolving power to carbohydrates due to their strong hydrogen bond basicity. The solubility of sugars in chloride based ionic liquids increases in the following order BMPyrCl < BMIMCl < EtOHMIMCl. The ionic liquids with a shorter chain cation have a larger dissolving power than those with long chain cations when their anions are identical.[28-30] Moreover, imidazolium based ionic liquids have stronger hydrogen bond basicity than pyrollidinium based ionic liquids.[33] The solubility of carbohydrates in ionic liquids decreases with an increase of the alkyl chain grafted on the cation. The solubility of sugars in a binary mixture of {IL + ethanol} follows the same trend as the solubility of sugars in pure ionic liquids with the exception of BMIMCl. The presence of ethanol in a mixture of {IL + sugar} decreases the solubility of sugars. For example, the solubility of fructose in a mixture of {DMIMMPh + ethanol} at 333.15 K is 80 g/l while its solubility in pure DMIMMPh is 650 g/l (0.50 mass fractions) at 331.5 K. In conclusion, ethanol has high efficiency when used as an antisolvent for extraction of sugars from different kinds of ionic liquids.

II.3.3.2. Effect of the structure of the carbohydrate

Figure II.2 shows the solubility of glucose, fructose, sucrose and lactose monohydrate in a binary mixture of (BMIMCl+EtOH) at a mixture ratio by weight =10, time =300 min, neglected water content and at different temperatures. It is obvious that the solubility increases in the following order lactose < sucrose < glucose < fructose. This behavior corrolates well with the

work of Hyvonen and P. Koivistoinen[56] who showed that fructose is more soluble than other sugars and hard to crystallize because it is more hygroscopic and holds onto polar solvents stronger than the others. Also maybe because fructose has lower melting point compared to other studied sugars. On the other hand, the solubility of di-saccharides, sucrose and lactose, exhibits a noticeably lower solubility than mono-saccharides, glucose and fructose. This behavior also correlates well with the work of J. A. Conceiçao et al.[47]who showed that sucrose has lower solubility than glucose because sucrose, as a di-saccharide, consists of two hexoses, glucose and fructose. Another reason is that di-saccharides have higher molecular weight and melting point than mono-saccharides. Table II.7 shows that fructose has higher solubility in pure ethanol if compared to the other sugars. This led to lower extraction performance of fructose from ionic liquids using ethanol as an antisolvent if compared with the other sugars.

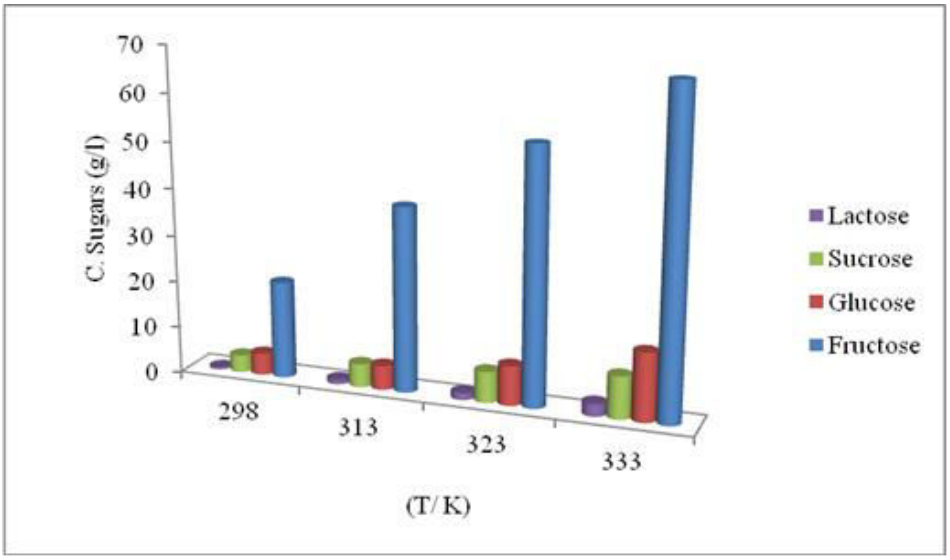

Figure II.2. The solubility of carbohydrates in a binary mixture of (BMIMCl+EtOH) at a mixture ratio by weight =10, time =300 min, neglected water content and at different temperatures

Table II.7. Solubility of sugars in water and ethanol

Solvent	T /K	Solubility (g/l)			
		Glucose	Fructose	Sucrose	Lactose
	293.15	900	3750	2000	
	298.15	1100		2074.1	233.12
	313.15			2345	235.97
Water	333.15			2885.7	592.73
	293.15	1.29	11.597	0.414	0.02
	298.15	1.31	18.20	0.599	0.11
	313.15		23.897	0.761	0.19
Ethanol	333.15		30.547	0.987	0.27

II.3.3.3. Effect of ethanol/ ionic liquid ratio

Figure II.3 presents the effect of (ethanol/ ionic liquid) ratio by weight on the solubility of the studied sugars in the binary mixture. It is shown that the solubility of the sugars increases with decreasing (ethanol/ ionic liquid) ratio for the studied ionic liquids. For example, the solubility of sucrose increases from 1.474 g/l to 6.716 g/l with decreasing the ethanol/ ionic liquid ratio by weight from 20 to 5 in a binary mixture of (BMIMCl + ethanol). The behavior can be explained using the solvatochromic parameters of binary mixtures (cosolvent + IL). Indeed, Yang et al [57] have shown that the π* values of (cosolvent + BMIMCl) mixtures increase with the concentration of BMIMCl, indicating the important role of an additional cosolvent on reducing the dipolarity/polarizability. Consequently, it is expected that these (cosolvent + BMIMCl) mixtures can have reduced affinity with polar compounds than pure IL. Moreover, the hydrogen-bond basicity values of mixtures are also lower than in pure IL. As discussed previously, a decreasing of these both solvatochromic parameters may lead to a decreasing of the solubility of sugars in solvents. This indicates the high efficiency of ethanol as an antisolvent. A high ethanol/ ionic liquid ratio is recommended for the satisfactory extraction of carbohydrates from their mixtures.

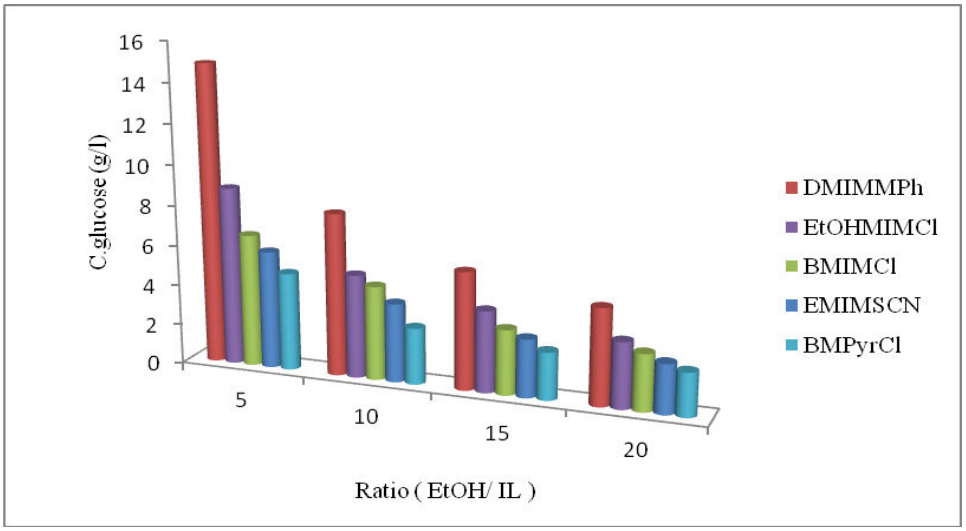

(a)

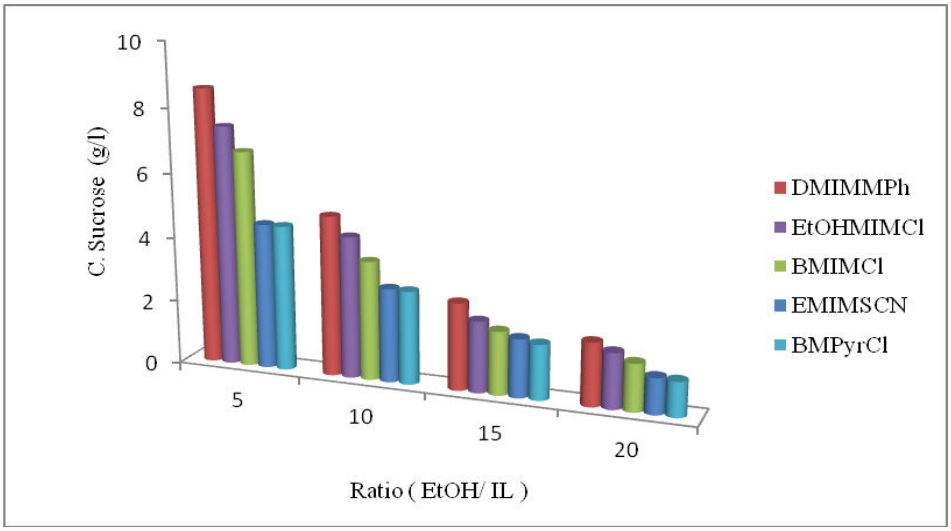

(b)

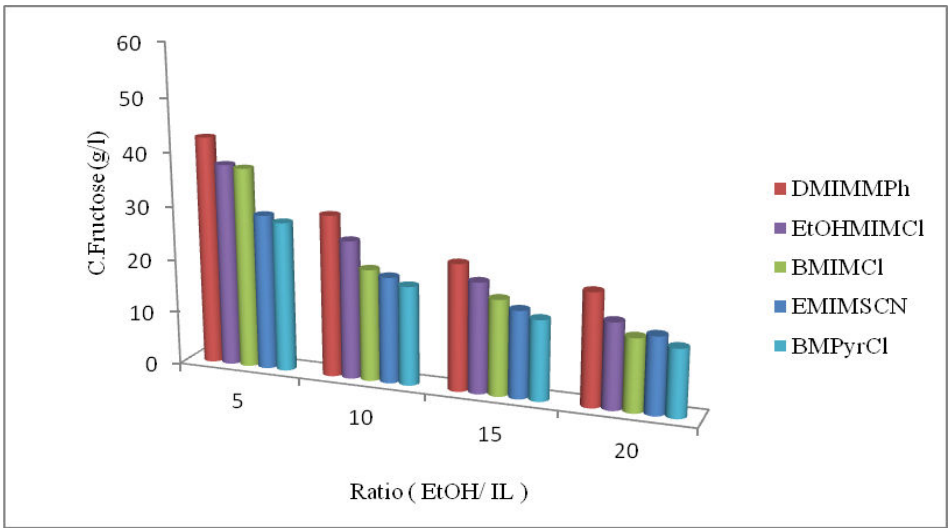

(c)

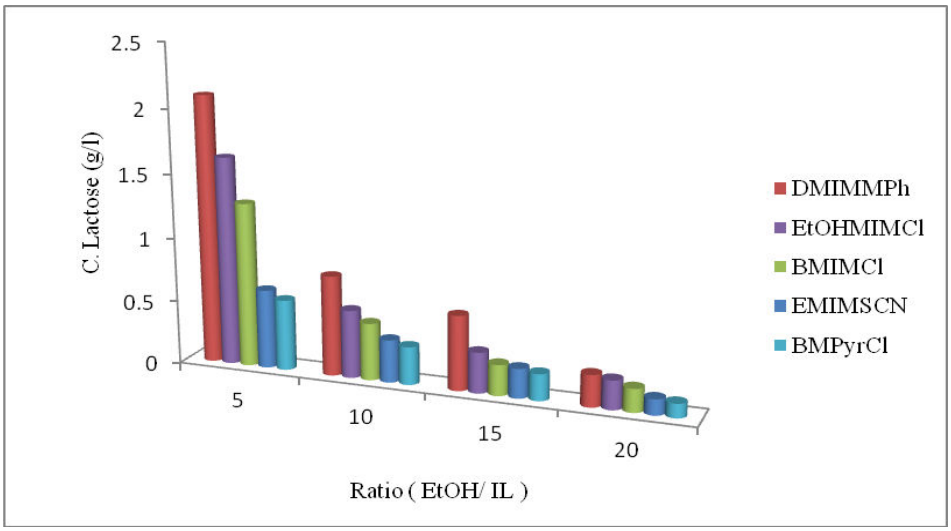

(d)

Figure II.3. The effect of EtOH / IL ratio by weight on the solubility of (a) glucose, (b) sucrose, (c) fructose and (d) lactose in the mixture at temperature = 298 K, time = 300 min and neglected water content

II.3.3.4. Effect of temperature

The effect of temperature on the solubility of the studied sugars in a mixture of {IL + ethanol} is illustrated in figure II.4. The solubility of carbohydrates is directly proportional to the temperature for the used ionic liquids mixtures. For example, the solubility of lactose increases from 0.446 g/l to 2.71 g/l with increasing temperature from 298 K to 333 K in a binary mixture of {BMIMCl + ethanol}. In fact, the raising of temperature increases the molecular thermal motion of the entire system and the volatility of a non volatile solute[38] resulting in an enhancement of the solubility of sugars in {IL + ethanol} mixtures. Therefore, a low temperature is recommended for the satisfactory extraction of carbohydrates from their mixtures.

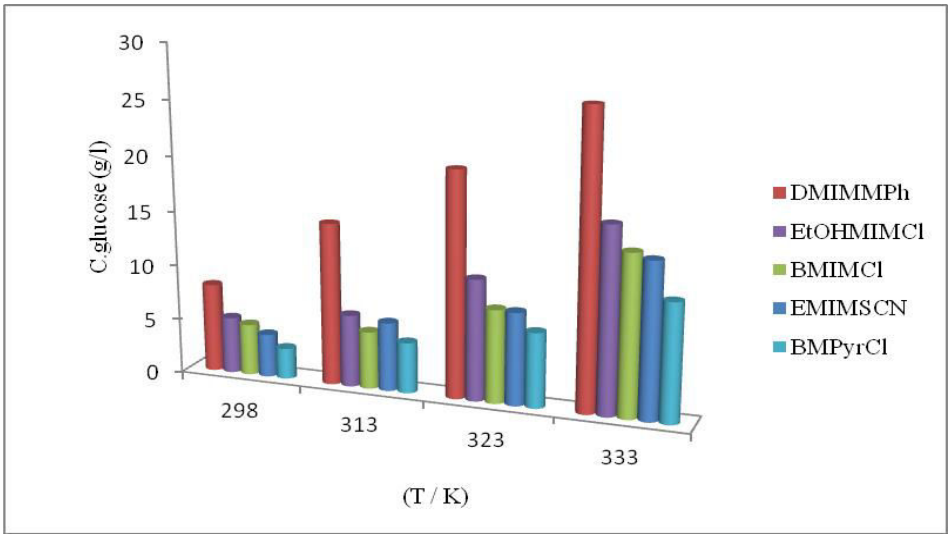

(a)

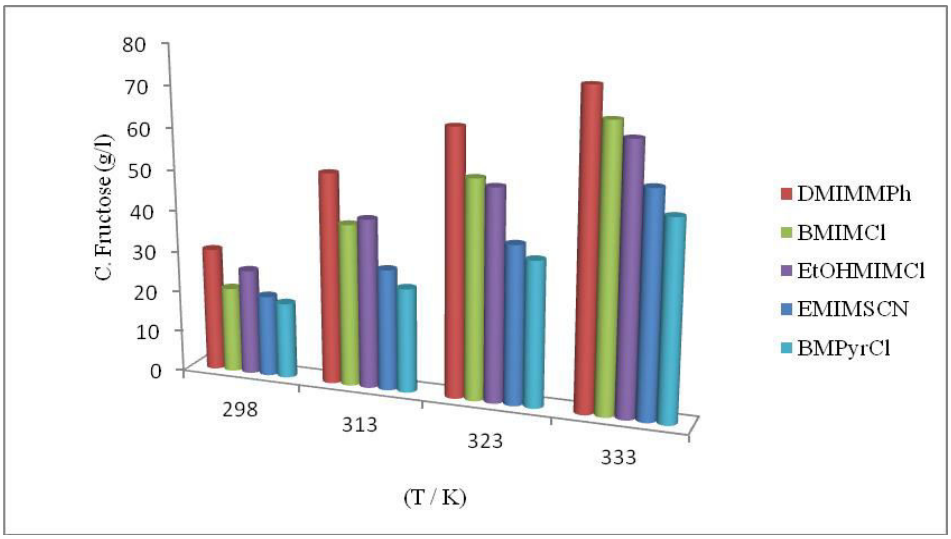

(b)

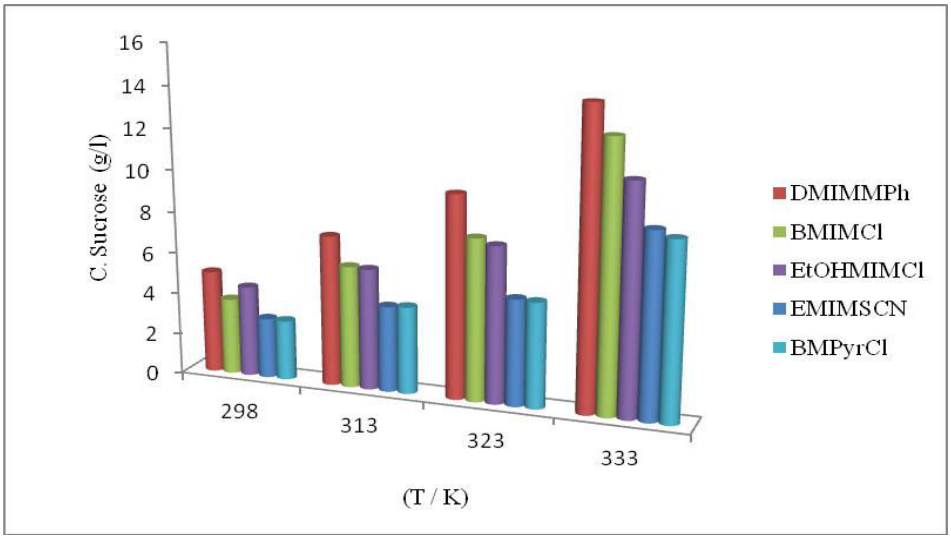

(c)

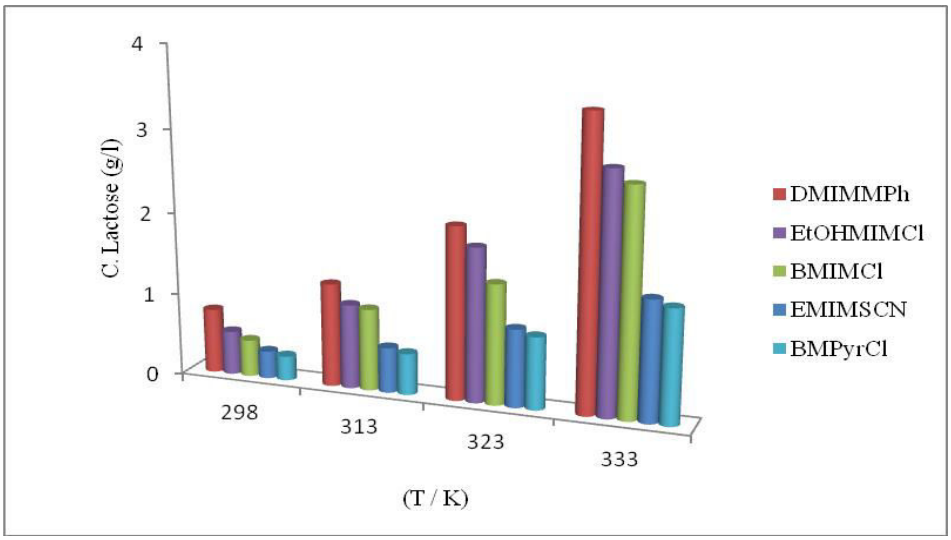

(d)

Figure II.4. The effect of temperature (K) on the solubility of (a) glucose, (b) fructose, (c) sucrose and (d) lactose in the mixture at EtOH/IL ratio by weight =10, time =300 min and neglected water content

II.3.3.5. Effect of water content

Figure II.5 shows the effect of water content on the solubility of the studied sugars in the mixtures of (IL + ethanol). It is known that water has a strong impact on the solubility of carbohydrates in ionic liquids as it significantly modifies the solvation ability of ionic liquids.[29] At 298 K, the solubility of glucose, fructose, sucrose and lactose in water reaches 1100, 3750, 2000 and 230 g/l respectively, so it would greatly affect the solubility of sugars in mixtures, table II.7. The solubility of sugars, especially fructose, sucrose and glucose, increases with

increasing the water content for the studied ionic liquids. For example, the solubility of fructose increases from 20.803 g/l to 48.942 g/l with increasing water content from 0% to 4% in a binary mixture of {BMIMCl + ethanol}. Therefore, negligible water content is recommended for the satisfactory extraction of sugars from their mixtures. This observation corresponds well to results obtained by dynamic simulations. Indeed, dynamic simulations showed that the water molecules initially located around the glucose molecules are rapidly uptaken by anions of the IL and most of the water shell around the glucose is replaced by anions. Calculations show that water acts as a solubility enhancer which disrupts glucose-glucose interaction and enhances glucose-solvent interaction (water+ IL) resulting in higher glucose solubility.

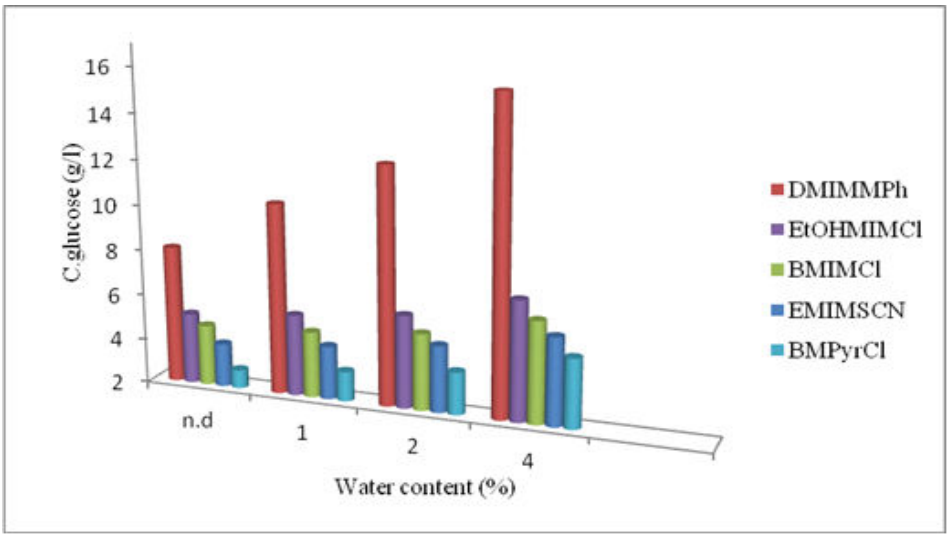

(a)

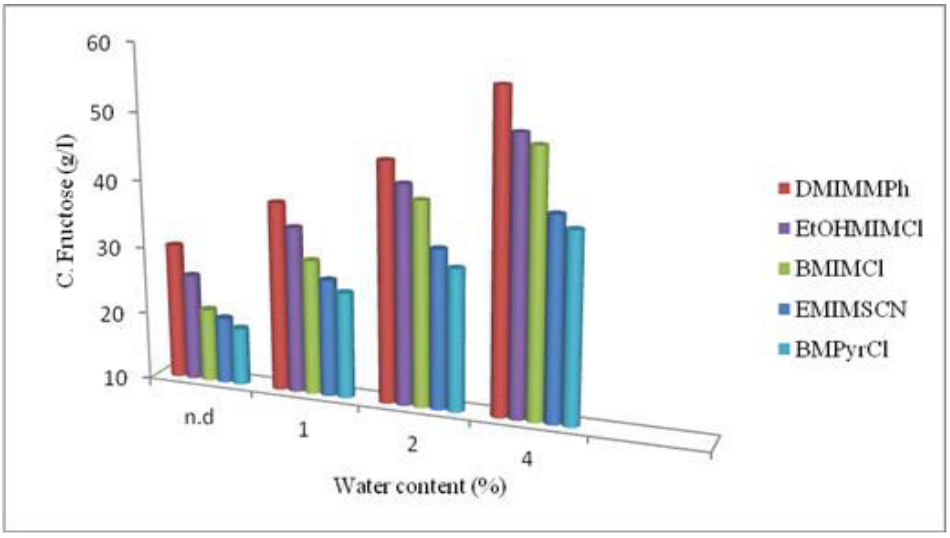

(b)

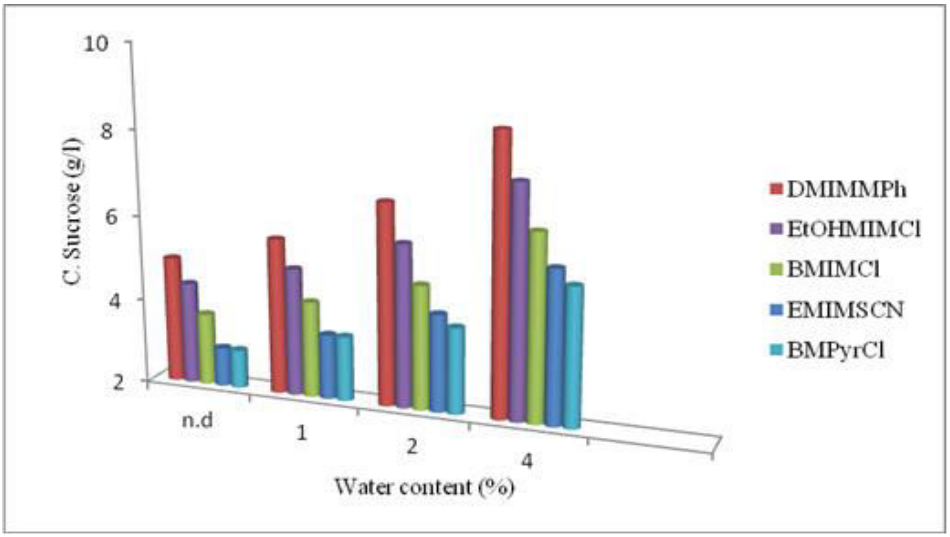

(c)

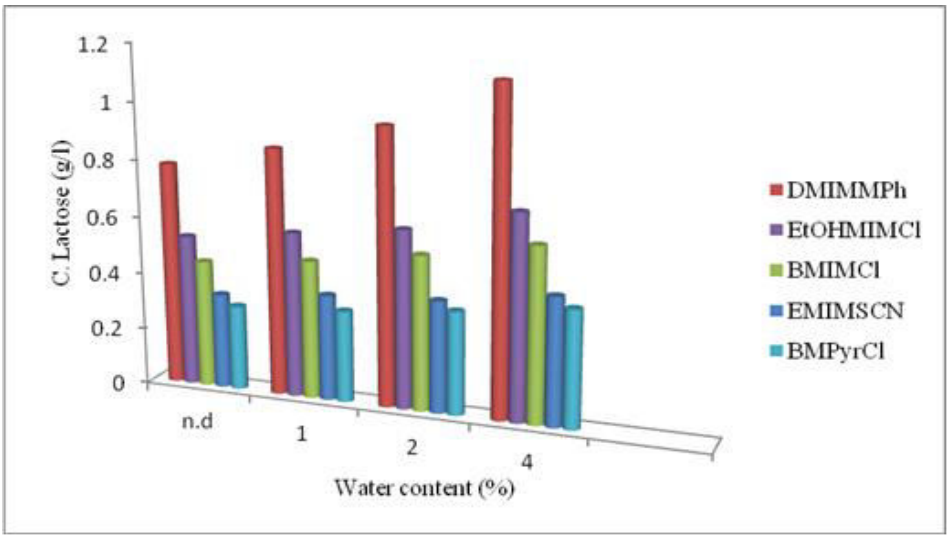

(d)

Figure II.5. The effect of water content (%) on the solubility of (a) glucose, (b) fructose, (c) sucrose and (d) lactose in the mixture at EtOH/IL ratio by weight =10, time =300 min and temperature =298 K

II.3.3.6. The dissolution rate of sugars solubility

Figure II.6 shows the dissolution rate of the solubility of the sudied sugars in the binary mixtures (BMIMCl + ethanol) at different temperatures. Most of the sugar dissolution occurs during the first 5 minutes in the binary mixtures. For example, the solubility of glucose at temperature 298 K increases rapidly from 0 to 3.89 g/l during the first five minutes and then increases slowly up to 4.664 g/l. During the first minutes, the dissolution rate of glucose in (BMIMCl + ethanol) is 0.8 g/l/min at 298 K, but after ten minutes the dissolution rate decreases greatly to be 0.002 g/l/min. As expected, the dissolution rate depends on the temperature of the system. It

increases from 0.8 to 2.32 g/l/min when the temperature increases from 298 K to 333 K. After ten minutes, the values of the dissolution rate are 0.002 and 0.018 g/l/min at 298 and 333K respectively. Thus, the equilibration time is prolonged when the temperature increases. In cases of glucose, sucrose and lactose, the mixture reaches the equilibrium at 200 minutes.

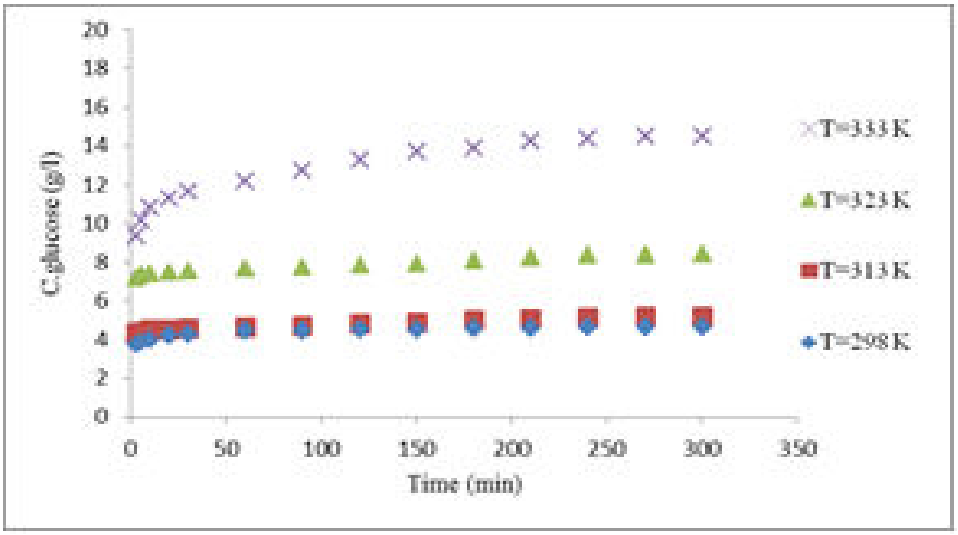

(a)

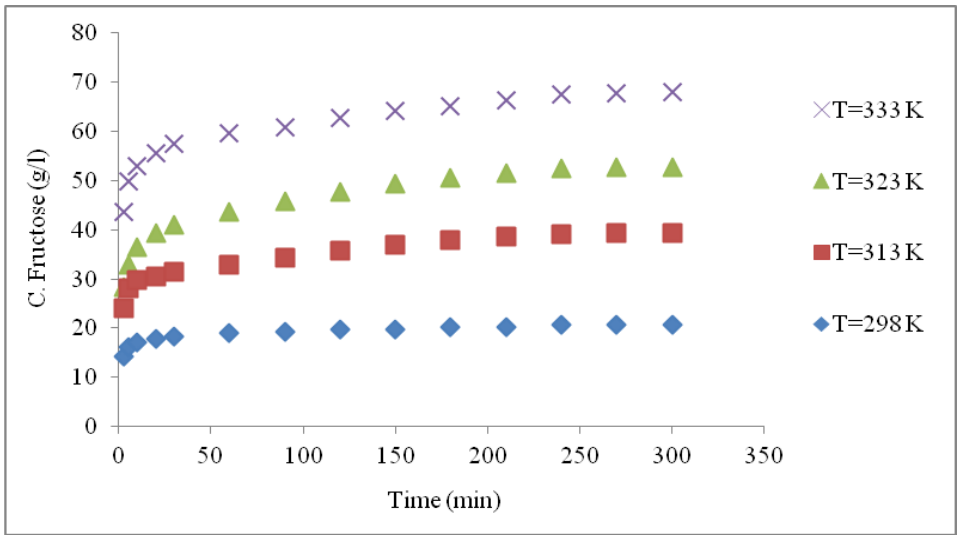

(b)

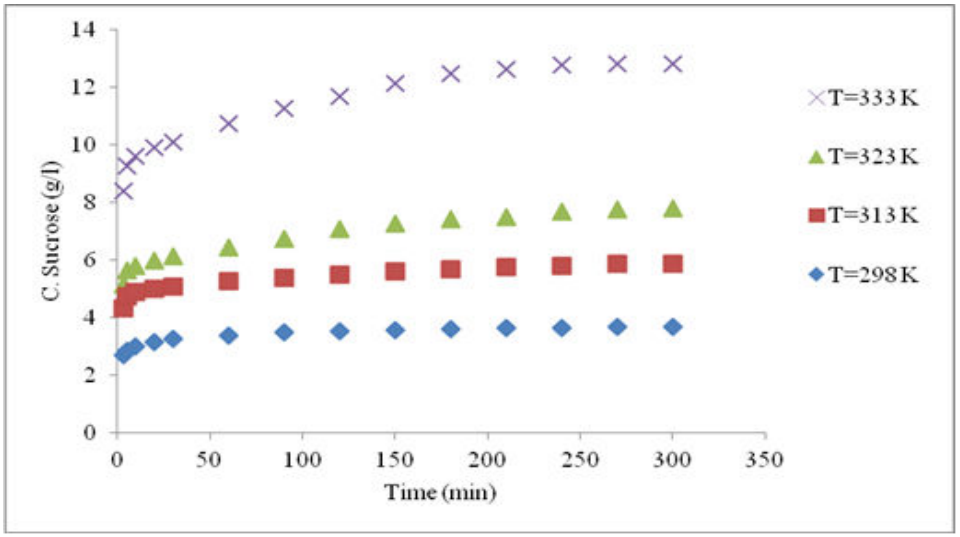

(c)

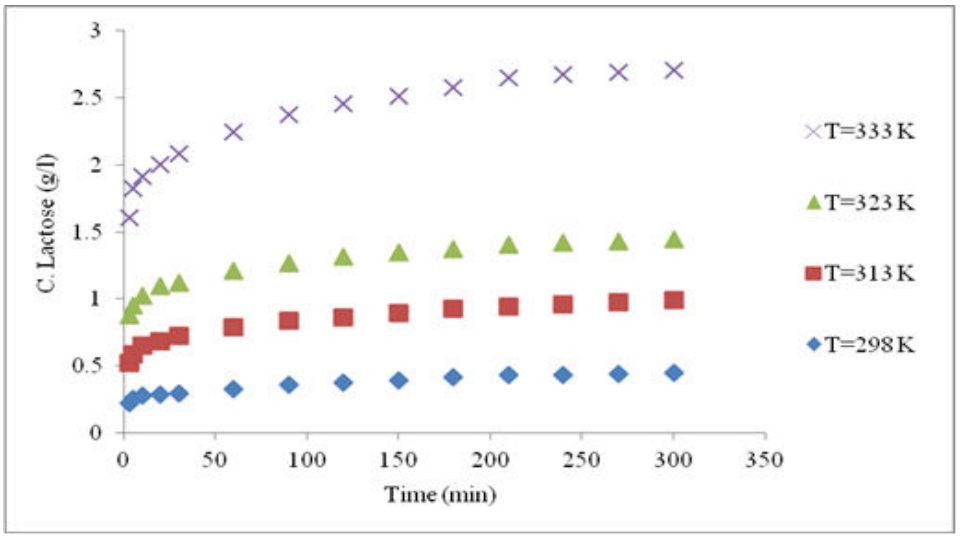

(d)

Figure II.6. Dissolution rate of (a) glucose, (b) fructose, (c) sucrose and (d) lactose in a mixture of (BMIMCl + EtOH) at EtOH/IL ratio by weight =10, neglected water content and temperature = ♦ 298, ■ 313, ▲ 323, and × 333 K

II.3.3.7. Applying 2^3Full-Factorial Design

An experimental design technique, 2^3Full-Factorial Design, is used to optimize the glucose solubility results and to evaluate the interaction between different parameters. The behavior of glucose in binary mixtures (ILs+ EtOH) is quite similar. Therefore, only the case of the glucose solubility in a binary mixture of (BMIMCl + EtOH) is presented in this section. Such an experiment allows studying the effect of each factor temperature, EtOH/ IL ratio and water content as well as the effects of interactions between factors on the glucose solubility. The analysis of variance (ANOVA) data for the system indicates the well fitting of the experimental

results to the factorial model equation and hence accuracy of this model, tables II.8 and II.9. The interaction between the different factors and their effect on the solubility of glucose in this system are shown in figures II.7 and II.8. It is obvious that no important interaction between the different factors is observed. The glucose solubility increases with increasing both temperature and water content and with decreasing the EtOH/ IL ratio. It is also clear that the main effective parameter on the glucose solubility is the temperature.

Table II.8. Estimated effects and coefficients for glucose solubility in (BMIMCl + EtOH) mixture, where T is the temperature (K), R is the (EtOH/ IL) ratio and W is the water content (%).

Term	Effect	Coef.
Constant		12.236
T	12.521	6.261
R	-7.274	-3.637
W	3.570	1.785
T*R	-3.093	-1.547
T*W	1.041	0.520
R*W	-0.721	-0.361
T*R*W	-0.328	-0.164

Table II.9. Analysis of Variance for glucose solubility in the binary mixture of (BMIMCl + EtOH).

Source	D.F.	Seq. SS	Adj. SS	Adj. MS
Main effects	3	444.872	444.872	148.291
2-way interactions	3	22.343	22.343	7.448
3-way interactions	1	0.215	0.215	0.215
Residual error	0	-	-	-
Total	7	467.430		

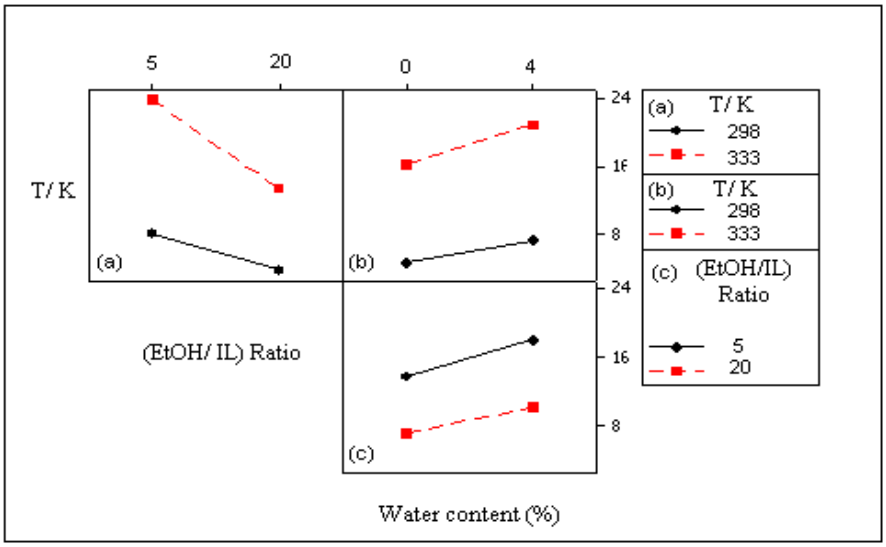

Figure II.7. The interaction between different variables on the solubility of glucose in a binary mixture of (BMIMCl + EtOH) at time 300 min.: a) at water content =2%, b) at EtOH/IL ratio by weight =12.5, c) at temperature =315.5 K.

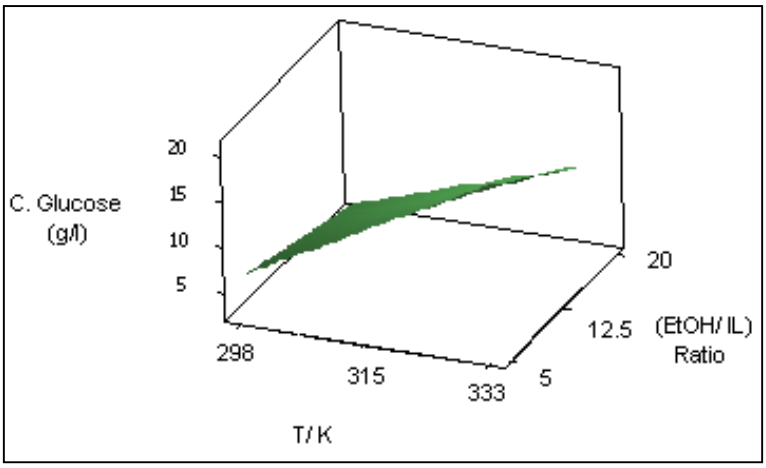

(a)

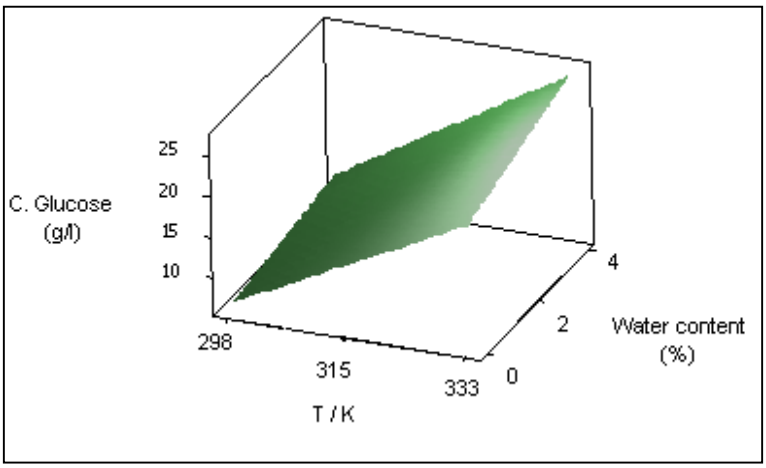

(b)

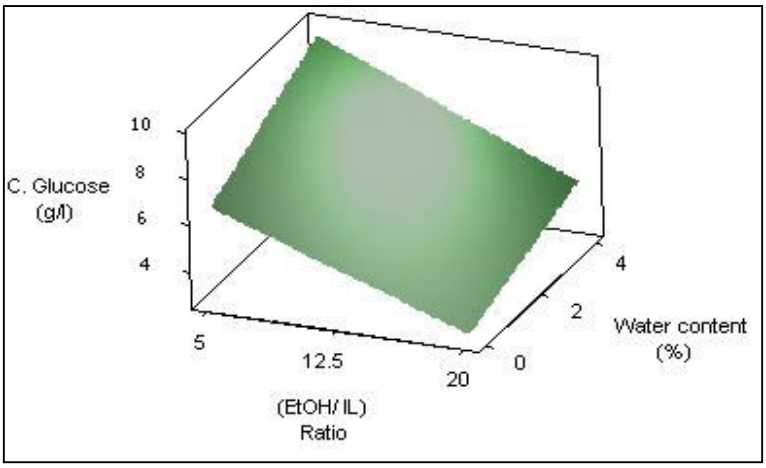

(c)

Figure II.8. Response surface plots of glucose concentration resulting from the main effects of (a) temperature and (EtOH/IL) ratio at fixed water content (W= 0 %), (b) temperature and water content at fixed (EtOH/IL) ratio (R= 5), (c) (EtOH/IL) ratio and water content at fixed temperature (T= 298K).

II.3.4. Extraction process using the antisolvent method

From the study of the dissolution of sugars in binary mixtures (ionic liquid + ethanol as an antisolvent), it is possible to evaluate the extraction percentage of sugars from ionic liquids. Table II.10 represents the extraction of glucose, fructose, sucrose and lactose from five ionic liquids using the antisolvent method described in the previous paragraph. In this study, the extraction is performed with the following characteristics: an {ethanol/ ionic liquid} ratio equal to 10, neglected water content, and a decrease of temperature from 313 K (or 323 or 333) to 298 K. Results indicate that the extracted percentage increases in the following order fructose < sucrose < glucose < lactose. This percentage increases with the increase of the temperature difference. For lactose, in the binary mixture (BMIMCl + ethanol), the extraction percentage is equal to 54.90 % when the temperature decreases from 313 K to 298 K, 69.18 % when the temperature decreases from 323 K to 298 K and 83.54 % if the temperature decreases from 333 K to 298 K.

The results of the extraction of sugars from IL using the anti solvent method with different anti-solvents are shown in table II.11. For these extractions, a solution containing 0.20 wt% of sugar was prepared in BMIMCl at 373 K. After the complete dissolution of sugar, an anti-solvent is added at 298 K. Due to the high extraction performance of ethanol, ionic liquids could be easily regenerated and reused in the process. This approach could be used in the industry. Nevertheless, extended work on the effect of different parameters on the extraction performance should be taken into consideration for the industrial feasibility.

Table II.10. The extraction % of the sugars from binary mixtures of the five ionic liquids at R= 10 and neglected water content.

Glucose					
Binary mixture of ethanol + IL	EMIMSCN	DMIMMPh	BMIMCl	EtOHMIMCl	BMPyrCl
Ex. % (from 313 K to 298 K)	37.15	45.13	21.91	21.76	39.05
Ex. % (from 323 K to 298 K)	53.33	60.39	51.89	53.21	58.63
Ex. % (from 333 K to 298 K)	72.08	69.58	72.03	69.39	73.71
Fructose					
Binary mixture of ethanol + IL	EMIMSCN	DMIMMPh	BMIMCl	EtOHMIMCl	BMPyrCl
Ex. % (from 313 K to 298 K)	32.798	41.247	47.183	37.303	27.104
Ex. % (from 323 K to 298 K)	48.441	53.101	60.629	49.645	47.503
Ex. % (from 333 K to 298 K)	63.296	60.019	69.418	59.903	61.390
Sucrose					
Binary mixture of ethanol + IL	EMIMSCN	DMIMMPh	BMIMCl	EtOHMIMCl	BMPyrCl
Ex. % (from 313 K to 298 K)	29.715	31.593	37.313	24.919	31.283
Ex. % (from 323 K to 298 K)	43.223	49.062	52.689	41.640	42.939
Ex. % (from 333 K to 298 K)	67.190	65.168	71.286	60.036	66.124
Lactose					
Binary mixture of ethanol + IL	EMIMSCN	DMIMMPh	BMIMCl	EtOHMIMCl	BMPyrCl
Ex. % (from 313 K to 298 K)	39.011	37.360	54.904	47.941	40.695
Ex. % (from 323 K to 298 K)	64.499	62.356	69.178	71.344	66.018
Ex. % (from 333 K to 298 K)	76.987	77.513	83.542	81.498	78.353

Table II.11. The extraction % of sugars from BMIMCl with different antisolvents at R= 20, T= 298.15 K and neglected water content.

Antisolvents	Glucose extracted %	Fructose extracted %	Sucrose extracted %	Lactose extracted %
	BMIMCl			
Ethanol	99	80	99	99
Dichloromethane	99	85	99	99
Acetonitrile	99	80	99	99

II.5. Conclusion

Ionic liquids have been suggested to replace volatile organic compounds in industrial separation processes. It was found that the antisolvent method is a good technique for the extraction of sugars from ILs. This work clearly shows the influence of the structure of both IL and sugar on the extraction performance. A successful extraction process requires high ethanol/ IL ratio, low temperature and low water content. The considerable decrease of the solubility of sugars in the binary mixtures proves the ability of ethanol to be an excellent antisolvent for separating sugars from various types of ionic liquids.

References

[1] H. Tadesse, R. Luque, Advances on biomass pretreatment using ionic liquids: An overview, Energy Environ. Sci., 4 (2011) 3913-3929.

[2] R. Henry, Evaluation of plant biomass resources available for replacement of fossil oil, Plant Biotechnol. J., 8 (2010) 288-293.

[3] M. Balat, H. Balat, C. Oz, Progress in bioethanol processing, Prog Energy Combust Sci., 34 (2008) 551-573.

[4] V. B. Agbor, N. Cicek, R. Sparling, A. Berlin, D. B. Levin, Biomass pretreatment: Fundamentals toward application, Biotechnology Advances, 29 (2011) 675-685.

[5] K. Nakashima, K. Yamaguchi, N. Taniguchi, S. Arai, R. Yamada, S. Katahira, N. Ishida, H. Takahashi, C. Ogino, A. Kondob, Direct bioethanol production from cellulose by the combination of cellulase-displaying yeast and ionic liquid pretreatment, Green Chem., 13 (2011) 2948-2953.

[6] C. E. Wyman, What is (and is not) vital to advancing cellulosic ethanol, Trends Biotechnol., 25 (2007) 153-157.

[7] G. Cheng, P. Varanasi, C. Li, H. Liu, Y. B. Melnichenko, B. A. Simmons, M. S. Kent, S. Singh, Transition of cellulose crystalline structure and surface morphology of biomass as a function of ionic liquid pretreatment and its relation to enzymatic hydrolysis, Biomacromolecules, 12 (2011) 933-941.

[8] H. Wang, G. Gurau, R. D. Rogers, Ionic liquid processing of cellulose, Chem. Soc. Rev., 41 (2012) 1519-1537.

[9] A. T. W. M. Hendriks, G. Zeeman, Pretreatments to enhance the digestibility of lignocellulosic biomass, Bioresour. Technol., 100 (2009) 10-18.

[10] A. P. Dadi, C. A. Schall, S. Varanasi, Mitigation of cellulose recalcitrance to enzymatic hydrolysis by ionic liquid pretreatment, Appl. Biochem. Biotechnol., 136-140 (2007) 407-421.

[11] N. Sun, M. Rahman, Y. Qin, M. L. Maxim, H. Rodríguez, R. Rogers, Complete dissolution and partial delignification of wood in the ionic liquid 1-ethyl-3-methylimidazolium acetate, Green Chem., 11 (2009) 646-655.

[12] C. Li, B. Knierim, C. Manisseri, R. Arora, H. V. Scheller, M. Auer, K. P. Vofgel, B. A. Simmons, S. Singh, Transition of cellulose crystalline structure and surface morphology of biomass as a function of ionic liquid pretreatment and its relation to enzymatic hydrolysis, Bioresour. Technol., 101 (2010) 4900-4906.

[13] I. P. Samayam, C. A. Schall, Ionic liquid induced changes in cellulose structure associated with enhanced biomass hydrolysis, Bioresour. Technol., 101 (2010) 3561-3566.

[14] M. J. Earle, J. M. S. S. Esperanca, M. A. Gilea, J. N. C. Lopes, L. P. N. Rebelo, J. W. Magee, K. R. Seddon, J. A. Widegren, The distillation and volatility of ionic liquids, Nature, 439 (2006) 831-834.

[15] U. Domanska, R. Bogel-Lukasik, Physicochemical properties and solubility of alkyl-(2-hydroxyethyl)-dimethylammonium bromide, J. Phys. Chem. B, 109 (2005) 12124-12132.

[16] H. S. Gao, C. Guo, J. M. Xing, J. M. Zhao, H. Z. Liu, Extraction and oxidative desulfurization of diesel fuel catalyzed by a Brønsted acidic ionic liquid at room temperature, Green Chem., 12 (2010) 1220-1224.

[17] Y. Y. Jiang, H. S. Xia, C. Guo, I. Mahmood, H. Z. Liu, Enzymatic hydrolysis of penicillin for 6-apa production in three-liquid-phase system, Appl Biochem Biotechnol., 144 (2010) 145-149.

[18] R. Hagiwara, T. Nohira, K. Matsumoto, Y. Tamba, A fluorohydrogenate ionic liquid fuel operating without humidification, Electrochem Solid-State Lett., 8 (2005) 231-233.

[19] B. Andrea, A. H. Wesley, S. Patrice, A. Balducci, W. A. Henderson, M. Mastragostino, Cycling stability of a hybrid activated carbon//poly(3-methylthiophene) supercapacitor with N-butyl-N-methylpyrrolidinium bis(trifluoromethanesulfonyl)imide ionic liquid as electrolyte, Electrochem Acta, 50 (2005) 2233-2237.

[20] G. W. Meindersma, M. Masse and A. B. DeHann, Ionic Liquids, *In Ullmann's Encylopedia of Industrial Chemistry* (Online); Wiley-VCH Verlag GmbH and Co.: Berlin, 2007; pp 1.

[21] H. A. Weingaertner, Understanding ionic liquids at the molecular level: facts, problems and controversies, Chem., Int. Ed., 47 (2008) 654-670.

[22] Y. Y. Jiang, C. Guo, H. S. Xia, I. Mahmood and C. Z. Liu, Magnetic nanoparticles supported ionic liquids for lipase immobilization: enzyme activity in catalyzing esterification, J Mol Catal B: Enzym., 58 (2009) 103-109.

[23] X. M. Hou, F. Zhou, Y. B. Sun, W. M. Liu, Ultrasound-assisted synthesis of dentritic ZnO nanostructure in ionic liquid, Mater Lett., 61 (2007) 1789-1792.

[24] R. P. Swatloski, S. K. Spear, J. D. Holbrey, R. D. Rogers, Dissolution of cellulose with ionic liquids, J. Am. Chem. Soc., 124 (2002) 4974-4975.

[25] S. Murugesan, R. J. Linhardt, Ionic liquids in carbohydrate chemistry - current trends and future direction, Curr. Org. Synth., 2 (2005) 437-451.

[26] F. Ganske, U. T. Bornscheuer, Lipase-catalyzed glucose fatty acid ester synthesis in ionic liquids, Org. Lett., 7 (2005) 3097-3098.

[27] O. A. El Seoud, A. Koschella, L. C. Fidale, S. Dorn, T. Heinze, Applications of ionic liquids in carbohydrate chemistry: a window of opportunities, Biomacromolecules, 8 (2007) 2629-2647.

[28] A. Pinkert, K. N. Marsh, S. S. Pang, M. P. Staiger, Ionic liquids and their interaction with cellulose, Chem. Rev., 109 (2009) 6712-6728.

[29] E. Z. Malgorzata, B. L. Ewa, B. L. Rafal, Solubility of carbohydrates in ionic liquids, Eneregy fuels, 24 (2010) 737-745.

[30] A. A. Rosatella, L. C. Branco, C. A. M. Afonso, Studies on dissolution of carbohydrates in ionic liquids and extraction from aqueous phase, Green Chem., 11 (2009) 1406-1413.

[31] A. P. Carneiro, O. Rodriguez, E. A. Macedo, Solubility of monosaccharides in ionic liquids – Experimental data and modeling, Fluid Phase Equil., 314 (2012) 22-28.

[32] R. M. Lau, F. van Rantwijk, K. R. Seddon, R. A. Sheldon, Lipase-catalyzed reactions in ionic liquids, Org. Lett., 2 (2000) 4189-4191.

[33] S. Park, R. J. Kazlauskas, Improved preparation and use of room temperature ionic liquids in lipase-catalyzed enantio- and regioselective acylations, J. Org. Chem., 66 (2001) 8395-8401.

[34] N. Kimizuka, T. Nakashima, Spontaneous self-assembly of glycolipid bilayer membranes in sugar-philic ionic liquids and formation of ionogels, Langmuir, 17 (2001) 6759-6761.

[35] S. A. Forsyth, D. R. MacFarlane, R. J. Thomson, M. von Itzstein, Rabid, clean and mild O-acetylation of alcohols and carbohydrates in an ionic liquid, Chem. Commun., 7 (2002) 714-715.

[36] D. R. MacFarlane, J. Golding, S. Forsyth, M. Forsyth, G. B. Deacon, Low viscosity ionic liquids based on organic salts of the dicyanamide anion, Chem. Commun., (2001) 1430-1431.

[37] Q. B. Liu, M. H. A. Janssen, F. van Rantwijk, R. A. Sheldon, Room-temperature ionic liquids that dissolve carbohydrates in high concentrations, Green Chem., 7 (2005) 39-42.

[38] W. Liu, Y. Hou, W. Wu, S. Ren, Y. Jing, B. Zhang, Solubility of glucose in ionic liquid + antisolvent mixtures, Ind. Eng. Chem. Res., 50 (2011) 6952-6956.

[39] U. Domanska, E. Bogel-Lukasik, R. Bogel-Lukasik, Solubility of 1-dodecyl-3-methyl-imidazolium chloride in alcohols (C2 - C12), J. Phys. Chem. B, 107 (2003) 1858-1863.

[40] Y. Fukaya, K. Hayashi, M. Wada, H. Ohno, Cellulose dissolution with polar ionic liquids under mild conditions: required factors for anions, Green Chem., 10 (2008) 44-46.

[41] C. Reichardt, T. Welton, Solvents and Solvent effects in Organic Chemistry, fourth edn. ISBN: 978-3-527-32473-6, Wiley-VCH, Weinheim, 2010.

[42] J.-M. Lee, Solvent properties of piperidinium ionic liquids, Chem. Eng. J., 172 (2011) 1066-1071.

[43] S. Zhang, X. Qi, X. Ma, L. Lu, Q. Zhang, Y. Deng, Investigation of cation-anion interaction in 1-(2-hydroxyethyl)-3-methylimidazolium-based ion pairs by density functional theory calculations and experiments, J. Phys. Org. Chem., 25 (2012) 248-257.

[44] J. Lee, J. M. Prausntiz, Polarity and hydrogen bond donor strength for some ionic liquids: Effect of alkyl chain length on the pyrrolidinium cation, Chem., Phys. Lett., 492 (2010) 55-59.

[45] G. J. Philip, A. J. David, F. Dongbao, Solvatochromic parameters for solvents of interest in green chemistry, P. Lam, Green Chem., 14 (2012) 1245-1259.

[46] A. Oehlke, K. Hofmann, S. Spange, New aspects on polarity of ionic liquids as measured by solvatochromic Probe, New J. Chem., 30 (2006) 533-536.

[47] L. J. A. Conceiçao, E. Bogel-Lukasik, R. Bogel-Lukasik, A new outlook on solubility of carbohydrates and sugar alcohols in ionic liquids, RSC Adv., 2 (2012) 1846-1855.

[48] D.A. Fort, R. P. Swatolski, P. Moyna, R. D. Rogers, G. Moyna, Use of ionic liquids in the study of fruit ripening by high-resolution 13C NMR spectroscopy: 'Green' solvents meet green bananas, Chem. Commun., (2006) 714-716.

[49] H. Zhang, G. Gurau, R.D. Rogers, Ionic liquid processing of cellulose, Chem Soc Rev., 41 (2012) 1519-1537.

[50] V. M. Egorov, S. V. Smirnova, A. A. Formanovsky, I. V. Pletnev, Y. A. Zolotov, Dissolution of cellulose in ionic liquids as a way to obtain test materials for metal-ion detection, Anal. Bioanal. Chem., 387 (2007) 2263-2269.

[51] H. Renon, J. M. Prausnitz, Local compositions in thermodynamic excess functions for liquid mixtures, AIChE J., 14 (1968) 135-144.

[52] D.S. Abrams, J. M. Prausnitz, Statistical thermodynamics of liquid mixtures: A new expression for the excess gibbs energy of partly or completely miscible systems, AIChE J., 21 (1975) 116-128.

[53] J. M. Prausnitz, R. N. Lichtenthaler, E.G. Azevedo, Molecular thermodynamics of fluid-phase equilibria, 2nd ed.; Prentice-Hall Inc.; Engelwood Cliffs, N J, 1986.

[54] L. D. Simoni, A. Chapeaux, J. F. Brennecke, M. A. Stadtherr, Asymmetric framework

for predicting liquid-liquid equilibrium of ionic liquid-mixed-solvent systems. 2. Prediction of ternary systems, Ind. Eng. Chem. Res., 48 (2009) 7257-7265.

[55] U. Domanska, Solubility of n-alkanols (C16, C18, C20) in binary solvent mixtures, Fluid Phase Equilib., 46 (1989) 223-248.

[56] L. Hyvonen, P. Koivistoinen, Fructose in food systems, Applied Science Publishers. pp. 133–144. ISBN 0-85334-997-5, 1982.

[57] Q. Yang, H. Xing, B. Su, K. Yu, Z. Bao, Y. Yang, Q. Ren, Improved separation efficiency using ionic liquid–cosolvent mixtures as the extractant in liquid–liquid extraction: A multiple adjustment and synergistic effect, Chem. Eng. J., 181-182 (2012) 334-342.

Chapter III. Study of the Interaction between Carbohydrates and Ionic liquids Using AB Initio Calculations

Previous work indicates that carbohydrates are soluble in some imidazolium based ionic liquids. For a better understanding of the behavior of such systems, theoretical quantum chemical calculation have become complementarities of experimental measurements. The goal of this chapter is to investigate the fundamental natures of the interaction between carbohydrates and imidazolium based ionic liquids using ab initio calculations and comparing these results with experimental data. Furthermore, a characterization study was made to investigate the changes in the cellulose structure during the process of solubility and regeneration with ionic liquids.

III.1. Introduction

Since ILs are interesting for so many different fields, these solvents are currently being intensively studied by using a great variety of experimental and theoretical methods.[1-8] Among these methods, ab initio calculations play an important role in understanding the special nature of ILs and their interactions with dissolved components or interfaces.[9-11] Recently, ionic liquids have become of great interest in the field of bioengineering, chemical and physical processes.[12-16] Ionic liquids efficiently dissolve carbohydrates[17], cellulose[18-22], and lignocellulosic biomass (e.g. miscanthus).[23-25] Hydrogen bonding in ILs has been extensively studied because it plays an important role in cation–anion and solvent–solute interactions, as revealed by both experimental and theoretical investigations.[26-30] For example, the hydrogen bond characteristics of ILs was said to be vitally important to design ILs as potential solvents for cellulose.[31-32]

H. Xu et al, 2012, [33] showed that both chloride anions and imidazolium cations of the IL interact with the cellulose via hydrogen bonds. However, the anions occupy the first coordination shell of the oligomer, and the strength and number of hydrogen bonds and the interaction energy between anions and the oligomer are much larger than those between cations and the oligomer. It is observed that the intra molecular hydrogen bond in the oligomer is broken under the combined effect of anions and cations. The present results emphasize that the chloride anions play a critically important role and the imidazolium cations present a remarkable contribution in the cellulose dissolution. This point of view is different from previous one that only underlines the importance of the chloride anions in the cellulose dissolution. The present results improve our understanding for the cellulose dissolution in imidazolium chloride ILs.[33]

The first part of this work aims to study, using ab initio quantum chemical methods, the optimized structures and H-bonding between cations and anions in different imidazolium based ionic liquids. In addition, the interaction of carbohydrates, glucose and cellulose building unit, with ionic liquids was investigated and compared with experimental results. The second part of the study is devoted to the evaluation of the process of dissolution and regeneration of cellulose from ionic liquids using the antisolvent method. A characterization study using various analytical techniques, such as X-ray diffracrion, infrared spectra, Scanning electron microscope, was performed to evaluate the efficiency of the produced cellulose to be used for biofuel production.

III.2. Methodology

The ab initio calculations were carried out using GAUSSIAN 98.[34] The minimum energy geometry of the cations and anions studied in this work were determined by performing calculations with density functional theory (DFT). The hybrid Becke 3−Lee−Yang−Parr, B3LYP, exchange-correlation function with the 6-311+G(d) basis set is employed for the geometry optimizations in this work.[35-38] It is known that the B3LYP/6-311+G(d) level is an excellent compromise between the computational cost and accuracy of the computational results. Moreover, the basis set was found to be suitable for the study of systems containing ILs and carbohydrates systems.[39,40] The geometry optimizations of the cation-anion pairs were carried out in a sequential process at the RHF/6-31G, B3LYP/6-31G(d), and B3LYP/6-311+G(d) levels of theory. The geometry of the cation-anion pairs was firstly optimized at the RHF/6-31G level. The resulting RHF/631G optimized structures were used as the initial structures for subsequent B3LYP/631G(d) geometry optimizations, and these optimized structures were in turn used as initial structures for the B3LYP/6-311+G(d) optimizations. Partial atomic charges were derived from the ion pair geometries using the CHELPG [41] method.

III.3. Experimental techniques

III.3.1. Materials

Microcrystalline cellulose (MCC) and avicel cellulose (AvC) were purchased from Sigma-Aldrich. The ionic liquids used in this work, 1-butyl-3-methylimidazolium chloride (BMIMCl), 1-ethanol-3- methylimidazolium chloride (EtOHMIMCl) and 1,3-dimethyl-imidazolium methyl phosphonate (DMIMMPh), with purity 98%, were from Solvionic, and 1-ethyl-3-methylimidazolium thiocyanate (EMIMSCN) with purity 95% was from Sigma Aldrich. These ionic liquids were dried under vacuum for 3 hours at 363 K before use.

III.3.2. Solubility and regeneration of cellulose

The solubility experiments of MCC and AvC cellulose in ionic liquids have been performed in jacketed glass cells at atmospheric pressure and at temperature ranges starting from 300 to 400 K. using a dynamic method described in chapter II.

For the extraction of cellulose, Water was added as an antisolvent to the resulting clear liquors, and a cellulose-rich extract was reconstituted from the liquor. This extract was washed with water until the IL completely removed and then dried overnight in an oven at 373 K prior to use.

The characterization of original and regenerated cellulose was performed using FTIR, XRD, ^{13}C NMR and SEM analyses. These techniques are well described in chapter IV.

III.4. Results and Discussion

III.4.1. Ionic liquids structure optimization and hydrogen bond formation

In this section, the optimized cation-anion pair geometries are presented and the interactions between the cation and anion are noted. The hydrogen bonding values of the cation-anion pairs are presented and discussed.

The optimized structures for cations and anions of ionic liquids and also for sugars, glucose and cellulose building unit, were obtained using the procedure described in part III.2 (see figuers III.1-III.3). The partial atomic charges for the optimized geometries, derived using the CHELPG method, are given in table III.1.

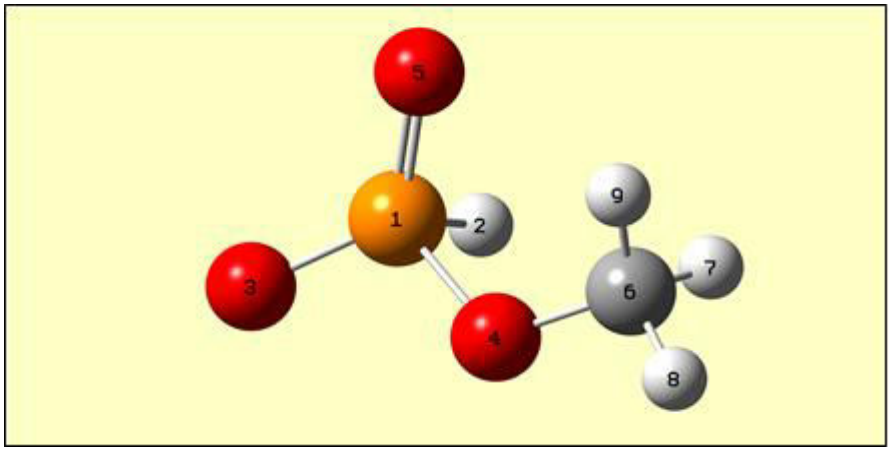

(a)

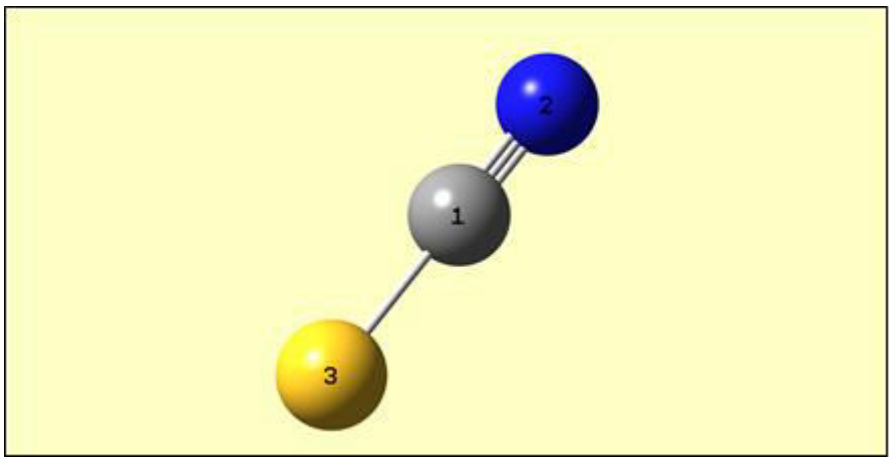

(b)

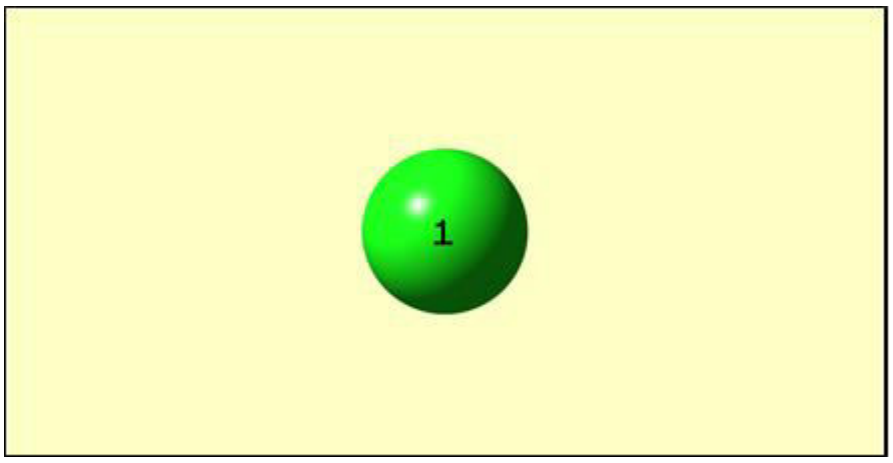

(c)

Figure III.1. Optimized geometries of A) MPh^-, B) SCN^- and C) Cl^- anions

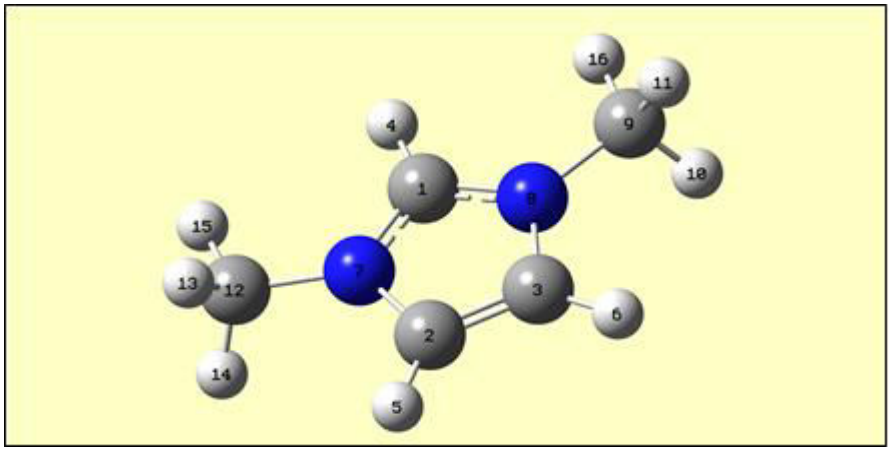

(a)

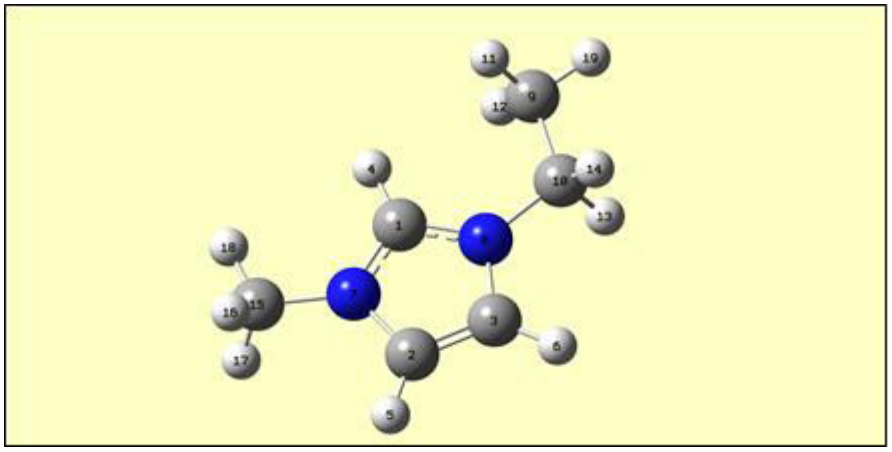

(b)

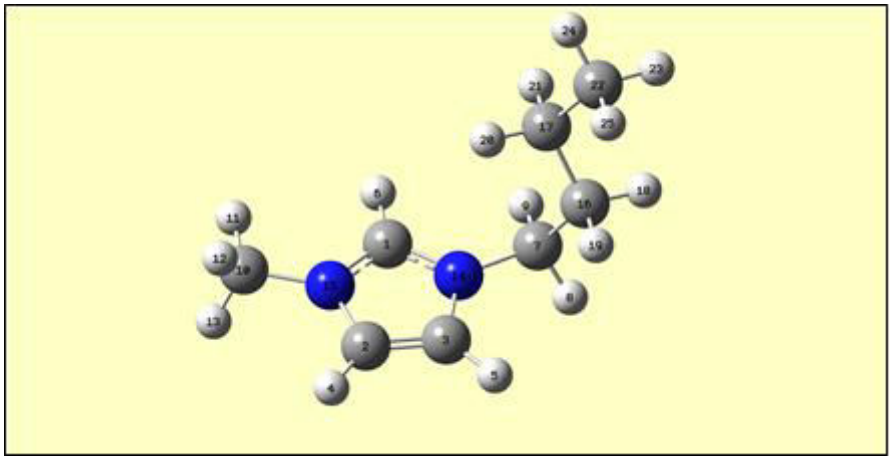

(c)

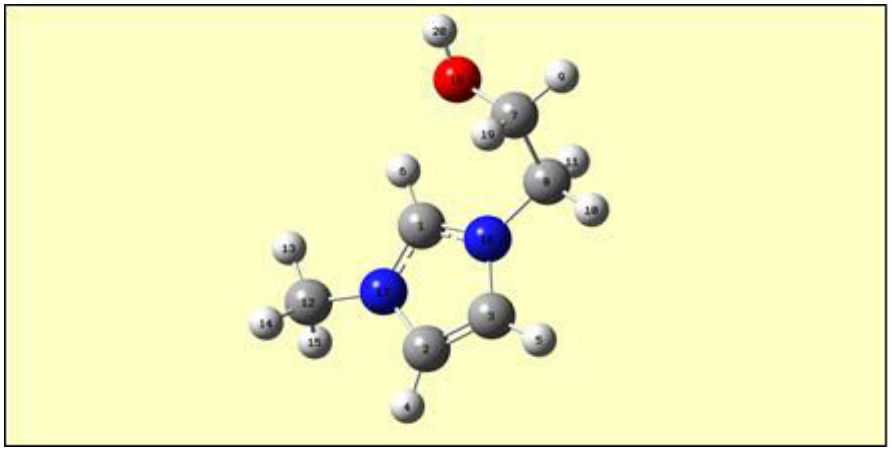

(d)

Figure III.2. Optimized geometries of a) $DMIM^+$, b) $EMIM^+$, c) $BMIM^+$and d) $EtOHMIM^+$ cations

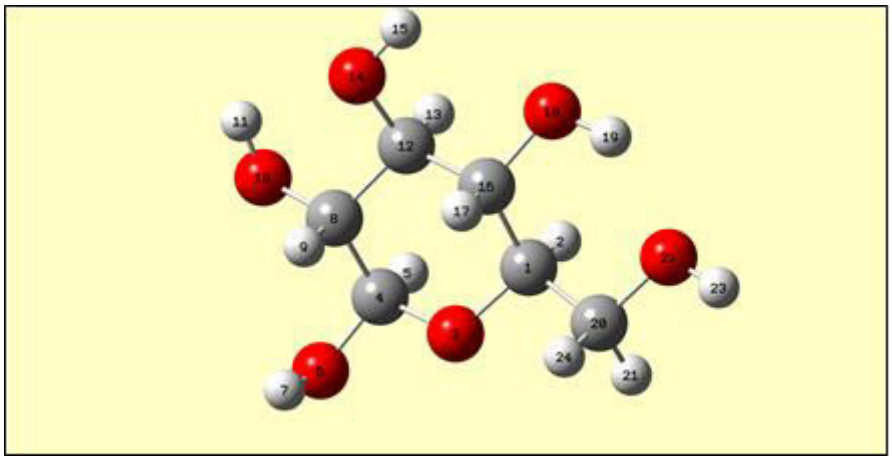

(a)

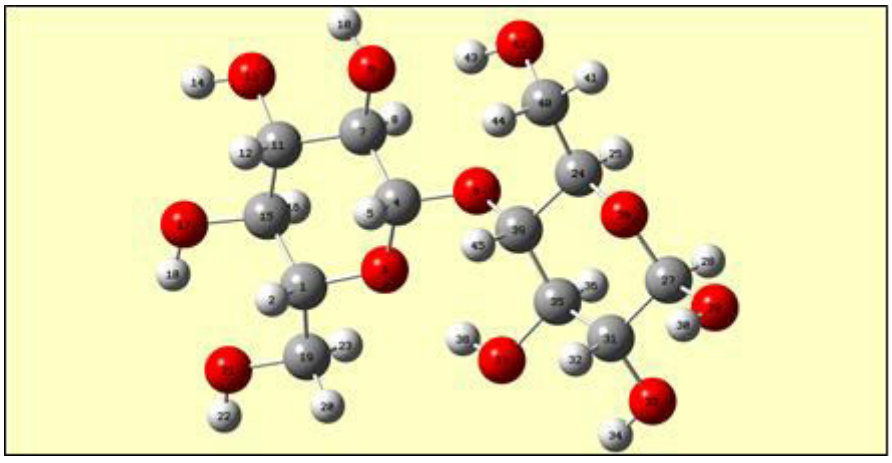

(b)

Figure III.3. Optimized geometries of a) glucose and b) cellulose building unit

Table III.1. Partial atomic charges for optimized structures of anions and cations of ILs and for sugars

Partial atomic charges									
Atom number	Anions			Cations				Sugars	
	MPh^-	SCN^-	Cl^-	$DMIM^+$	$EMIM^+$	$BMIM^+$	$EtOHMIM^+$	Glucose	Cellobiose
1	1.405	0.591	-1.0	-0.130	-0.044	-0.096	0.004	0.324	0.302
2	-0.238	-0.805		-0.147	-0.107	-0.160	-0.088	0.011	0.015
3	-0.884	-0.786		-0.147	-0.127	-0.142	-0.195	-0.778	-0.813
4	-0.578			0.226	0.204	0.213	0.199	0.853	0.920
5	-0.875			0.215	0.203	0.218	0.217	0.007	-0.039
6	0.267			0.215	0.196	0.199	0.202	-0.757	-0.638
7	-0.005			0.189	0.120	-0.158	0.394	0.461	0.070
8	-0.043			0.189	0.075	0.109	-0.195	0.072	0.104
9	0.001			-0.222	-0.179	0.111	0.037	0.073	-0.837
10				0.140	0.044	-0.276	0.119	-0.793	0.533
11				0.140	0.067	0.151	0.138	0.520	0.367
12				-0.222	0.067	0.153	-0.185	0.320	0.011
13				0.140	0.083	0.148	0.133	0.025	-0.798
14				0.140	0.083	0.143	0.133	-0.791	0.504
15				0.138	-0.224	0.209	0.131	0.504	0.202
16				0.138	0.143	0.081	0.178	0.143	0.050
17					0.143	0.158	0.077	0.062	-0.814
18					0.140	0.037	-0.770	-0.799	0.514
19					0.114	0.001	-0.011	0.510	0.369
20						-0.046	0.482	0.392	0.019
21						-0.017		0.014	-0.824
22						-0.257		-0.842	0.484
23						0.069		0.482	0.002
24						0.089		-0.009	0.364
25						0.065			0.010
26									-0.845
27									0.949
28									-0.020
29									-0.769
30									0.456
31									0.030
32									0.079
33									-0.806
34									0.524
35									0.431
36									-0.006
37									-0.880
38									0.562
39									0.078
40									0.480
41									0.045
42									-0.912
43									0.572
44									-0.081
45									0.049

III.4.1.1. Optimized structures of ionic liquids

The interaction energy ΔE can be calculated using the following equation[11,42]

$$\Delta E\ (KJ\ mol^{-1}) = 2625.5^{*}\ [E[cation]^{+}\ [anion]^{-} - (E[cation]^{+} + E[anion]^{-})] \quad (III.1)$$

Where $E[cation]^{+}\ [anion]^{-}$ is defined as the total energy of the system and $E[cation]^{+} + E[anion]^{-}$ is defined as the sum of the energy of the pure compositions.

The interaction energies are corrected by the basis set superposition error (BSSE) and zero-point energy (ZPE). Thus, the corrected interaction energy ΔE_{Corr} could be calculated as follows:[11,42]

$$\Delta E_{Corr} = \Delta E + \Delta E_{BSSE} + \Delta E_{ZPE} \quad (III.2)$$

Where ΔE_{BSSE} is the correction of BSSE and ΔE_{ZPE} is the correction of ZPE.

To obtain the stable configurations of DMIMMPh, the anion MPh^{-} is located at several different positions around the cation. The initial configurations are fully optimized. Three representative configurations, A_1, A_2 and A_3 are selected, where the MPh^{-} anion is placed at carbon number 2, 4 and 5 of the imidazolium ring in $DMIM^{+}$ cation, respectively. The interaction energy of A_1 is larger than that of A_2 and A_3. Thus, the conformer A_1 have better probability than other conformers. Therefore, the conformer A_1 is chosen as the best optimized structure of DMIMMPh ionic liquid. The same trend was found with the BMIMCl, EtOHMIMCl and EMIMSCN ionic liquids, where the highest interaction energies between anions and cations in the ionic liquids studied were found when the anion was placed at the imidazolium C2 carbon. The best optimized structure for BMIMCl ionic liquid is in agreement with the work of P. A. Hunt et al., 2006, [10] who also found that the best optimized structure for BMIMCl is when Cl^{-} is placed at C2 of $BMIM^{+}$. The interaction energies results of the studied ionic liquids are listed in table III.2, the best optimized structures are shown in figure III.4 and the data of the bond ring distances of the best optimized ionic liquids are given in table III.3.

It could be also noticed that the most stable ionic liquid ion pairs have the anion positioned in front of the C2-H; however, the anion is shifted slightly toward the less bulky group, methyl group, at C6 and lies slightly above the plane of the imidazolium ring.

On the other hand, the presence of hydroxyl group at C8 in EtOHMIMCl, makes it a better hydrogen bond donor than C6–H. Hence, the Cl^{-} anion is shifted slightly toward the OH-C8, figure III.4. This behavior is in a good agreement with the work of S. Zhang et al., 2012.[32]

Comparing the interaction energies of the best conformer A_1 (see table III.2) for the pure optimized imidazolium based ionic liquids showed that ΔE and ΔE_{Corr} increase in the following order: EMIMSCN < BMIMCl ≈ EtOHMIMCl < DMIMMPh.

Table III.2. Comparison between different structure geometries of DMIMPh, BMIMCl, EtOHMIMCl and EMIMSCN where, A_1: Anion at C2 A_2: Anion at C4 A_3: Anion at C5

DMIMMPh			
At level: B3LYP/6.311+G (d)	A_1	A_2	A_3
Total E (a. u.)	-913.210	-913.122	-913.100
ΔE (KJ mol^{-1})	-540.418	-309.209	-250.721
ΔE_{BSSE} (KJ mol^{-1})	5.915	2.569	1.313
ΔE_{ZPE} (KJ mol^{-1})	3.707	-3.458	-4.051
ΔE_{Corr} (KJ mol^{-1})	-530.796	-310.098	-253.459
Hydrogen bond strength range (Å)	1.83-2.44	2.39-2.98	1.98-3.11
Dipole moment (debye)	10.061	19.277	25.010
BMIMCl			
At level: B3LYP/6.311+G (d)	A_1	A_2	A_3
Total E (a. u.)	-883.599	-883.576	-883.543
ΔE (KJ mol^{-1})	-371.246	-309.433	-223.686
ΔE_{BSSE} (KJ mol^{-1})	1.254	1.677	2.054
ΔE_{ZPE} (KJ mol^{-1})	-1.226	-3.497	-4.115
ΔE_{Corr} (KJ mol^{-1})	-371.218	-311.253	-225.747
Hydrogen bond strength range (Å)	2.05-2.69	2.11-2.75	2.17-2.89
Dipole moment (debye)	10.2991	13.122	13.778
EtOHMIMCl			
At level: B3LYP/6.311+G (d)	A_1	A_2	A_3
Total E (a. u.)	-880.160	-880.146	-880.125
ΔE (KJ mol^{-1})	-377.635	-330.410	-276.107
ΔE_{BSSE} (KJ mol^{-1})	1.554	2.230	2.110
ΔE_{ZPE} (KJ mol^{-1})	-1.045	-2.640	-3.965
ΔE_{Corr} (KJ mol^{-1})	-377.126	-330.820	-277.962
Hydrogen bond strength range (Å)	2.09-2.23	2.17-2.58	2.22-2.41
Dipole moment (debye)	14.221	16.875	18.409
EMIMSCN			
At level: B3LYP/6.311+G (d)	A_1	A_2	A_3
Total E (a. u.)	-835.774	-835.761	-835.749
ΔE (KJ mol^{-1})	-338.353	-277.840	-243.562
ΔE_{BSSE} (KJ mol^{-1})	1.875	1.981	2.145
ΔE_{ZPE} (KJ mol^{-1})	2.337	-1.546	-2.667
ΔE_{Corr} (KJ mol^{-1})	-334.141	-277.405	-244.084
Hydrogen bond strength range (Å)	1.71-2.56	1.84-2.76	1.91-2.99
Dipole moment (debye)	17.065	18.003	18.654

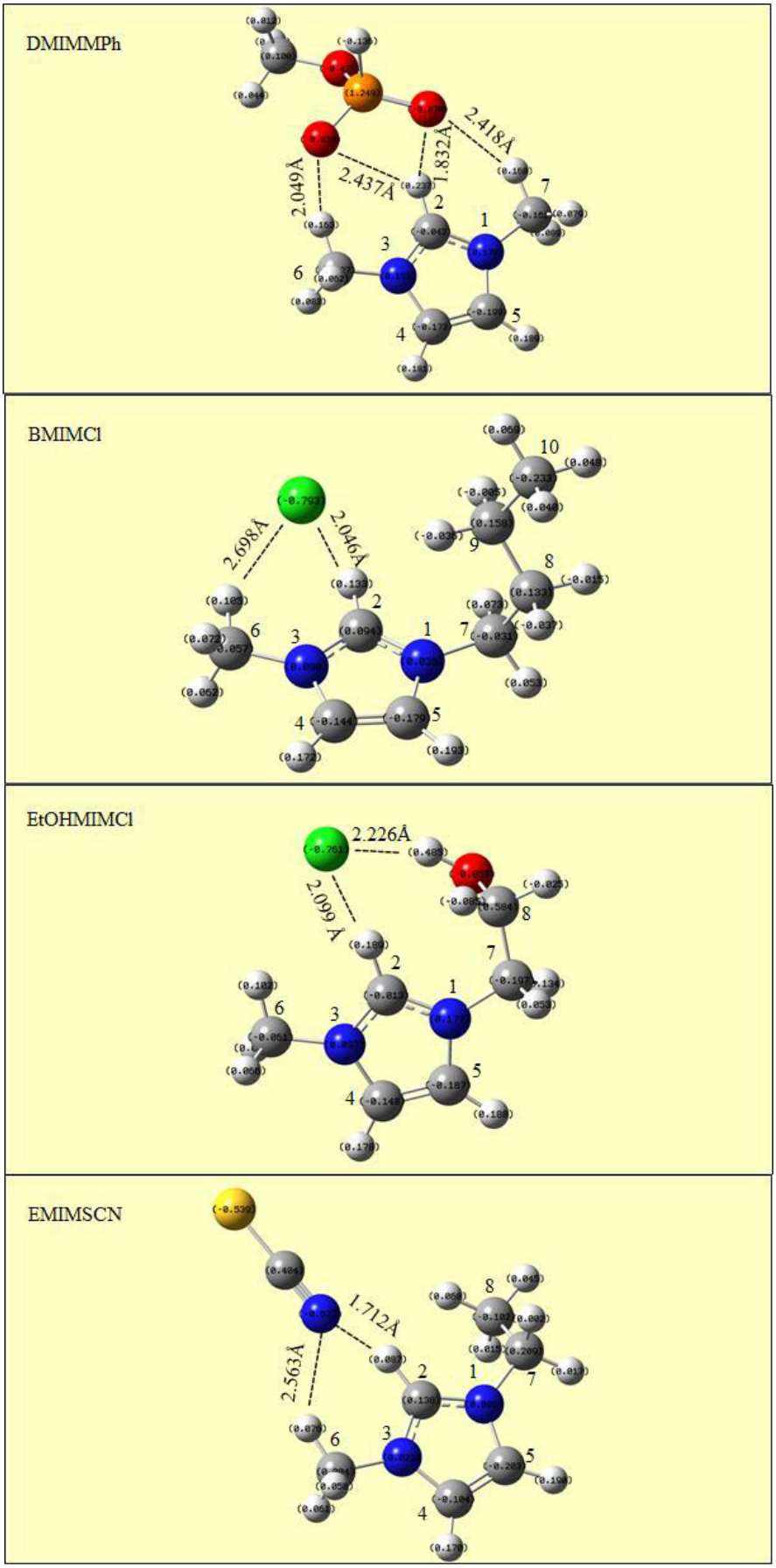

Figure III.4. The most stable geometries of DMIMPh, BMIMCl, EtOHMIMCl and EMIMSCN ionic liquids

Table III.3. Ring bond distances for the optimized structures of ionic liquids

Bond type	Level	Bond distance (Å)			
		BMIMCl	DMIMMPh	EtOHMIMCl	EMIMSCN
N^1-C^2	RHF/6.31G	1.325	1.316	1.327	1.328
	B3LYP/6.31G(d)	1.351	1.337	1.351	1.351
	B3LYP/6.311+G (d)	1.349	1.336	1.346	1.349
C^2-H	RHF/6.31G	1.089	1.072	1.061	1.089
	B3LYP/6.31G(d)	1.115	1.095	1.073	1.129
	B3LYP/6.311+G (d)	1.109	1.094	1.099	1.113
C^2-N^3	RHF/6.31G	1.326	1.316	1.323	1.326
	B3LYP/6.31G(d)	1.349	1.336	1.349	1.351
	B3LYP/6.311+G (d)	1.348	1.335	1.347	1.348
N^3-C^4	RHF/6.31G	1.390	1.379	1.387	1.389
	B3LYP/6.31G(d)	1.397	1.386	1.395	1.397
	B3LYP/6.311+G (d)	1.396	1.385	1.397	1.396
C^4-H	RHF/6.31G	1.064	1.068	1.063	1.064
	B3LYP/6.31G(d)	1.076	1.079	1.075	1.076
	B3LYP/6.311+G (d)	1.073	1.077	1.073	1.073
C^4-C^5	RHF/6.31G	1.346	1.341	1.344	1.345
	B3LYP/6.31G(d)	1.367	1.364	1.366	1.367
	B3LYP/6.311+G (d)	1.364	1.361	1.364	1.364
C^5-H	RHF/6.31G	1.064	1.068	1.063	1.064
	B3LYP/6.31G(d)	1.076	1.079	1.075	1.076
	B3LYP/6.311+G (d)	1.073	1.077	1.073	1.073
C^5-N^1	RHF/6.31G	1.390	1.379	1.390	1.389
	B3LYP/6.31G(d)	1.399	1.385	1.398	1.399
	B3LYP/6.311+G (d)	1.399	1.384	1.398	1.398
N^3-C^6	RHF/6.31G	1.465	1.465	1.466	1.467
	B3LYP/6.31G(d)	1.476	1.470	1.471	1.473
	B3LYP/6.311+G (d)	1.475	1.471	1.473	1.474
N^1-C^7	RHF/6.31G	1.475	1.465	1.472	1.477
	B3LYP/6.31G(d)	1.480	1.469	1.479	1.486
	B3LYP/6.311+G (d)	1.480	1.468	1.485	1.485

III.4.1.2. Hydrogen bonding interaction

It is now well established that cation anion H-bonding occurs in some imidazolium-based ionic liquids.[43-45] In 1998, G. A. Jeffrey found that a normal O···H hydrogen bond is formed when

O···H < 2.7 Å and C— H···O > 90°.[46] Otherwise, a criterion that the interaction distance be less than the sum of the respective van der Waals radii has also been used.

In case of BMIMCl, when the conformer A1 is taken, the distances of Cl···H vary from 2.05 to 2.67 Å, which is much longer than the covalent bond distance of H···Cl (1.31 Å) and shorter than the van der Waals distance of Cl···H (2.95 Å). These values are within the accepted criteria of the C−H···Cl hydrogen bond, which implies that the Cl^- forms hydrogen bonds with N−C−H fragments of $BMIM^+$ (2.95 Å > H.B > 1.31 Å). It is found that there are two H bonds formed between $BMIM^+$ and Cl^-; the corresponding bond lengths and angles of H bonds between $BMIM^+$ and Cl^- are as follows: Cl···H−C2, 2.046 Å; Cl···H−C6, 2.698 Å; angle of C2−H−Cl, 159.75°; and angle of C6−H−Cl, 146.49°. These results are in good agreement with the work of P. A. Hunt et al, 2006,[10] who have shown that a strong H-bond is formed when the C-H···Cl distance is lower than 2.3 Å. The H-bond is weak if 2.3< r < 2.75 Å. The maximum distance is thus shorter than the van der Waals radii limit for a H-bond.

The same trend is found with O---H in DMIMMPh where: 2.72 Å > H.B > 0.942 Å and N---H in EMIMSCN where: 2.75 Å > H.B > 1 Å.

In EtOHMIMCl, the presence of hydroxyl group OH at C8 makes it a better hydrogen bond donor than C6–H. Hence, Strong hydrogen-bonding interaction occurred between Cl^- anion and OH on the cation (O–H---Cl). Key H-bonding anion-cation distances and angles of the best geometries of the studied ionic liquids are summarized in table III.4.

Table III.4. Hydrogen Bonding Formation, where r (Å) is the bond length in angstrom and ∠° is the bond angle in degree

Bond type	Level	BMIMCl		DMIMMPh		EtOHMIMCl		EMIMSCN	
		r (Å)	∠°	r (Å)	∠°	r (Å)	∠°	r (Å)	∠°
C2-H…anion	RHF/6.31G	2.075	175.41	2.163	140.91	2.891	90.03	1.787	166.99
	B3LYP/6.31G(d)	2.033	154.26	2.288	132.09	2.786	99.46	1.642	170.68
	B3LYP/6.311+G (d)	2.046	159.75	2.437	129.59	2.099	170.99	1.712	162.42
C6-H…anion	RHF/6.31G	3.331	136.77	2.215	153.62	2.785	126.17	2.835	136.88
	B3LYP/6.31G(d)	2.591	147.42	2.048	159.57	2.624	132.10	2.795	136.24
	B3LYP/6.311+G (d)	2.698	146.49	2.049	162.44	3.129	141.05	2.563	140.47
C8-OH…anion	RHF/6.31G					2.283	147.15		
	B3LYP/6.31G(d)					2.096	156.64		
	B3LYP/6.311+G (d)					2.226	152.83		

III.4.2. Interaction of ionic liquids with carbohydrates

The results obtained for the interaction between the glucose and the anion or the cation but also the IL are presented in table III.5. All optimized structures are shown in figures III.5- III.7. The interaction of the glucose-anion systems increase in the following order: glucose-SCN^- < glucose-Cl^- < glucose-MPh^-. This is mainly due to the fact that the MPh^- anion has a higher hydrogen bond basicity and a higher polarity than the Cl^- and SCN^- anions. It is also obvious that the absolute values of interaction energies and hydrogen bonding of glucose-cation systems are smaller than those obtained on glucose-anion systems, suggesting that the anion plays a dominant role in the interaction of ionic liquids with carbohydrates. These results are in good agreement with the work of A. Casas et al., 2012,[47]. The authors have demonstrated that the anion has the main role in the dissolution process of carbohydrates, in which the H-bonding forces are the major interactions.

Results concerning the binary systems {glucose + IL} are listed in table III.5. The interaction of glucose-IL systems increases in the following order: glucose-EMIMSCN < glucose-EtOHMIMCl < glucose-BMIMCl < glucose-DMIMMPh. This observation is in good agreement with the experimental results obtained in a previous work.[48, 49]

It was shown in table III.2 that the interaction energy between ion pairs of pure EtOHMIMCl is slightly higher than that of BMIMCl. Nevertheless, BMIMCl interacts higher than EtOHMIMCl with glucose. This is maybe due to the presence of the hydroxyl group in the cation which is competing with glucose for hydrogen bond donation to the anion and hence decreases the solubility of the glucose in the corresponding IL. This could be further explained from the hydrogen bonding values shown in figure III.7 (B and C).

The cellulose-building unit, cellobiose, interacts similarly to glucose with anions and cations of ionic liquids. All results are presented in table III.6 and optimized geometries are shown in figures III.8-III.10. The comparison of the interaction energies and the hydrogen bonding formation of glucose-Ils and cellulose-Ils systems showed that ionic liquids interact with glucose higher than with cellulose. This is may be explained due to the high molecular weight and the strong β-(1→4)-glycosidic linkages between cellulose molecules when compared with glucose. This could be further proved by the values of the interaction energies and inter- and intra-hydrogen bonds in the cellulose-cellulose and glucose-glucose systems presented in table III.7 and figure III.11.

Table III.5. The interaction between glucose and ionic liquids

Glucose with DMIMMPh			
At level : B3LYP/6.311+G (d)	Glucose-MPh^-	Glucose-$DMIM^+$	Glucose-DMIMMPh
Total E (a. u.)	-1295.169	-992.407	-1600.597
ΔE (KJ mol^{-1})	-175.68	-81.889	-116.567
ΔE_{BSSE} (KJ mol^{-1})	2.373	1.451	4.011
ΔE_{ZPE} (KJ mol^{-1})	9.542	6.081	14.546
ΔE_{Corr} (KJ mol^{-1})	-163.765	-74.357	-98.010
Hydrogen bond strength (Å)	1.61-2.65	1.9-2.56	1.8-2.8
Dipole moment (debye)	7.07	12.68	9.54
Glucose with BMIMCl			
At level: B3LYP/6.311+G (d)	Glucose-Cl^-	Glucose-$BMIM^+$	Glucose-BMIMCl
Total E (a. u.)	-1147.520	-1110.350	-1570.782
ΔE (KJ mol^{-1})	-152.542	-98.719	-102.261
ΔE_{BSSE} (KJ mol^{-1})	3.945	1.652	4.757
ΔE_{ZPE} (KJ mol^{-1})	14.558	12.902	17.694
ΔE_{Corr} (KJ mol^{-1})	-134.039	-84.165	-79.810
Hydrogen bond strength (Å)	2.24-2.59	1.91-1.98	2.2-2.58
Dipole moment (debye)	6.82	7.16	11.27
Glucose with EtOHMIMCl			
At level: B3LYP/6.311+G (d))	Glucose-Cl^-	Glucose-$EtOHMIM^+$	Glucose-EtOHMIMCl
Total E (a. u.)	-1147.520	-1107.303	-1567.346
ΔE (KJ mol^{-1})	-152.542	-136.008	-90.134
ΔE_{BSSE} (KJ mol^{-1})	3.945	4.892	4.692
ΔE_{ZPE} (KJ mol^{-1})	14.558	24.071	22.24
ΔE_{Corr} (KJ mol^{-1})	-134.039	-107.045	-63.202
Hydrogen bond strength (Å)	2.24-2.59	1.88-2.43	2.17-2.46
Dipole moment (debye)	6.82	5.23	13.452
Glucose with EMIMSCN			
At level: B3LYP/6.311+G (d)	Glucose-SCN^-	Glucose-$EMIM^+$	Glucose-EMIMSCN
Total E (a. u.)	-1178.149	-1031.958	-1523.261
ΔE (KJ mol^{-1})	-132.16	-109.291	-80.601
ΔE_{BSSE} (KJ mol^{-1})	2.985	1.554	4.223
ΔE_{ZPE} (KJ mol^{-1})	13.661	11.776	15.088
ΔE_{Corr} (KJ mol^{-1})	-115.514	-95.961	-61.290
Hydrogen bond strength (Å)	2.16	2.05-2.84	1.84-2.82
Dipole moment (debye)	6.234	16.254	15.887

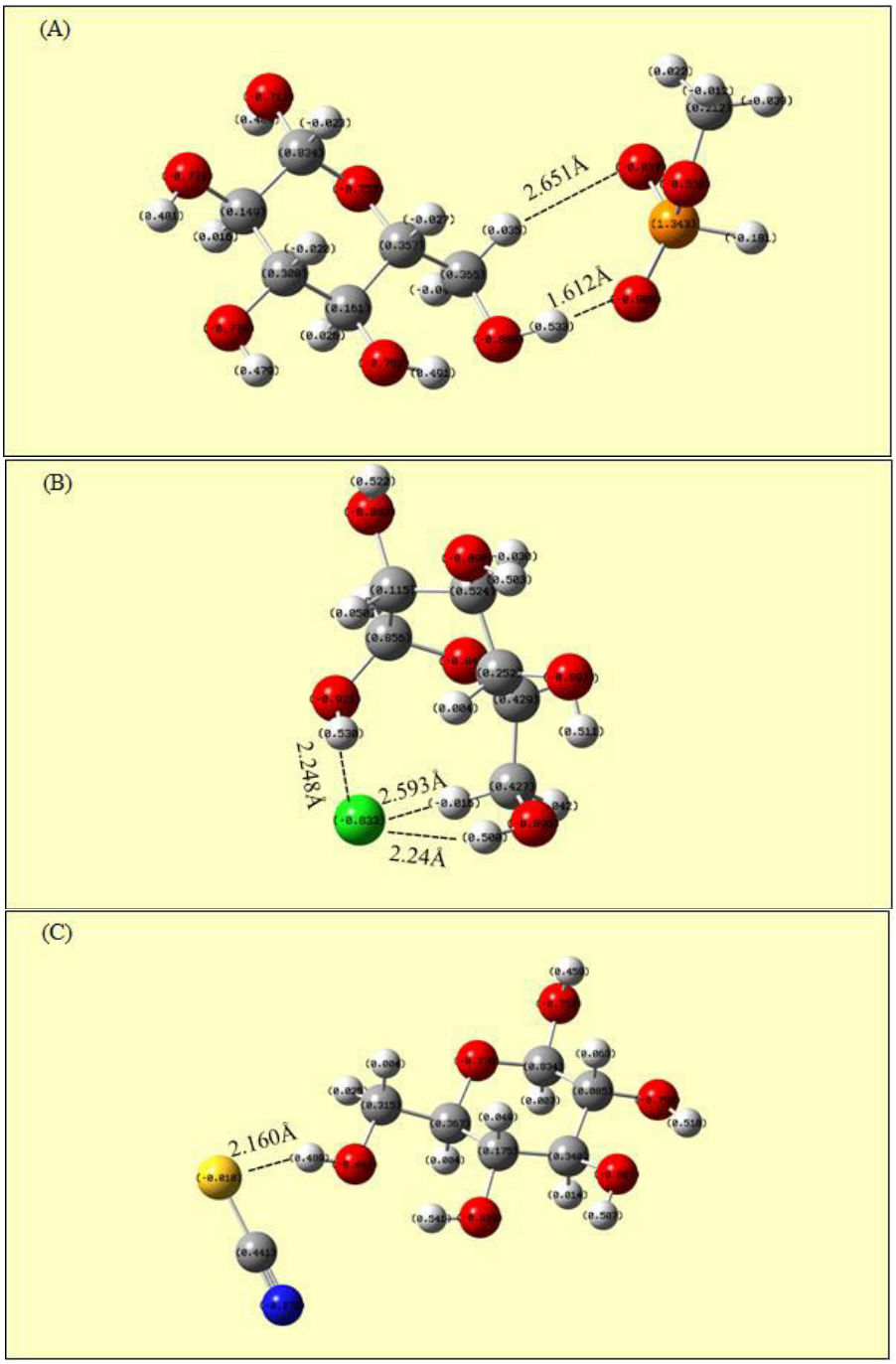

Figure III.5. Optimized structures of glucose with A) MPh^-, B) Cl^- and C) SCN^- anions

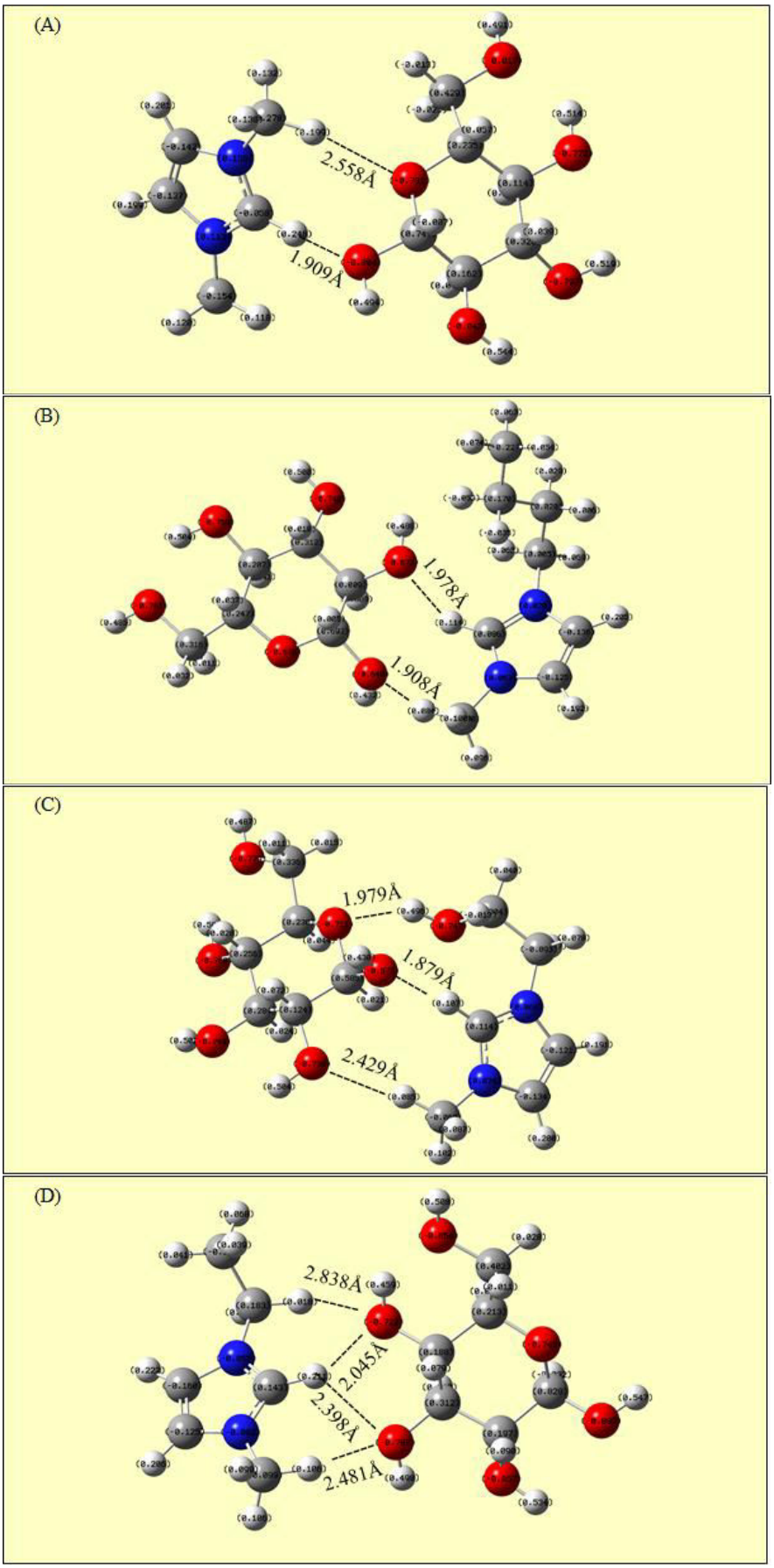

Figure III.6. Optimized structures of glucose with A) $DMIM^+$, B) $BMIM^+$, C) $EtOHMIM^+$ and D) $EMIM^+$ cations

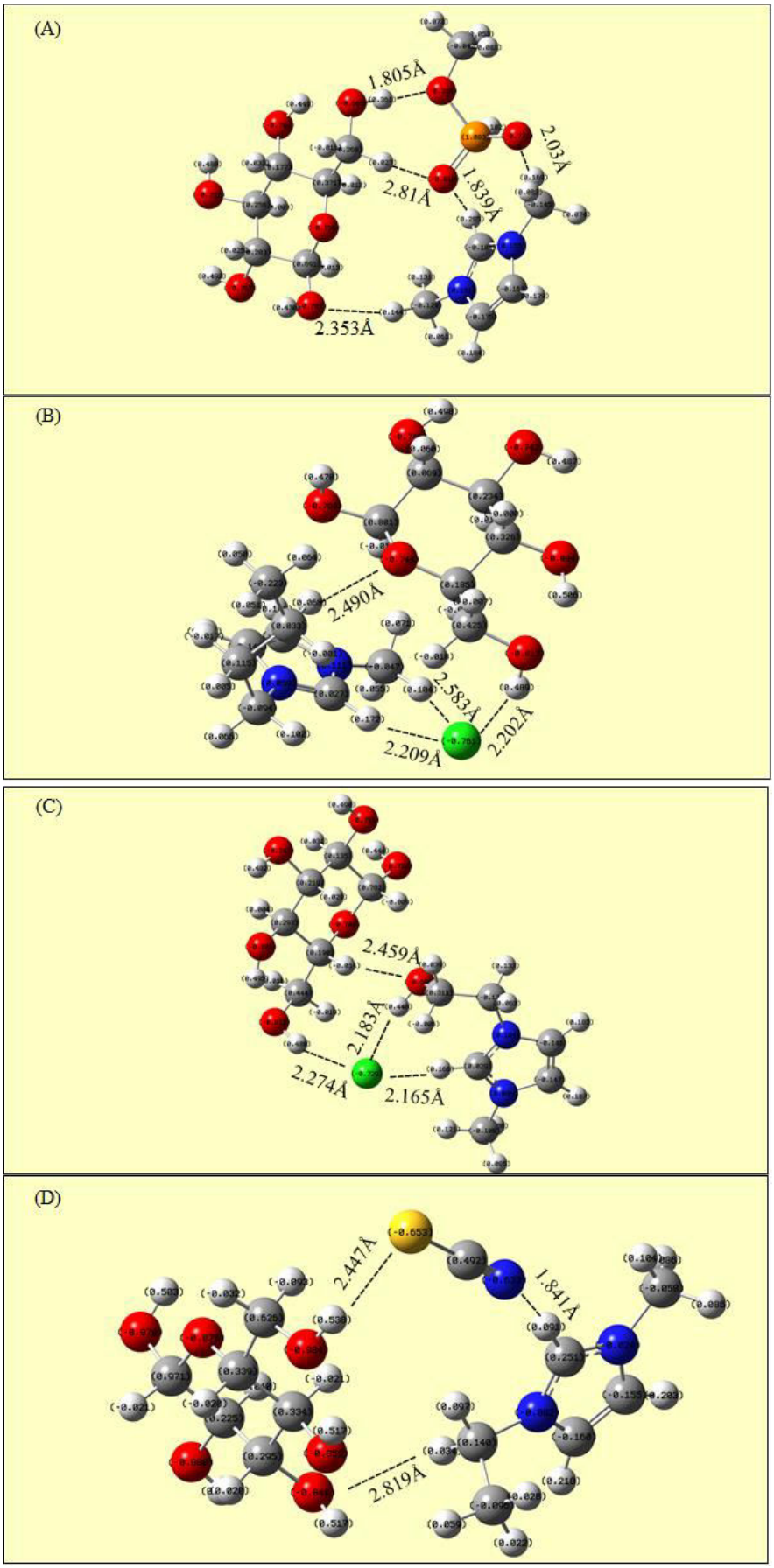

Figure III.7. The interaction of glucose with A) DMIMMPh, B) BMIMCl C) EtOHMICl and D) EMIMSCN

Table III.6. The interaction between cellulose building unit and ionic liquids

Cellulose building unit with DMIMMPh			
At level : B3LYP/6.311+G (d))	Cellulose-MPh^-	Cellulose-$DMIM^+$	Cellulose-DMIMMPh
Total E (a. u.)	-1905.992	-1603.058	-2211.271
ΔE (KJ mol^{-1})	-163.053	-68.240	-110.68
ΔE_{BSSE} (KJ mol^{-1})	7.890	5.912	8.049
ΔE_{ZPE} (KJ mol^{-1})	33.052	29.219	31.629
ΔE_{Corr} (KJ mol^{-1})	-122.111	-33.109	-71.002
Hydrogen bond strength (Å)	1.67-2.72	2.1-2.48	1.62-2.14
Dipole moment (debye)	4.863	20.999	4.292
Cellulose building unit with BMIMCl			
At level : B3LYP/6.311+G (d)	Cellulose-Cl^-	Cellulose-$BMIM^+$	Cellulose-BMIMCl
Total E (a. u.)	-1758.230	-1721.070	-2182.005
ΔE (KJ mol^{-1})	-120.652	-73.664	-97.568
ΔE_{BSSE} (KJ mol^{-1})	5.116	3.17	7.645
ΔE_{ZPE} (KJ mol^{-1})	22.13	21.395	24.655
ΔE_{Corr} (KJ mol^{-1})	-93.406	-49.099	-65.268
Hydrogen bond strength (Å)	2.3-2.84	1.96-2.45	2.15-2.86
Dipole moment (debye)	5.832	18.986	14.003

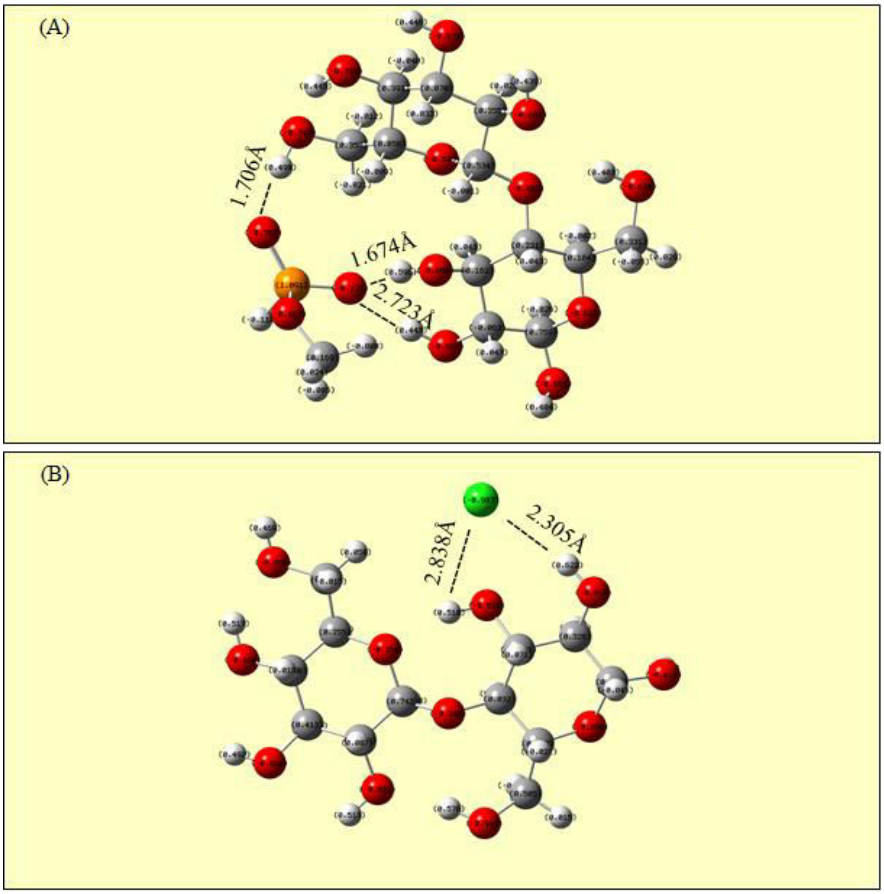

Figure III.8. Optimized structures of cellulose with A) MPh^- and B) Cl^- anions

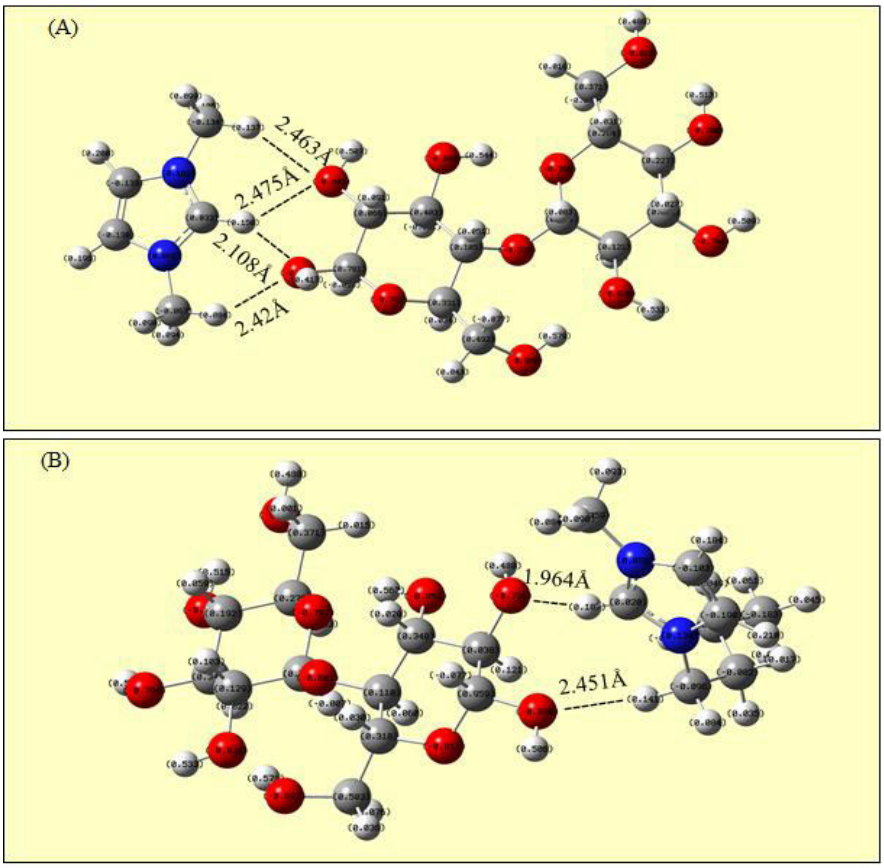

Figure III.9. Optimized structures of cellulose with A) $DMIM^+$ and B) $BMIM^+$ cations

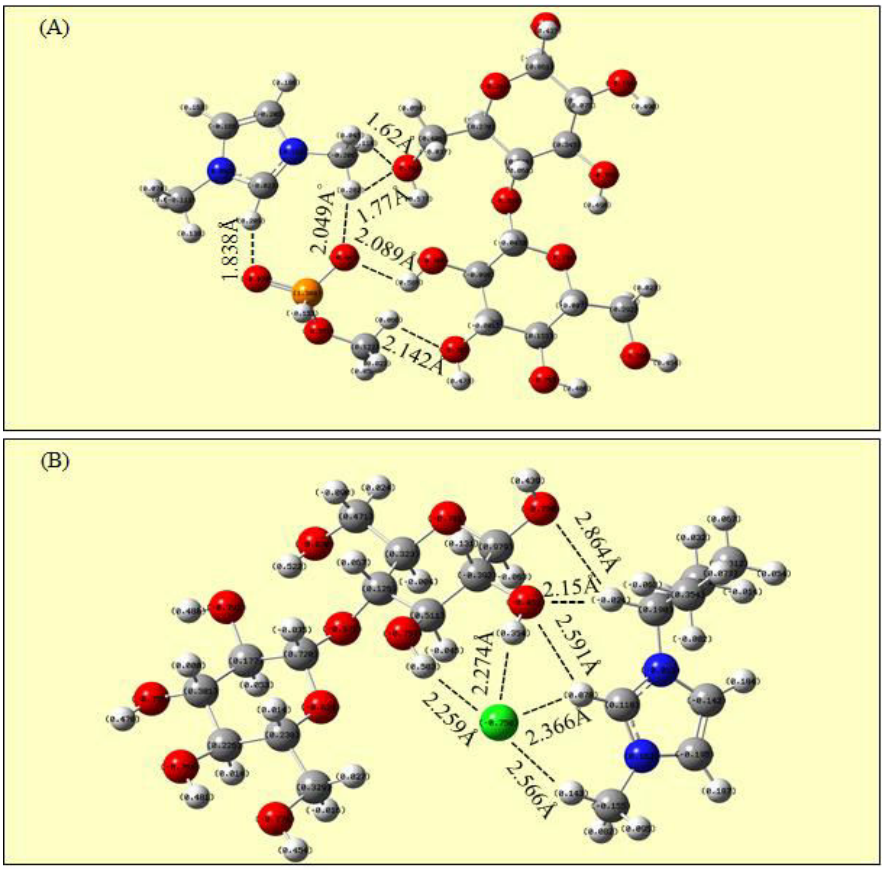

Figure III.10. The interaction of cellulose with A) DMIMMPh and B) BMIMCl

Table III.7. The interaction results of cellulose-cellulose and glucose-glucose systems

At level : B3LYP/6.311+G (d)	Glucose-Glucose	Cellulose- Cellulose
Total E (a. u.)	-1374.702	-2595.034
ΔE (KJ mol^{-1})	-37.416	-74.535
ΔE_{BSSE} (KJ mol^{-1})	2.224	2.69
ΔE_{ZPE} (KJ mol^{-1})	13.553	25.77
ΔE_{Corr} (KJ mol^{-1})	-21.639	-46.075
Hydrogen bond strength (Å)	1.9-2.16	1.64-2.44
Dipole moment (debye)	4.73	12.23

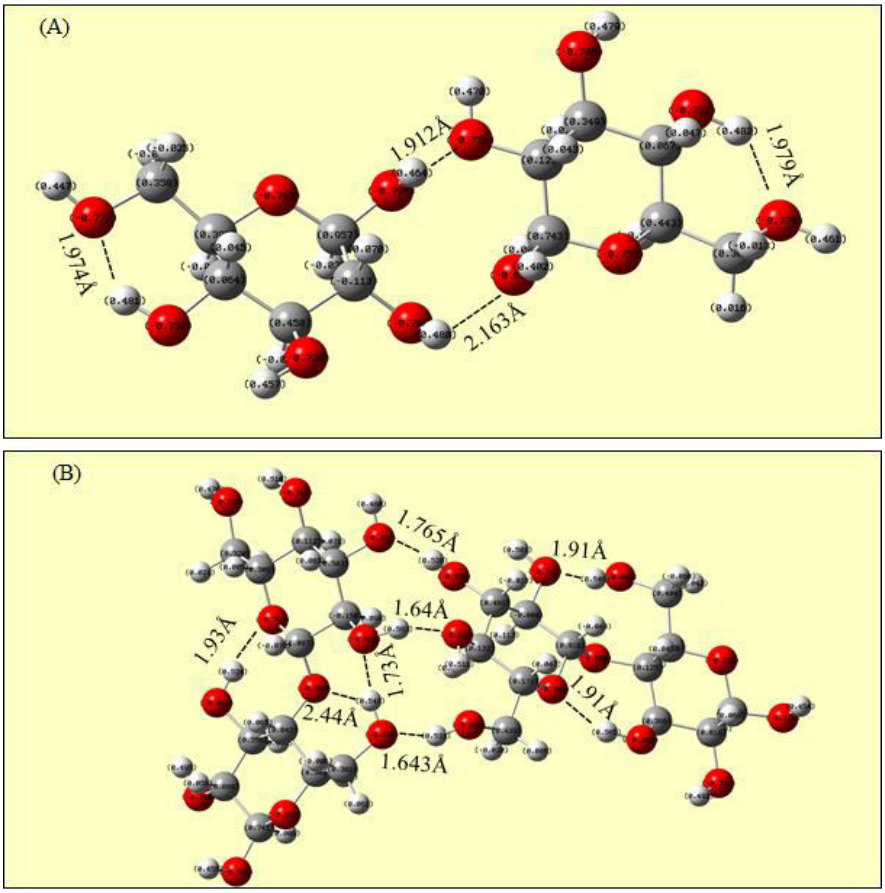

Figure III.11. The inter- and intra-hydrogen bonds in the A) glucose-glucose and B) cellulose-cellulose systems

III.4.3. Effect of water on IL-cellulose system

The presence of water affect the activity of the ILs because water exhibits a strong interaction with ILs, especially hydrophilic ILs, such as MPh^- and Cl^- anion based ionic liquids. Figure III.12 and table III.8 present the interaction energies and hydrogen bonds formed in the systems DMIMMPh-nH_2O and BMIMCl-nH_2O where n = 1 and 2. It demonstrates that the interaction energy tends to increase with the increase of the water content indicating that the higher the water content, the stronger the interaction with ionic liquids. For example, the values of

interaction energy obtained for the system composed of two water molecules in presence of BMIMCl is more important than the value obtained with the system {BMIMCl-cellulose}. This indicates that BMIMCl is available prior to interacting with a water molecule, resulting in the precipitation of the cellulose.

The influence of the water molecule on IL-cellulose is further investigated as follows: the optimized configuration of BMIMCl-cellulose was taken as an original configuration and a series of possible initial configurations are obtained by adding water molecules. All initial configurations are optimized and checked to be a true minimum through a frequency calculation. Subsequently, water molecules are removed from the optimized configurations, and then the interaction energies are carried out between the BMIMCl-cellulose. When two water molecules are added to the BMIMCl-cellulose system, the value of interaction energy of BMIMCl-cellulose is decreased of about 36 kJ mol^{-1}. This indicates that the hydrogen bonds between BMIMCl and cellulose are weaken or even destroyed by the addition of water, figure III.13. The hydrogen bonds in the cellulose-cellulose system formed again, resulting in the precipitation of the cellulose. Therefore, water could be used as an antisolvent for the regeneration of cellulose.

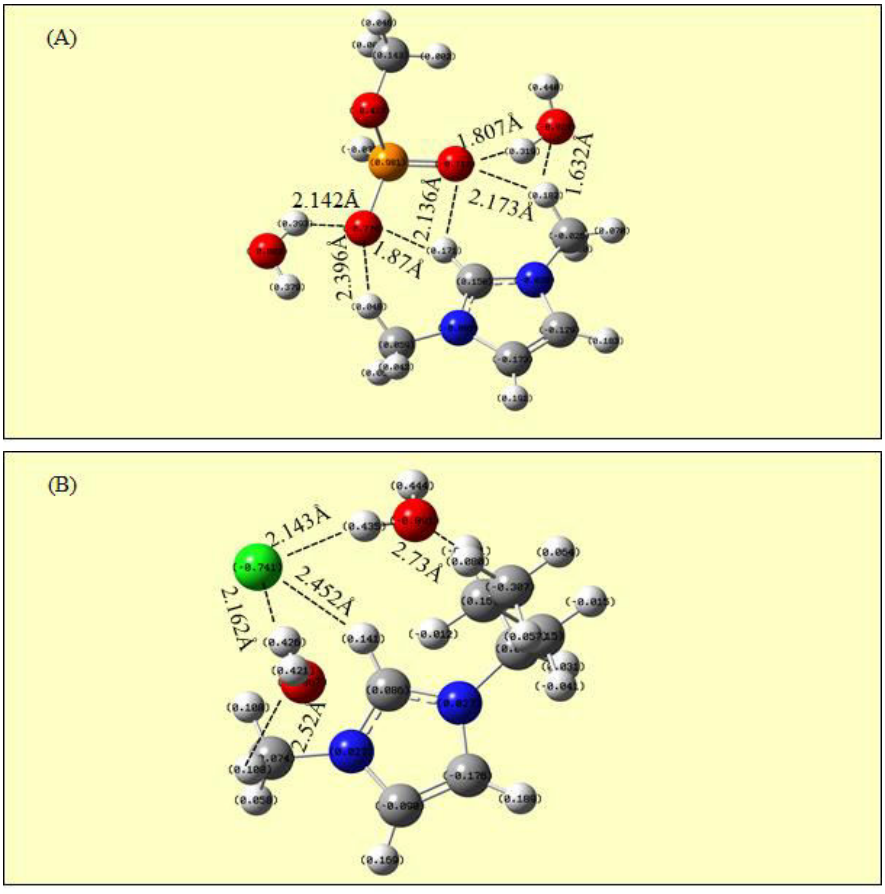

Figure III.12. Optimized structures of A) DMIMMPh-2H_2O and B) BMIMCl-2H_2O systems

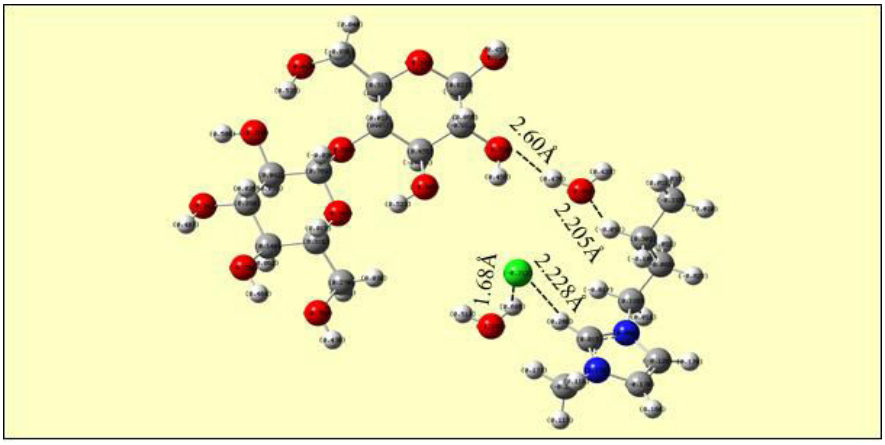

Figure III.13. The effect of water on cellulose-BMIMCl system

Table III.8. The results of IL-water systems

At level: B3LYP/6.311+G (d)	BMIMCl-H_2O	BMIMCl-2H_2O	DMIMMPh-H_2O	DMIMMPh-2H_2O
Total E (a. u.)	-959.882	-1036.294	-989.391	-1065.778
ΔE (KJ mol^{-1})	-85.631	-154.085	-129.436	-176.883
ΔE_{BSSE} (KJ mol^{-1})	1.476	2.250	1.669	2.378
ΔE_{ZPE} (KJ mol^{-1})	9.870	16.689	10.552	22.746
ΔE_{Corr} (KJ mol^{-1})	-74.285	-135.146	-117.215	-151.759
Hydrogen bond strength (Å)	1.98-2.61	2.14-2.73	1.87-2.15	1.63-2.39
Dipole moment (debye)	10.998	8.848	10.693	8.604

III.4.4. Experimental study on the dissolution and regeneration of cellulose

III.4.4.1. Solubility of cellulose in ionic liquids

Solid-liquid equilibria (SLE) of microcrystalline cellulose (MCC) and avicel cellulose (AvC) in ionic liquids, was carried out in a large range of temperature (313-393 K). The experimental results are presented in table III.9. It is obvious that the solubility of cellulose in imidazolium based ionic liquids increases in the following order EMIMSCN < EtOHMIMCl < BMIMCl < DMIMMPh. It was demonstrated from the ab initio calculation results that ionic liquids could dissolve cellulose molecules by disrupting their inter- and intra-molecular hydrogen bonding network and forming new IL-cellulose hydrogen bonds promoting their dissolution.

As expected from the theoretical results, it is found that the solubility of cellulose is higher in DMIMMPh than other ionic liquids and this maybe related to its high interaction energy, strong hydrogen bonding formation, with its high hydrogen bond basicity and polarity. It is indicated from ab initio calculations that the nature of the ionic liquid's anion significantly influence the interaction between ionic liquid and cellulose. The experimental studies confirm those observations. Strong H-bond-acceptor anions, such as phosphonate and chloride anions,

effectively dissolve cellulose. The solubility results of MCC and AvC in BMIMCl at 383 K are similar to the those published in the literature.[50] The solubility of MCC cellulose is slightly lower than that of AvC in studied ionic liquids and this maybe related to the higher particle size (≈80 µm) of MCC compared to AvC (≈50 µm).

As indicated in the ab initio results, water could be successfully used as an antisolvent for the regeneration of cellulose from ionic liquids. The regenerated cellulose was characterized with different techniques. Moreover, ionic liquids could be recycled by evaporating water under vacuum for reuse.

Table III.9. Solubility data of microcrystalline cellulose (MCC), avicel cellulose (AvC) and alkaline lignin in DMIMMPh, BMIMCl, EtOHMIMCl and EMIMSCN ionic liquids

DMIMMPh			
MCC		AvC	
Mass fraction	T/K	Mass fraction	T/K
1.001	313.15	1.001	314.15
3.000	335.65	3.033	334.70
5.001	350.45	5.009	348.15
8.003	363.10	8.005	361.85
10.037	372.30	10.073	369.00
12.036	380.00	12.007	379.35
13.047	383.15	14.002	383.25
BMIMCl			
MCC		AvC	
Mass fraction	T/K	Mass fraction	T/K
1.002	343.15	1.009	343.15
3.001	346.65	3.007	346.45
5.001	352.70	5.009	350.75
6.505	359.65	8.016	365.00
8.008	368.65	10.088	380.10
10.029	385.15	12.005	393.25
EtOHMIMCl			
MCC		AvC	
Mass fraction	T/K	Mass fraction	T/K
1.003	356.15	1.002	356.15
2.003	360.65	2.008	360.25
3.006	364.55	3.004	364.10
5.014	372.00	5.012	371.50
7.006	379.45	7.003	378.25
8.004	383.15	8.204	383.15
EMIMSCN			
MCC		AvC	
Mass fraction	T/K	Mass fraction	T/K
1.001	333.15	1.009	333.15
2.003	347.35	2.001	346.55
3.001	359.55	3.004	357.95
4.004	370.65	4.008	368.35
5.013	379.25	5.010	375.50
6.005	386.90	6.001	384.10

III.4.4.2. Characterization of the regenerated cellulose

The XRD, FTIR, NMR and SEM analyses are designed to determine whether the process of dissolution and regeneration of celullose in ionic liquids is accompanied with a physical change or chemical change.

The FTIR spectra of original MCC and regenerated celluloses presented in figure III.14 are similar, and there are no new peaks appearing in the spectrum of regenerated cellulose compared to the original one. The intensity of the broad band at the 3600-3100 cm^{-1} region, which is characteristic of hydrogen bonds from the spectra of regenerated cellulose, decreases and shifts to higher wave number values, compared to the original MCC. This could be correlated with the scission of the intra- and inter-molecular hydrogen bonds. The adsorption bands at the 1500-899 cm^{-1} region are strongly reduced in intensity. In addition, the intensity of the "crystallinity band"[51] at 1430 cm^{-1}, which assigned to a symmetric CH_2 bending vibration, decreased. This indicates the reduction in the degree of crystallinity of the regenerated cellulose. Moreover, the increase of the intensity of the FTIR amorphous" absorption band[51,52] at 898 cm^{1}, which assigned to C–O–C stretching at β-(1→4)-glycosidic linkages, indicates the formation of regenerated amorphous cellulose.

The XRD spectra of the original MCC and the regenerated cellulose are shown in figure III.15. The original MCC sample shows two prominent peaks near 2θ of 15° and 22° indicating the characteristic diffraction pattern of crystalline cellulose while the regenerated cellulose displays a slightly broad amorphous diffraction peak near 2θ of 21° indicating the formation of amorphus cellulose.[51,52]

The intensities of the FTIR and XRD peaks in the cellulose regenerated with DMIMMPh are smaller than cellulose regenerated with other ionic liquids. DMIMMPh is more efficient and hence destroy the inter and intramolecular hydrogen bonds among cellulose molecules, leading to lower crystallinity in the regenerated cellulose.[54]

Figure III.16 shows the NMR spectrum of original MCC and the regenerated cellulose. Results showed that the spectrum of microcrystalline cellulose have characteristic peaks at 105 (C_1), 89 (C_4, crystalline), 83 (C_4, amorphous), 72 and 75 (C_2, C_3 and C_5), 65 (C_6, crystalline) and 62 ppm (C_6, amorphous).[55,56] The spectrum of microcrystalline cellulose, contains all the characteristic peaks above, although the chemical shifts (ι) had ±1 ppm deviation. The peak of regenerated cellulose from DMIMMPh-IL solution highly weakened at 65 and 89 ppm, while enlarged at 62 ppm, which could be an evidence that crystallinity decreased. The spectra for both microcrystalline and regenerated cellulose are similar to each other, except for the characteristic

peaks of crystallinity. The crystallinity index value calculated with the NMR C_4 peak separation method or Newman's method[56] is about 74 for microcrystalline cellulose while it is only 32 for the regenerated cellulose.

Figure III.17 shows MEB images of the microcrystalline cellulose (MCC) and the regenerated cellulose. There is a difference between the highly intensive crystalline structure in microcrystalline cellulose (MCC) and the porous structure of the regenerated cellulose. The regenerated cellulose is amorphous, porous and with high surface area.

From the different analysis, it could be concluded that there are no chemical reactions occurring during the dissolution and regeneration process. This means that ionic liquids could be used as solvents for the recovery and regeneration of cellulose from biomass materials. The pretreated cellulose becomes more accessible to the enzymes that convert the carbohydrate polymers into fermentable sugars and hence for biofuel production.[57]

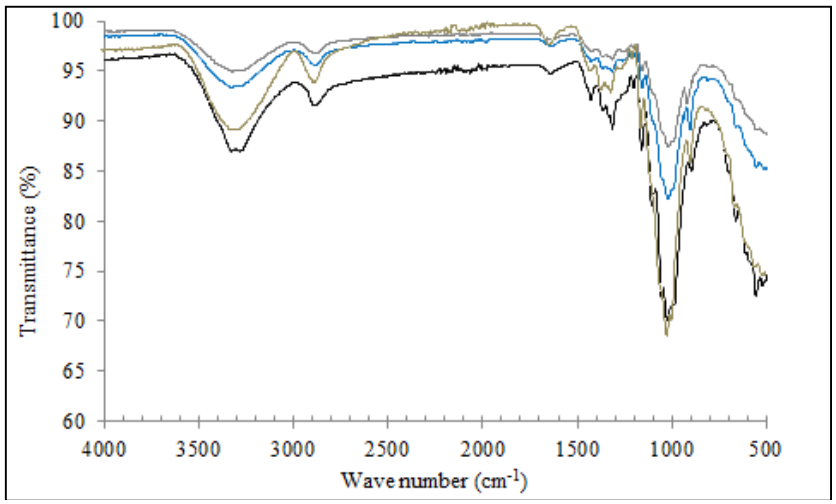

Figure III.14. FTIR of ■) microcrystalline cellulose and cellulose regenerated ■) EtOHMIMCl, ■) BMIMCl and ■) DMIMMPh ionic liquids

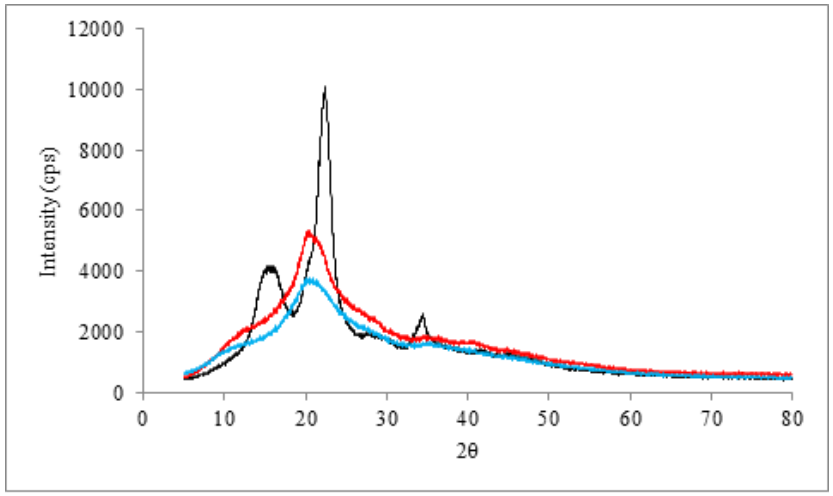

Figure III.15. XRD of ■) microcrystalline cellulose and cellulose regenerated ■) BMIMCl and ■) DMIMMPh ionic liquids

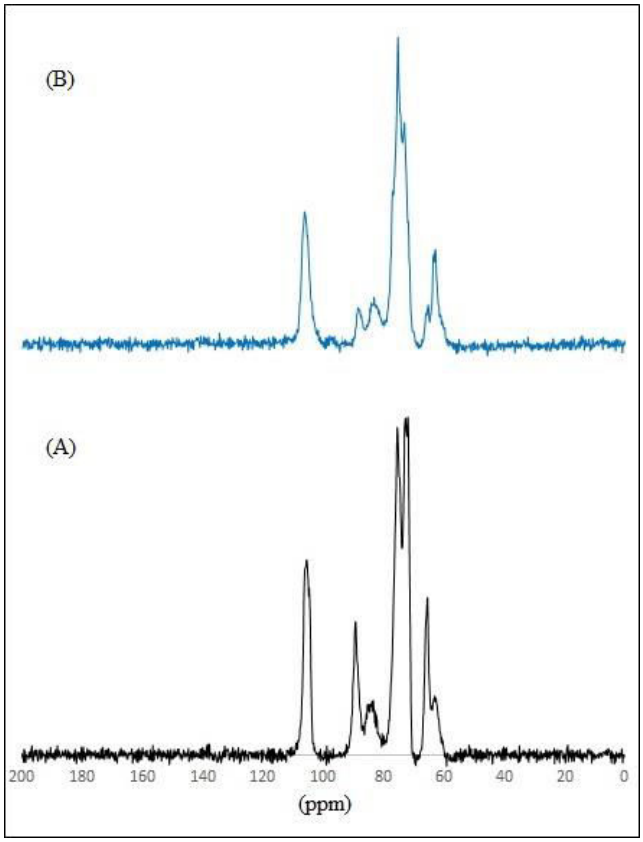

Figure III.16. ^{13}C CP/MAS NMR spectra of (A) microcrystalline cellulose and (B) regenerated cellulose

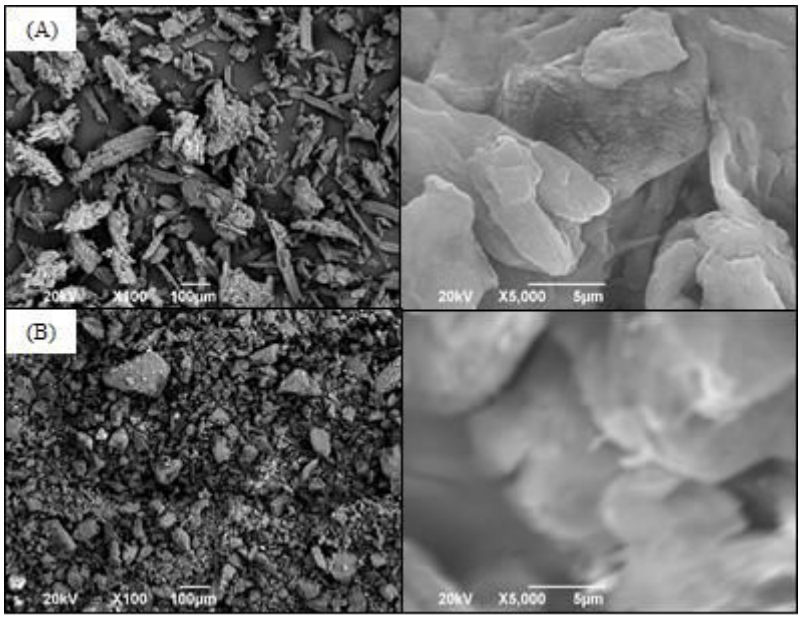

Figure III.17. MEB images of A) microcrystalline cellulose and B) regenerated cellulose

III.5. Conclusion

This study presents the geometry optimization of four imidazolium based ionic liquids DMIMMPh, BMIMCl, EtOHMIMCl and EMIMSCN. It is obvious that anions and cations of ionic liquids interact via hydrogen bonding formation. The interaction energy data and the possibility of hydrogen bonding formation of glucose and cellulose building unit with ionic liquids indicate that DMIMMPh is more efficient than other ionic liquids. This result is in a good agreement with the experimental data. It is also concluded that water could be used as an antisolvent for the regeneration of cellulose. The experimental results proved that the process of cellulose dissolution and regeneration using ionic liquids is accompanied only with a physical change.

References

[1] A. Khelassi-Sefaoui, F. Mutelet, I. Mokbel, J. Jose, L. Negadi, Measurement and correlation of vapour pressures of pyridine and thiophene with [EMIM][SCN] ionic liquid, J.Chem.Thermodynamics, 72 (2014) 134-138.

[2] H. A. Weingaertner, Understanding ionic liquids at the molecular level: facts, problems and controversies, Chem., Int. Ed., 47 (2008) 654-670.

[3] F. Mutelet, El-Sayed R. E. Hassan, T. W. Stephens, W. E. Acree, G. A. Baker, Activity coefficients at infinite dilution for organic solutes dissolved in three 1-alkyl-1-methylpyrrolidinium bis(trifluoromethylsulfonyl)imide ionic liquids bearing short linear alkyl side chains of three to five carbons, J. Chem. Eng. Data, 58 (2013) 2210-2218.

[4] W. Leitner, A greener solution, Nature, 423 (2003) 930-931.

[5] W. L. Wong, P-H. Chan, Z.-Y. Zhou, K.-H. Lee, K.-C. Cheung, K.-Y. Wong, A Robust ionic liquid as reaction medium and efficient organocatalyst for carbon dioxide fixation, ChemSusChem, 1 (2008) 67-70.

[6] C. Thurier, C. Fischmeister, C. Bruneau, H. Olivier-Bourbigou, P. H. Dixneuf, Ethenolysis of Methyl Oleate in Room-Temperature Ionic Liquids, ChemSusChem, 1 (2008) 118-122.

[7] E. R. Cooper, C. D. Andrews, P. S. Wheatley, P. B. Webb, P. Wormald, R. E. Morris, Ionic liquids and eutectic mixtures as solvent and template in synthesis of zeolite analogues, Nature, 430 (2004) 1012-1016.

[8] W. Xu, E. I. Cooper, C. A. Angell, Ionic Liquids: Ion Mobilities, Glass Temperatures, and Fragilities, J. Phys. Chem. B, 107 (2003) 6170-6178.

[9] J. Kiefer, K. Obert, A. Bçsmann, T. Seeger, P. Wasserscheid, A. Leipertz, Quantitative analysis of alpha-d-glucose in an ionic liquid by using infrared spectroscopy, Chem. Phys. Chem., 9 (2008) 1317-1322.

[10] P. A. Hunt and I. R. Gould, Structural characterization of the 1-butyl-3-methylimidazolium chloride ion pair using ab initio methods, J. Phys. Chem. A, 110 (2006) 2269-2282.

[11] W. Ji, Z. Ding, J. Liu, Q. Song, X. Xia, H. Gao, H. Wang, W. Gu, Mechanism of lignin dissolution and regeneration in ionic liquid, Energy Fuels, 26 (2012) 6393-6403.

[12] F. van Rantwijkl, R. M. Lau, R. A. Sheldon, Biocatalytic transformations in ionic liquids, Trends Biotechnol., 21 (2003) 131-138.

[13] S. Park, R. J. Kazlauskas, Biocatalysis in ionic liquids - advantages beyond green technology, Curr. Opin. Biotechnol., 14 (2003) 432-437.

[14] U. Kragl, M. Eckstein, N. Kaftzik, Enzyme catalysis in ionic liquids, Curr. Opin. Biotechnol., 13 (2002) 565-571.

[15] R. A. Sheldon, R. M. Lau, M. J. Sorgedrager, F. van Rantwijk, K. R. Seddon, Biocatalysis in ionic liquids, Green Chem., 4 (2002) 147-151.

[16] Z. Yang, W. B. Pan, Ionic liquids: Green solvents for nonaqueous biocatalysis, Enzyme Microb. Technol., 37 (2005) 19-28.

[17] S. H. Lee, D. T. Dang, S. H. Ha, W-J. Chang, Y-M. Koo, Lipase-catalyzed synthesis of fatty acid sugar ester using extremely supersaturated sugar solution in ionic liquids, Biotechnol. Bioeng., 99 (2008) 1-8.

[18] R. P. Swatloski, S. K. Spear, J. D. Holbrey, R. D. Rogers, Dissolution of cellulose with ionic liquids, J. Am. Chem. Soc., 124 (2002) 4974-4975.

[19] B. Kosan, C. Michels, F. Meister, Dissolution and forming of cellulose with ionic liquids, Cellulose, 15 (2008) 59-66.

[20] Y. Fukaya, K. Hayashi, M. Wada, H. Ohno, Cellulose dissolution with polar ionic liquids under mild conditions: required factors for anions, Green Chem., 10 (2008) 44-46.

[21] M. B. Turner, S. K. Spear, J. D. Holbrey, D. T. Daly, R. D. Rogers, Ionic liquid-reconstituted cellulose composites as solid support matrices for biocatalyst immobilization, Biomacromolecules, 6 (2005) 2497-2502.

[22] M. Bagheri, H. Rodriguez, R. P. Swatloski, S. K. Spear, D. T. Daly, R. D. Rogers, Ionic liquid-based preparation of cellulose-dendrimer films as solid supports for enzyme immobilization, Biomacromolecules, 9 (2008) 381-387.

[23] I. Kilpeläinen, H. Xie, A. King, M. Granstrom, S. Heikkinen, D. S. Argyropoulos, Dissolution of wood in ionic liquids, J. Agric. Food Chem., 55 (2007) 9142-9148.

[24] D. A. Fort, R. C. Remsing, R. P. Swatloski, P. Moyna, G. Moyna, R. D. Rogers, Can ionic liquids dissolve wood? Processing and analysis of lignocellulosic materials with 1-n-butyl-3-methylimidazolium chloride, Green Chem., 9 (2007) 63-69.

[25] Y. Pu, N. Jiang, A. J. Ragauskas, Ionic liquid as a green solvent for lignin, J. Wood Chem. Technol., 27 (2007) 23-33.

[26] P. Kolle, R. Dronskowski, Hydrogen Bonding in the Crystal Structures of the Ionic Liquid Compounds Butyldimethylimidazolium Hydrogen Sulfate, Chloride, and Chloroferrate(II,III), Inorg. Chem., 43 (2004) 2803-2809.

[27] A. Wulf, K. Fumino, R. Ludwig, Spectroscopic evidence for an enhanced anion-cation interaction due to hydrogen bonding in pure imidazolium Ionic Liquids, Angew. Chem. Int. Ed., 49 (2010) 449-453.

[28] R. C. Remsing, J. L. Wildin, A. L. Rapp, G. Moyna, Hydrogen-bonding in ionic liquids revisited: An NMR study of deuterium isotope effects in 1-n-butyl-3-methylimidazolium Chloride, J. Phys. Chem. B, 111 (2007) 11619-11621.

[29] K. Dong, S. J. Zhang, D. X. Wang, X. Q. Yao, Hydrogen bonds in imidazolium ionic liquids, J. Phys. Chem. A, 110 (2006) 9775-9782.

[30] K. Fumino, A. Wulf, R. Ludwig, The cation-anion interaction in ionic liquids probed by far-infrared spectroscopy, Angew. Chem. Int. Ed., 47 (2008) 3830-3834.

[31] H. Ohno, Y. Fukaya, Task specific ionic liquids for cellulose technology, Chem. Lett., 38 (2009) 2-7.

[32] S. Zhang, X. Qi, X. Ma, L. Lu, Q. Zhang, Y. Deng, Investigation of cation-anion interaction in 1-(2-hydroxyethyl)-3-methylimidazolium-based ion pairs by density functional theory calculations and experiments, J. Phys. Org. Chem., 25 (2012) 248-257.

[33] H. Xu, W. Pan, R. Wang, D. Zhang, C. Liu, Understanding the mechanism of cellulose dissolution in 1-butyl-3-methyl imidazolium chloride ionic liquid via quantum chemistry calculations and molecular dynamics simulations, J Comput Aided Mol Des, 26 (2012) 329-337.

[34] M. J. Frisch, G. W. Trucks, H. B. Schlegel, G. E. Scuseria, M. A. Robb, J. R. Cheeseman, J. A. Montgomery, Jr., T. Vreven, K. Kudin, J. C. N. Burant, J. M. Millam, S. S. Iyengar, J. Tomasi, V. Barone, B. Mennucci, M. Cossi, G. Scalmani, N. Rega, G. A. Petersson, H. Nakatsuji, M. Hada, M. Ehara, K. Toyota, R. Fukuda, J. Hasegawa, M. Ishida, T. Nakajima, Y. Honda, O. Kitao, H. Nakai, M. Klene, X. Li, J. E. Knox, H. P. Hratchian, J. B. Cross, C. Adamo, J. Jaramillo, R. Gomperts, R. E. Stratmann, O. Yazyev, A. J. Austin, R. Cammi, C. Pomelli, J. W. Ochterski, P. Y. Ayala, K. Morokuma, G. A. Voth, P. Salvador, J. J. Dannenberg, V. G. Zakrzewski, S. Dapprich, A. D. Daniels, M. C. Strain, O. Farkas, D. K. Malick, A. D. Rabuck, K. Raghavachari, J. B. Foresman, J. V. Ortiz, Q. Cui, A. G. Baboul, S. Clifford, J. Cioslowski, B. B. Stefanov, G. Liu, A. Liashenko, P. Piskorz, I. Komaromi, R. L. Martin, D. J. Fox, T. Keith, M. A. Al-Laham, C. Y. Peng, A. Nanayakkara, M. Challacombe, P. M. W. Gill, B. Johnson, W. Chen, M. W. Wong, C. Gonzalez, J. A. Pople, Gaussian 03, revision E.01, Gaussian, Inc.: Pittsburgh, PA, 2003.

[35] A. D. Becke, Density-functional thermochemistry. III. The role of exact exchange, J. Chem. Phys., 98 (1993), 5648-5652.

[36] C. Lee, W. Yang, R. G. Parr, Development of the colle-salvetti correlation-energy formula into a functional of the electron density, Phys. Rev. B, 37 (1988) 785-789.

[37] S. H. Vosko, L. Wilk, M. Nusair, Accurate spin-dependent electron liquid correlation energies for local spin density calculations: a critical analysis, J. Phys. Chem., 58 (1980) 1200−1211.

[38] P. J. Stephens, F. J. Devlin, C. F. Chabalowski, M. J. Frisch, Ab initio calculation of vibrational absorption and circular dichroism spectra using density functional force fields, J. Phys. Chem., 98 (1994) 11623-11627.

[39] Z. D. Ding, Z. Chi, W. X. Gu, S. M. Gu, J. H. Liu, H. J. Wang, Theoretical and experimental investigation on dissolution and regeneration of cellulose in ionic liquids, Carbohydrate Polymers, 89 (2012) 7-16.

[40] X. L. Zhang, W. H. Yang, W. Blasiak, Modeling study of woody biomass: Interactions of cellulose, hemicellulose, and lignin, Energy Fuels, 25 (2011) 4786-4795.

[41] C. M. Breneman, K. B. Wiberg, Determining atom-centered monopoles from molecular electrostatic potentials: The need for high sampling density in formamide conformational analysis, J. Comp. Chem., 11 (1990) 361-373.

[42] J. Zhou, J. Mao, S. Zhang, Ab initio calculations of the interaction between thiophene and ionic liquids, Fuel Processing Technology, 89 (2008) 1456-1460.

[43] C. Chiappe, D. Pieraccini, Ionic liquids: solvent properties and organic reactivity, J. Phys. Org. Chem., 18 (2005) 275-297.

[44] J. S. Wilkes, M. J. Zaworotko, Air and water stable 1-ethyl-3-methylimidazolium based ionic liquids, J. Chem. Soc. Chem. Commun., 13 (1992) 965-967.

[45] P. B. Hitchcock, K. R. Seddon, T. Welton, Hydrogen-bond acceptor abilities of tetrachlorometallate (II) complexes in ionic liquids, J. Chem. Soc., Dalton Trans, 17 (1993) 2639-2643.

[46] G. A. Jeffrey, The ups and downs of C–H hydrogen bonds, J. Mol. Structure, 485-486 (1999) 293-298.

[47] A. Casas, J. Palomar, M. V. Alonso, M. Oliet, S. Omar, F. Rodriguez, Comparison of lignin and cellulose solubilities in ionic liquids by COSMO-RS analysis and experimental validation Ind. Crops Prod., 37 (2012) 155-163.

[48] El-Sayed R. E. Hassan, F. Mutelet, S. Pontvianne, J-C. Moise, Studies on the dissolution of glucose in ionic liquids and extraction using the antisolvent method, Environ. Sci. Technol., 47 (2013) 2809-2816.

[49] El-Sayed R. E. Hassan, F. Mutelet, J-C. Moise, From the dissolution to the extraction of carbohydrates using ionic liquids, RSC Adv., 3 (2013) 20219-20226.

[50] H. Wang, G. Gurau, R. D. Rogers, Ionic liquid processing of cellulose, Chem. Soc. Rev., 41 (2012) 1519-1537.

[51] D. Ciolacu, F. Ciolacu, V. I. Popa, Amorphus cellulose-structure and characterization, Cellulose Chem. Technol., 45 (2011) 13-21.

[52] W-Z. Li, M-T. Ju, Y-N. Wang, L. Liu and Y. Jiang, Separation and recovery of cellulose from Zoysia japonica by 1-allyl-3-methylimidazolium chloride, Carbohydrate Polymers, 92 (2013) 228- 235.

[53] P. Mansikkamaki, M. Lahtinen, K. Rissanen, Structural changes of cellulose crystallites induced by mercerisation in different solvent systems; determined by powder X-ray diffraction method, Cellulose, 12 (2005) 233-242.

[54] X. Wanga, H. Li, Y. Cao, Q. Tang, Cellulose extraction from wood chip in an ionic liquid 1-allyl-3-methylimidazolium chloride (AmimCl), Bioresource Tech., 102 (2011) 7959-7965.

[55] R. H. Newman, Homogeneity in cellulose crystallinity between samples of Pinus radiata wood, Holzforschung, 58 (2004) 91-96.

[56] H. Lateef, S. Grimes, P. Kewcharoenwong, B. Feinberg, Separation and recovery of cellulose and lignin using ionic liquids: a process for recovery from paper-based waste, J. Chem. Technol. Biotechnol., 84 (.2009) 1818-1827.

[57] H. Tadesse, R. Luque, Advances on biomass pretreatment using ionic liquids: An overview, Energy Environ. Sci., 4 (2011) 3913-3929.

Chapter IV. Use of Ionic Liquids in the Pretreatment of Miscanthus for Biofuel Production

Biomass, as fuel source, is renewable, environmentally friendly and abundant in the natural world. It is of great interest to produce green energy and bio-products from lignocellulose which contains up to 35-50% cellulose. Miscanthus is a promising biomass energy crop due to its relatively low maintenance and high energy content. This chapter presents an environmentally friendly method of extracting cellulose from miscanthus using imidazolium based ionic liquids, and also provides a new approach for utilizing biomass resources. The parameters affecting the extraction process are the ionic liquid structure, miscanthus mass fraction, temperature, and time. The regenerated cellulose could be hydrolyzed efficiently into glucose using cellulase enzyme with glucose hydrolysis efficiency exceeds 97%. The hydrolysate is converted successfully into bioethanol with fermentation using saccharomyces cerevisaie yeast with an ethanol conversion rate reaches up to 90%.

IV.1. Introduction

Biomass, the sustainable resource, has obvious potential as a renewable starting material for the production of fuel-grade ethanol and materials according to the biorefinery philosophy.[1,2] Lignocellulosic biomass is capable of delivering liquid fuels and chemical products on a large scale. The major constituents lignocellulosic feedstock are cellulose, hemicellulose, and lignin.[3] Indeed, Production of ethanol from sugars or starch negatively impacts the economics of the process, thus making ethanol more expensive compared with fossil fuels. Hence, the technology development of producing ethanol has shifted towards the utilization of lignocellulosic materials to lower production costs.[4] Pretreatment is considered to be a major unit operation in a biorefinery to convert lignocellulosic biomass into bio-ethanol, which accounts for 16–19% of its total capital.[5,6] Bioethanol production from cellulosic materials mainly consists of three steps: the first step is the pretreatment of lignocellulose to enhance the enzymatic digestibility of polysaccharide components; the second step is the hydrolysis of cellulose and hemicellulose to fermentable sugars; and the third step is the fermentation of these sugars into liquid fuels.[7-10]

Among biomass feedstocks, miscanthus has attracted considerable attention as a possible dedicated energy crop. Indeed, miscanthus could be an interesting raw material for industrial bioconversion processes, as its carbohydrate content reaches up to 75%.[11] Miscanthus primarily consists of a complex mixture of lignin, hemicellulose, and semi crystalline cellulose. Pretreatment of miscanthus is required to disrupt the lignin-carbohydrate complex, decrease cellulose crystallinity and partially remove lignin and hemicelluloses. The pretreated cellulose becomes more accessible to the enzymes that convert the carbohydrate polymers into fermentable sugars.[3,12]

Different technologies have been reported for the pretreatment of miscanthus such as one-step extrusion/sodium hydroxide,[13] ammonia fiber expansion,[14] dilute acid pre-soaking combined with wet explosion,[15] sodium chlorite,[16] ethanol organosolv process,[11] a procedure using a mixture of acetic acid/hydrochloric acid or formic acid/hydrochloric acid,[17] and soaking in aqueous ammonia.[18] These technologies give good results concerning the sugar conversion, while a full recovery of the lignocellulosic components should be one of the major goals of optimizing the conversion of biomass to ethanol. Thus, the main goal of the pretreatment process is to recover the cellulose in an amorphous form and free from lignin as possible, thereby facilitating its enzymatic hydrolysis and to develop a process that could be applied at the industrial scale.[11]

Ionic liquids (ILs) as design solvents demonstrate a great variety of physicochemical properties. Their most common properties are: high polarity,[19] great thermal stability,[20] high conductivity, large electrochemical window, great solvent power,[21] negligible volatility, and nonflammability.[22] These unique properties of ionic liquids allow their use in biomass pretreatment and extraction processes.[23–26] ILs have the ability to dissolve biomass by an effective disruption of the complex network of noncovalent interactions between carbohydrates and lignin.[27] The most commonly used ionic liquids for this application are based on imidazolium cations (e.g. 1-butyl, 3- methyl imidazolium chloride (BMIMCl), and 1-ethyl-3-methylimidazolium acetate (EMIMOAc). Cellulose could be precipitated efficiently from IL solution using the antisolvent method. An antisolvent is added to the solution mixture, promoting carbohydrate precipitation as a recovered material. Lignin and other soluble compounds are partially extracted to the liquid phase.[28] Lignin can be further recovered from the antisolvent/IL mixture using ethanol.[29,30] The cellulose-rich extract is significantly less crystalline, has a higher surface area and is very susceptible to enzymatic hydrolysis. Indeed, a small number of studies has been published on the ionic liquid-pretreatment, enzymatic hydrolysis and fermentation of miscanthus. K. Shill et al., 2010,[31] studied the solubility of miscanthus in EMIMAOC ionic liquid. The lignin was partially removed and the hydrolysis conversion rate reached up to 100% at time 44 hr and temperature 343 K using a 40 wt% K_3PO_4 solution as an antisolvent. H. Rodriguez et al., 2011,[32] studied the enhancement of miscanthus delignification via the addition of gaseous ammonia or oxygen. The preatreatment with EMIMOAC, at 9 bar absolute air, or ammonia, or oxygen, or a combination of both at temperature 413K for 3hr, gives a final product of 10% lignin content. Padmanabhan et al., 2011,[33] found that acetate, chloride and phosphate imidazolium based ionic liquids could dissolve miscanthus up to 5%. In 2012, S. Padmanabhan et al.[34] also studied the miscanthus delignification using ethylenediamine solvent mixtures. They were able to remove up to 78% of lignin from miscanthus at 343 K without disrupting the cellulose structure.

Enzymatic hydrolysis process has many advantages such as the very mild conditions (pH = 4.8 and temperature 323K) which give high yields. The maintenance costs are low compared to alkaline and acid hydrolysis due to no corrosion problems.[35, 36] Hydrolysis without preceding pre-treatment yields typically lower than 20%, whereas yields after pre-treatment often exceed 90%.[37] Enzymatic hydrolysis is attractive because it produces better yields than acid-catalyzed hydrolysis and enzyme manufacturers have recently reduced costs substantially using modern biotechnology.[38,39]

Yeast is currently the most popular method for converting cellulosic sugars into ethanol. The

most common type of yeast used is Saccharomyces cerevisiae, also known as Brewer's yeast or Baker's yeast.[40] S. cerevisiae has a relatively high tolerance to ethanol and inhibitor compounds. Furthermore, this yeast gives high ethanol yields from glucose. Similar to most bacteria, this yeast is unable to ferment xylose and other pentose sugars efficiently.[40]

This study is mainly divided into five parts, the first part aims to study the influence of the structure of imidazolium based ionic liquids on the solubility of miscanthus in a temperature range from 363 K to 403 K. Solubility data have been compared with those in the literature. The ionic liquids used in this work are 1-butyl-3-methylimidazolium chloride (BMIMCl), 1-ethanol-3-methylimidazolium chloride (EtOHMIMCl) 1,3-dimethyl-imidazolium methyl phosphonate (DMIMMPh) and 1-ethyl-3-methylimidazolium thiocyanate (EMIMSCN). The second part of the article is devoted to the evaluation of the extraction of cellulose from ionic liquids using the antisolvent method. The influence of different parameters such as miscanthus size, miscanthus weight %, temperature, time, precipitant type, and the structure of the IL on the performance of the extraction were evaluated. A Box-Benhken design expert was applied to evaluate the best conditions for the extraction of cellulose from miscanthus using the ionic liquids 1-butyl-3-methylimidazolium chloride and 1,3-dimethyl-imidazolium methyl phosphonate. In the third part, we studied the influence of the dissolution of miscanthus in a mixture of {ethylene diamine + dimethyl sulfoxide} as a step prior to the addition of ionic liquids in order to enhance the delignification process.

Then, a characterization study using various analytical techniques such as X-ray diffraction, Infra-red spectra, scanning electron microscope, was performed to evaluate the efficiency of the produced cellulose for biofuel production.

In the last part, the produced amorphous cellulose is subjected to hydrolysis and fermentation for biofuel production. Hydrolysis yield and ethanol conversion rate were estimated in order to evaluate the different processes.

IV.2. Experimental techniques

IV.2.1. Materials and miscanthus preparation

Miscanthus x Gigantus (MxG) was harvested in spring 2009 at a local site from Courcelles-Chaussy (France). The dried miscanthus was milled to a particle size below 3 mm using a Wiley mill. Miscanthus samples were screened to different sizes: 2-1mm, 1-0.4mm, 0.4-0.2mm, 0.2-0.08mm, 0.08-0.04mm, and <0.04mm particles.

Ash and extractables removal for miscanthus was obtained via the treatment with water for 5 minutes at temperature 383.15 K. Then, miscanthus was dried in an oven at 383.15 K for 2 days. The oven-dried samples were stored in a dessicator to avoid moisture. Table 4 shows the composition of miscanthus before and after ash and extractables removal process.
Ethyl alcohol absolute with a mass fraction purity of 0.999 was from Carlo Erba. Acetonitrile with a mass fraction purity of 0.999 was from Sigma-Aldrich. Ethylene diamine (EDA) and Ethylene glycol (EG) with a mass fraction purity of 0.995 were purchased from Fluka. Dimethyl sulfoxide (DMSO) with a mass fraction purity of 0.998 was purchased from Fisher Scientific. The ionic liquids used in this work, 1-butyl-3-methylimidazolium chloride (BMIMCl), 1-ethanol-3- methylimidazolium chloride (EtOHMIMCl) and 1,3-dimethyl-imidazolium methyl phosphonate (DMIMMPh) with purity 98%, were from Solvionic, and 1-ethyl-3-methylimidazolium thiocyanate (EMIMSCN) with purity 95% was from Sigma Aldrich. These ionic liquids were dried under vacuum for 3 hours at 343 K before use.

Cellulase Enzymes: Cellulases from T. reesei (Celluclast 1.5L Product # C2730-50mL) and β-glucosidase (Novo188 Product # C6105-50mL) were purchased from Sigma Aldrich. The activity of the Celluclast 1.5L was reported to be 800EGU/g, and of Novo188 to be 258CBU/g. The IUPAC Filter Paper Assay was performed on the Celluclast 1.5L and found to be 130 FPU/mL of solution. [41]

IV.2.2. Miscanthus dissolution

Solid-liquid equilibrium phase diagrams of the {miscanthus-ILs} systems were obtained at atmospheric pressure and at temperature ranges starting from 363 to 403 K. A desired amount of IL and miscanthus were loaded into a prepared jacketed glass cell. The cell was sealed and connected to the temperature controller. The mixture was vigorously stirred at desired temperatures. A dark viscous miscanthus suspension was obtained. The solution was centrifuged to determine if any solid residues remained. The solubility measurements were confirmed by the visual observation of the solution under microscope. The miscanthus dissolution was calculated according to equation 1.

IV.2.3. Cellulose extraction and residue separation

For the extraction of cellulose, dimethyl sulfoxide (DMSO) was added to ILs (20: 80 wt %) to form a clear solution with stirring. The use of DMSO as a co-solvent has no noticeable effect on the solubility of carbohydrates in ionic liquids and reduces the viscosity of the mixtures.[42] Although DMSO is a solvent for carbohydrate-free lignin, native lignin in miscanthus has a

complex structure with many linkages between the lignin units and between lignin and carbohydrates, which prevent it from dissolution in DMSO.[43] A 3 wt % miscanthus was dissolved in IL/DMSO solution, after dissolution, the suspension was filtered through a glass filter to remove the undissolved residue. Water was added to the resulting clear liquors and a cellulose-rich extract was reconstituted from the liquor. This extract and the undissolved residue were respectively washed with water until the IL was completely removed and then dried overnight in an oven at 373 K prior to use. The miscanthus dissolution rate, the regeneration rate, the recovery of miscanthus components and the mass loss were calculated as following:

$$R_{diss}\,(\%) = [(M_o - M_r) / M_o] \times 100 \qquad \text{(IV.1)}$$

$$R_{reg}\,(\%) = (M_{ex} / M_o) \times 100 \qquad \text{(IV.2)}$$

$$\text{Recovery}_{(cell)}\,(\%) = [\,(M_{ex} \times C_{ex\text{-}cell})\ /\ (M_o \times C_{o\text{-}cell})] \times 100 \qquad \text{(IV.3)}$$

$$\text{Mass loss}\,(\%) = [M_o - (M_{ex} + M_r + M_{lig\text{-}ex})] \times 100 \qquad \text{(IV.4)}$$

Where: R_{diss} is the rate of dissolution, R_{reg} is the rate of regeneration, $\text{Recovery}_{(cell)}$ is the recovery of cellulose, M_o is the mass of the original miscanthus added, M_r is the mass of residue, M_{ex} is the mass of cellulose-rich extract, $M_{lig\text{-}ex}$ is the lignin-rich extract, $C_{o\text{-}cell}$ is the cellulose content in the original miscanthus and $C_{ex\text{-}cell}$ is the cellulose content in the extract. The recovery of hemicellulose and lignin were calculated in a similar way to the recovery of cellulose.

IV.2.4. Enhancement of miscanthus delignification

Miscanthus delignification studies were performed using three EDA-containing solvent mixtures as shown in table IV.11. The mass ratio of solvent to miscanthus (10:1) was loaded into a prepared cell. The cell was sealed and connected to the temperature controller. The mixture was vigorously stirred at temperature 348 K during 4 hr. The suspension was cooled to room temperature and filtered. The solid residue was washed several times with water to remove any residual solvent. As EDA–containing solvent is alkaline pH (≈12), washing was continued until the pH of the wash became neutral. The recovered solid residue was dried in a vacuum oven at 383 K. The filtrate was acidified to pH 2.0 with a 1 M HCl to precipitate the lignin-rich material.

IV.2.5. Determination of cellulose, lignin and hemicelluloses content

IV.2.5.1. Determination of lignin content

The acid-insoluble lignin content in the raw and the pretreated miscanthus was determined by using two-step acid hydrolysis according to the laboratory analytical procedure (LAP) provided by the National Renewable Energy Laboratory (NREL).[44,45] Firstly, 1.5 ml of a 72% (w/w) H_2SO_4 solution was added to 0.10 g of extracted miscanthus sample in a 50 ml conical flask. Hydrolysis was carried out for 2 h in a water bath shaker at 303 K and 150 rpm. Upon completion, 56 ml of deionized water was added to dilute the acid to a final concentration of 4% (w/w). Then, second hydrolysis was carried out by autoclaving the reaction mixture at a temperature of 394 K and pressure at 2 atm during 1 h in an autoclave. The solid residue remaining after the two-step hydrolysis was filtered and dried overnight in an oven to constant weight. The dried residue which is acid insoluble lignin was further placed in a furnace at 823 K for 2 h to determine the acid-insoluble ash content. The percentage of acid insoluble lignin, Kalson lignin, was calculated and corrected for the ash content. The acid-soluble lignin content was determined from absorbance at 280 nm.[31]

IV.2.5.2. Determination of cellulose content

Cellulose content of raw and pretreated miscanthus samples was determined using cellulose isolation method as described in Sun et al.[46] An acetic/nitric acid reagent consisting of 80% acetic acid and concentrated nitric acid in a ratio of 10:1 (v/v) was prepared. 0.10 g of extracted miscanthus sample was weighed into 15 ml conical tubes with known weight. Subsequently, 3 ml of acetic/nitric reagent was added into each tube and mixed vigorously. The tubes were capped and heated for 10 min at 383 K. Reaction was continued for 30 min at 393 K. Once completed, the tubes were cooled and 10 ml of deionized water was added. The treatment with acetic/nitric reagent efficiently removed lignin and hemicellulose in the sample, leaving cellulose in the mixture, which was obtained by centrifugation at 4000 rpm for 20 min (Centrifuge 5810, Eppendorf). Supernatant was decanted and the residue was washed twice with deionized water and centrifuged. Residue was then dried in the tube at 333 K in an oven during 24 h. Cellulose content in the samples is determined by gravimetric analysis.

IV.2.5.3. Determination of hemicellulose content

The hemicellulose content in the sample was obtained by the difference between the holocellulose and cellulose contents. Therefore, holocellulose, which is the sum of hemicellulose and cellulose in the biomass, was first determined according to the sodium chlorite method reported by Teramoto et al.[47] In few words, 0.5 g of the extracted miscanthus sample was treated with 30 ml of deionized water containing 0.04 ml of acetic acid and 0.4 g of sodium chlorite ($NaClO_2$) for 1 h at 348 K. Subsequently, 0.04 ml of acetic acid and 0.2 g of $NaClO_2$ were added to the mixture every 1 h for 3 h. Once completed, the residue was filtered, washed with deionized water and acetone, and then dried overnight to constant weight. The solid residue obtained after the reaction with $NaClO_2$ in acetate buffer was weighed and hemicellulose content was determined from the difference between holocellulose and cellulose content.

IV.2.6. Charecterization of the regenerated cellulose-rich extract

IV.2.6.1. XRD analysis

X-ray diffraction (XRD) for the untreated miscanthus, cellulose-rich extracts and residues were determined with Cu Ka1 radiation at 30 kV and 15 mA. Patterns were recorded in the range of 2θ = 5 - 80 degree with a scan speed of 1degree.min^{-1}, using a Rigaku MiniFlex II X-ray diffractometer.

The crystallinity index, CrI, was estimated using Segal's method[48,49] as following:

$$CrI = [(I_{002} - I_{am}) / I_{002}] \times 100 \quad \text{(IV.5)}$$

Where: I_{002}: is the highest peak intensity of the crystalline fractions at 2θ = 22.5 degree; I_{am}: is the low intensity peak of amorphous region at 2θ = 18 degree.

IV.2.6.2. NMR analysis

Untreated and treated miscanthus samples ground to pass a 40-mesh screen, were packed in 4-mm-diameter zirconium oxide rotors fitted with Kel-F caps for solid-state nuclear magnetic resonance (NMR) analysis. Cross-polarization/magic angle spinning (CP/MAS) ^{13}C NMR experiments were performed on a Bruker Avance-400 spectrometer operating at a ^{13}C frequency of 100.59 MHz. Glycine was used for the Hartman-Hahn matching procedure and as an external

standard for the calibration of the chemical shift scale relative to tetramethylsilane. All spectra were acquired at ambient temperature using a Bruker 4-mm MAS probe.
The crystallinity index, CrI, was estimated using Newman's method[49,50] as following:

$$CrI = [A_{CrC} / (A_{CrC} + A_{AmC})] \times 100 \quad \text{(IV.6)}$$

Where $A_{CrC:}$ the area of the peak at 89 ppm, which assigned to the C_4 crystalline cellulose; $A_{AmC:}$ the area of the peak at 83 ppm, which assigned to the C_4 amorphus cellulose.
The structures of pure and recycled DMIMMPh were determined by ^{1}H NMR spectroscopy, Bruker Avance 300 apparatus (300, 13 MHz, 25 °C) using acetone-d6 as solvent.

IV.2.6.3. FTIR analysis

The IR spectra of the untreated miscanthus, cellulose-rich extracts and residues were determined using an ALPHA Fourier Transform IR spectrometer with an OPUS/Mentor software. A small amount of samples, enough to cover the surface of platinum diamond ATR crystal probe was used. Twenty-four scans were acquired for each spectrum.

IV.2.6.4. SEM analysis

SEM images were obtained using a JSM6700F scanning electron microscope. Samples were fixed to a metal-base specimen holder using double-sided adhesive tape, coated with Au/Pd and observed at 20 kV accelerating voltage.

IV.2.7. Enzymatic hydrolysis process

The miscanthus and cellulose-rich extract samples were placed in a 100mL volumetric flask with additional citrate Buffer (50 mM pH 4.8) for a total mass ≈30 g. Celluclast was added at a loading of 20FPU/g of cellulose for each reaction, with β-glucosidase added at a 1:1 volume ratio. The enzymatic hydrolysis was conducted at 323 K with shaking at 250 rpm in a Sanyo Incubating Orbital Shaker. Samples, (0.5–2mL), were removed and analyzed by HPLC for glucose concentration. Reactions were run in duplicate, with samples taken from each reactor and run twice on the HPLC. The hydrolysis efficiency is calculated using the following formula:

Glucose hydrolysis efficiency (%) = [(glucose concentration (g/l) × volume of reaction (l)) / (mass of sample (g) ×fraction cellulose in sample)] × 0.9 ×100 (IV.7)

Xylose hydrolysis efficiency (%) = [(xylose concentration (g/l) × volume of reaction (l)) / (mass of sample (g) × fraction hemicellulose in sample)] ×0.88×100 (IV.8)

Where: the value 0.9 in eq. IV.7 is equivalent to: [molecular weight of cellulose unit (162.14) / molecular weight of glucose unit (180.16)] and the value 0.88 in eq. IV.8 is equivalent to: [molecular weight of hemicellulose, xylan, unit (132.11) / molecular weight of xylose unit (150.13)].

An HPLC (SHIMADZU, USA) with a SHODEX Asahipak NH2-50 4E column (Shodex, Japan) and a differential refractive index detector (SHIMADZU, USA) was employed for analyzing concentrations of glucose and xylose in the mixtures. The column oven temperature was 308 K, the mobile phase was a mixture of acetonitrile and water with a ratio (75:25), and the flow rate was 1.5 ml/min. The correlation coefficient of the sugar standard curve by the HPLC reached a value of 0.999. The expanded relative uncertainty of sugar was estimated at 1.0%. The equilibration temperature was measured with an uncertainty of 0.2 K.

IV.2.8. Fermentation of the hydrolysates

IV.2.8.1. Yeast and culture conditions:

In this study, the produced hydrolysates were fermented using baker's yeast (Yeast from S. cerevisaie, YSC2, Sigma Aldrich). The method described by Yan Lin et al.[51] was followed in this study with some modifications. Yeast was maintained on agar slants with ATCC Medium No.1245, which contains (in g l^{-1}): bacto-yeast extract 10; bacto-peptone 20; glucose 20, and bacto-agar 20. The prepared media was sterilized at 121°C for 20 min. Pre-cultures were inoculated from agar slants and grown at 30°C overnight in 250 ml shake-flasks with mineral medium containing (in g l^{-1}): bacto-yeast extract 10; bacto peptone 20 and glucose 20 while stirring at 100 rpm. Pre-cultures of (10 ml) were used to inoculate 500 ml baffled shake-flasks containing 250 ml of the above media. The inoculum was grown for approximately 24h. Yeast biomass solutions were then centrifuged and the sediment was used as inoculum for ethanol fermentation.

IV.2.8. 2. Batch fermentation

Ethanol fermentation was performed under anaerobic condition in a 100 mL shake flask at 100 rpm. The 1:10 ratio of inoculum: hydrolysate, as the sole carbon source, was used to conduct the fermentation. The experiments were carried out for 7 days under isothermal conditions, at 30° C and monitored by harvesting samples for glucose and ethanol analyses. Each run was duplicated and the average data was reported.

Cell growth was determined by measuring the optical density (OD) at 600 nm using a spectrophotometer (UV-1600,SHIMADZU). The cell dry weight was obtained using a calibration curve. The cell dry weight was proportional to cell turbidity and absorbance at 600 nm.[52] Biomass concentration was determined by the use of the dry weight method.[53] Accordingly, samples were centrifuged, and then the settled solids were washed with distilled water and dried for 2 h at 105°C.

Ethanol concentration was determined using a Brucker 450 gas chromatograph. The GC operating conditions are given in Table IV.1. All GC analyses were repeated three times to check reproductibility. The sample concentration was given according to the area of each chromatograph peak and the calibration curve made prior for all the solutes.

Table IV.1. GC operating conditions for composition analysis

Injector Temperature	250°C
Carrier Gas	Helium
Capillary column	WCOT Ulti-Metal coated with HT-SIMDIST-CB (10 m × 0.53 mm × 0.53 μm)
Flow rate	2 $mL.min^{-1}$
Column Oven	100°C
Detector Type	FID
Detector Temperature	250°C

IV.3. Results and discussion

In this work, four ionic liquids, EtOHMIMCl, DMIMMPh, BMIMCl and EMIMSCN were investigated in order to evaluate the dissolution of miscanthus and the extraction of cellulose. The influence of different parameters is studied in order to define the optimum conditions of the extraction process.

IV.3.1 Solubility of miscanthus in ionic liquids

ILs are capable of dissolving complex macromolecules and polymeric materials with high efficiency by breaking the inter and intra-molecular hydrogen bonding network of polysaccharides and promoting their dissolution.[54] This mechanism has been observed to proceed as follows: The ion pairs in BMIMCl dissociate into individual Cl^- and $Bmim^+$ ions. Free Cl^- ions associate with cellulose hydroxyl protons, and free $Bmim^+$ cations associate with cellulose hydroxyl oxygen groups. These disrupt hydrogen bonding in cellulose and cause its dissolution. Solid-liquid equilibria (SLE) of miscanthus in ionic liquids, was carried out in a large range of temperatures (363-403 K). Figure IV.1 presents the solubility of miscanthus in four ionic liquids. It was found that the solubility of miscanthus is higher in DMIMMPh than other ionic liquids. As discussed in chapter III, this is related to its high hydrogen bond basicity and polarity. This observation indicates that the nature and size of the ionic liquid's anion significantly influence the solubility of miscanthus. Our studies confirm those observations. Strong H-bond-acceptor anions, such as chloride and phosphonate anions, effectively dissolve miscanthus, figure IV.2. The high solubility of miscanthus in phosphonate-based ILs compared to other studied ionic liquids may be of interest in technology because these ILs are free of halogens. These ILs are also less-toxic, non-corrosive and biodegradable.[54]

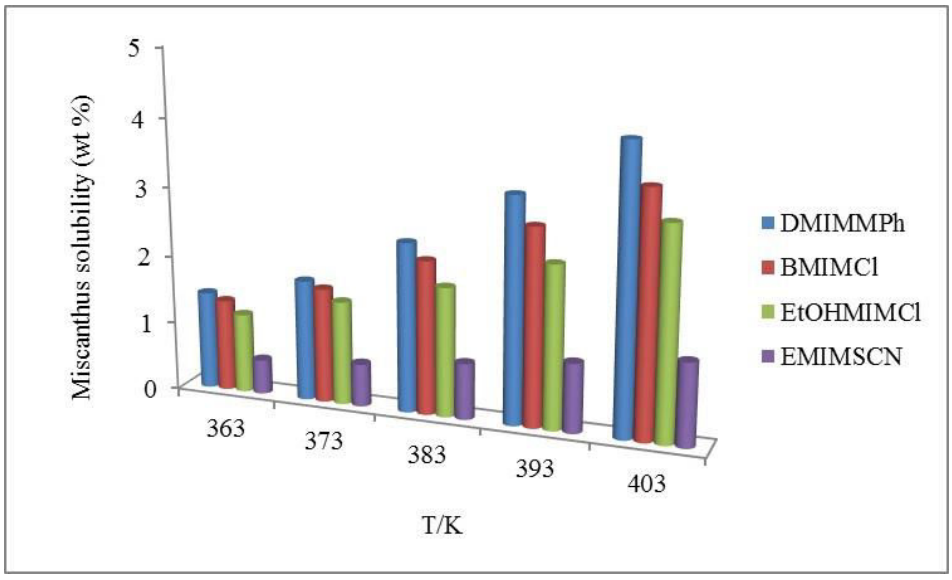

Figure IV.1. The solubility of miscanthus in ionic liquids

On the other hand, the nature of the IL's cation and the alkyl-chain length on the cation also play a role in the dissolution process. Swotloski et al. have reported that the solubility of cellulose in ILs decreased with the increasing size of the cations such as lengthy alkyl groups

substituted on the imidazolium ring.[54] It is suggested that, in salt solutions with small, strong polarizing cations and large polarizable anions, intensive interactions with cellulose occur. Results obtained on the solubility of miscanthus in ionic liquids and the data published in the literature[33,42,55-57] proved that phosphonate- and chloride-based ionic liquids are good solvents for miscanthus. Table IV.2 shows the published solubility data for miscanthus and other lignocellulosic-biomass materials. The solubility results presented in this work are in agreement with the work of S. Padmanabhan et al., 2011. The direct comparison with the published solubility data of other lignocellulosic biomass materials is not possible due to differences in solutes and/or pretreatment conditions. However, the trends reported in those studies are similar.

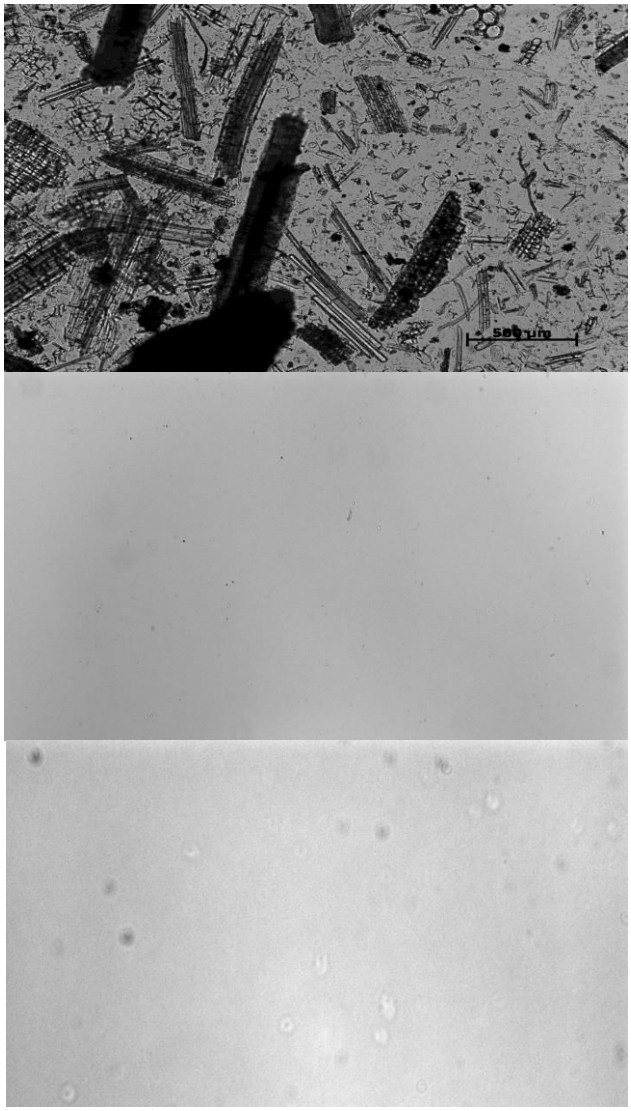

Figure IV.2. Microscopic images for raw miscanthus (0.2 mm size) in water (top), miscanthus dissolved in DMIMMPh (middle), and for miscanthus dissolved in BMIMCl (bottom).

Table IV.2 Dissolution of different biomass species in imidazolium based ionic liquids, data from this work and from the litrature

Biomass	Ionic Liquid	Solubility (wt%)	Time (hr)	Temperature (K)	Reference
Miscanthus	DMIMMPh	1.42	24	363.15	This work
	DMIMMPh	1.75	18	373.15	
	DMIMMPh	2.45	15	383.15	
	DMIMMPh	3.25	12	393.15	
	DMIMMPh	4.10	12	403.15	
	BMIMCl	1.33	24	363.15	
	BMIMCl	1.66	15	373.15	
	BMIMCl	2.22	15	383.15	
	BMIMCl	2.84	12	393.15	
	BMIMCl	3.50	10	403.15	
	EtOHMIMCl	1.22	24	363.15	
	EtOHMIMCl	1.5	18	373.15	
	EtOHMIMCl	1.87	18	383.15	
	EtOHMIMCl	2.35	15	393.15	
	EtOHMIMCl	2.75	12	403.15	
	EMIMSCN	0.50	24	363.15	
	EMIMSCN	0.62	24	373.15	
	EMIMSCN	0.81	24	383.15	
	EMIMSCN	1.00	24	393.15	
	EMIMSCN	1.20	24	403.15	
	EMIMOAC	5	6-8	393.15	33
	BMIMOAC	4	8-10	393.15	33
	BMIMCl	3	8	393.15	33
	EMIMCl	4	8	393.15	33
	DMIMDMP	4	10	393.15	33
	EMIMDMP	4	15	393.15	33
	EMIMHSO4	2	12-14	393.15	33
	BMIMSCN	<1	>24	403.15	33
Southern yellow pine	EMIMOAC	4.93	16	383.15	42
Southern yellow pine	BMIMCl	2.6	16	383.15	42
Wool keratin	BMIMCl	4	10	373.15	55
Pine	AMIMCl	1.3	24	373.15	56
Pine	AMIMCl	3.35	24	393.15	56
Poplar wood	EMIMOAC	5	12	383.15	57

IV.3.1.1. Effect of miscanthus particle size

Table IV.3 shows the solubility results of different miscanthus sizes, 2-1mm, 1mm- 400 micron, 400-200 micron, 200-80 micron, and 80-40 micron and <40 micron particles, in BMIMCl. It is obvious that reduction of miscanthus particle size increases its solubility in ionic liquids. When the particle size of miscanthus is reduced from 2 mm to 0.2 mm, the time required for dissolution declines. While a particle size below 80 micron gives better dissolution results, the

additional cost of grinding to very small miscanthus particles is not justified. So the size below 0.2 mm was suggested as a suitable size for our studies.

Table IV.3. Effect of miscanthus paricle size on the solubility in BMIMCl at 373 K

Miscanthus size (mm)	Miscanthus solubility (wt %)	Time (hr)
2-1mm	0.97	36
1-0.4mm	1.43	24
0.4-0.2mm	1.57	18
0.2-0.08mm	1.64	12
0.08-0.04mm	1.67	12
< 0.04mm	1.68	10

IV.3.1.2. Effect of temperature and dissolution rate

Recent studies reported on the solubility of lignocellulosic biomass in ionic liquids, showed that temperature and time significantly influence the solubility process. In fact, high temperatures lead to better solubility, but this may cause degradation of cellulose and hemicelluloses. Figure IV.3 shows the influence of temperature and time on the rate of dissolution of miscanthus (<0.2 mm particle size) in DMIMMPh and BMIMCl. As expected, the rate of dissolution of miscanthus is slightly faster at higher temperatures. The rate of dissolution of miscanthus in BMIMCl is higher than in DMIMMPh. No significant increase in the solubility of miscanthus, in BMIMCl and in DMIMMPh, was observed after 12 and 18 hr respectively.

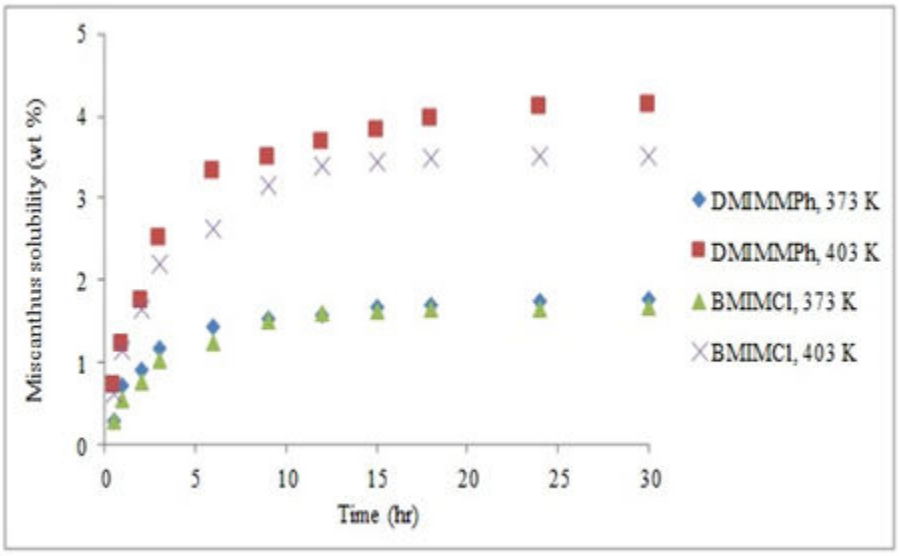

Figure IV.3. Effect of temperature on the miscanthus solubility in DMIMMPh and BMIMCl as a function of time at temperatures 373 and 403 K

IV.3.2. Extraction and regeneration of cellulose from miscanthus using ionic liquids

IV.3.2.1. Ash and extractables removal

In order to reduce the ash and extractables content of miscanthus and to expand the intermolecular pores, miscanthus was treated with hot water. Table IV.4 shows the results of pretreatment of miscanthus at 373 K for 5 min. Wei-Zun Li et al., 2013, [58] showed that water treatment at temperature 373 K for 5 min would not destroy the molecular configuration of lignocellulosic biomass. XRD and IR analyses show no difference before and after water pre-treatment, figures IV.8 and IV.14. The treated miscanthus was dried at 378 K to be ready for the extraction processes.

Table IV.4. Miscanthus treatment with H_2O at 373 K for 5 min for ash and extractables removal

Miscanthus components (%)	Before treatment	After treatment
Cellulose	40.5	42.5
Lignin	27.0	28.5
Hemicellulose	24.5	26.0
Ash content	3.6	0.7
Others (extractables)	4.4	2.3

IV.3.2.2. Effect of antisolvent type

The dissolved cellulose can be easily regenerated by precipitating it out from ionic liquids through the addition of anti-solvent. Water, methanol, ethanol and acetone are excellent anti-solvents that effectively precipitate cellulose from IL. When anti-solvent such as water is added in the IL and biomass mixture, the ions of IL form hydrogen bonds with water molecules and they are displaced into the aqueous phase. The interactions between IL and cellulose are shielded by the hydrodynamic shells built up by water molecules around the ions of IL. Consequently, cellulose which previously interacted with IL is expelled and rebuilt its intra and intermolecular hydrogen bonds and then precipitated.[44,59,60] Subsequently, the precipitate is separated from IL by filtration. Table IV.5 shows the effect of antisolvent type on the extraction of cellulose form miscanthus using BMIMCl ionic liquid at temperature 373 K during 6 hr with a mixture containing 3% miscanthus mass fraction. The effect of antisolvent on the extraction process was investigated using various antisolvents such as water, ethanol, acetone, water-acetone (50:50) and water-DMSO (50:50). In fact, the extraction process did not affect greatly with changing the antisolvent. Hence, water was suggested as a suitable antisolvent for our studies.

Table IV.5. Effect of antisolvent type on the extraction process

Antisolvent type	Cellulose grade (%)	Cellulose recovery (%)
Water	67.93	68.57
Ethanol	64.70	66.62
Acetone	66.55	67.20
Water- Acetone	67.30	67.90
Water-DMSO	68.42	66.84

IV.3.2.3. Effect of type of ionic liquid

Table IV.6 presents the effect of the structure of ionic liquid on the cellulose extraction process. The extraction process was performed at temperature 373 K, during 6 hr, with a mixture containing 3% miscanthus mass fraction and water as an antisolvent. The cellulose-rich extract composition shown in table IV.6 proves that cellulose extraction efficiency, high cellulose yield with low lignin yield, increases in the following order: EMIMSCN < EtOHMIMCl < BMIMCl < DMIMMPh. This is in a good agreement with the miscanthus solubility results. This behaviour could be explained, as discussed in the solubility part, due to the difference in hydrogen bond basicity and polarity between ionic liquids.

Table IV.6. Effect of type of ionic liquid on the extraction processes

Solvent	Cellulose grade %	Cellulose recovery %	Hemicellulose grade %	Hemicellulose recovery %	Lignin grade %	Lignin recovery %	Others (ash & unknown products) %
DMIMMPh	70.03	72.14	15.47	25.56	11.69	18.29	2.80
BMIMCl	67.93	68.57	16.67	26.98	12.49	19.15	2.90
EtOHMIMCl	67.03	65.98	16.97	26.78	12.99	19.42	3.00
EMIMSCN	54.05	44.10	22.95	30.04	19.99	24.77	3.00

IV.3.2.4. Effect of temperature

Brandt et al.[61] found that swelling and dissolution in ILs is temperature-dependent, and that better dissolution and regeneration rates are obtained at temperatures beyond 373 K. Figure IV.4 shows the dissolution rate, cellulose recovery, cellulose grade, cellulose regeneration rate and mass loss of miscanthus in DMIMMPh ionic liquid at 5% miscanthus mass fraction, time 6 hr and water as an antisolvent. It is obvious that the dissolution rate increases when the temperature increases from 363 to 403 K. Nevertheless, the cellulose grade, recovery and regeneration rate increase from 363 to 383 K. At temperature higher than 383 K, these parameters strongly decrease except for cellulose grade due to the degradation occurrence. Mass loss results indicate that temperature has a great effect on the extraction efficiency. The

mass loss increased from 1.42 % at 363 K to 42.54% at 403 K. Temperature higher than 380 K leads to high degradation and hence low extraction efficiency.[56]

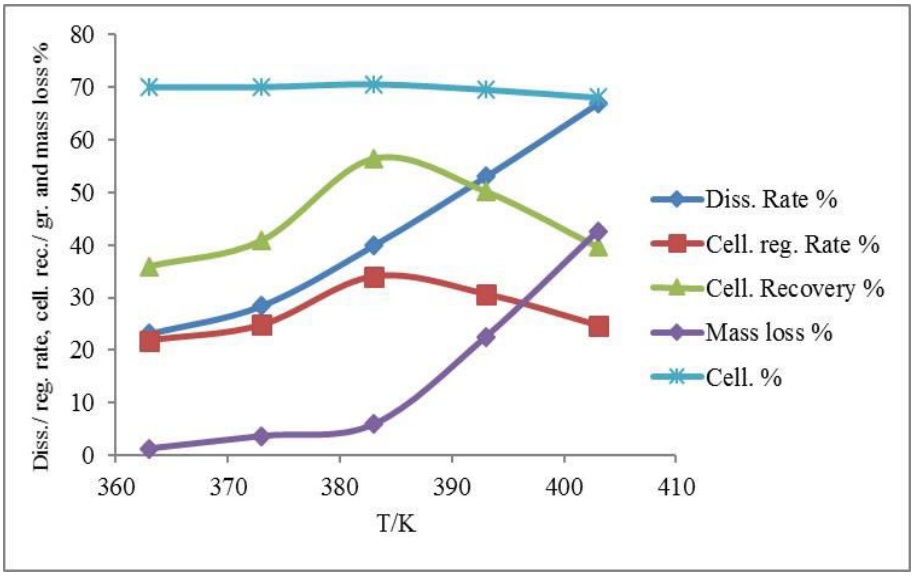

Figure IV.4. The effect of temperature (K) on the extraction process

IV.3.2.5. Effect of time

The kinetics of the miscanthus dissolved in DMIMMPh were studied as a function of dissolution time. Figure IV.5 shows the dissolution rate %, cellulose recovery%, cellulose grade%, cellulose regeneration rate% and mass loss % miscanthus in DMIMMPh. The measeurements were performed in these conditions: at 3 % miscanthus mass fraction, temperature of 373 K, and water as an antisolvent. As expected, the dissolution rate increased with increasing reaction time from 1 to 24 hours. The cellulose grade, recovery and regeneration rate highly increase from 1 to 12 hr. After 12 hrs, these parameters decrease due to the degradation occurrence. The mass loss increased from 0.95% at 1 hr to 13.82% at 24 hrs indicating that the polymer degradation increases with time.

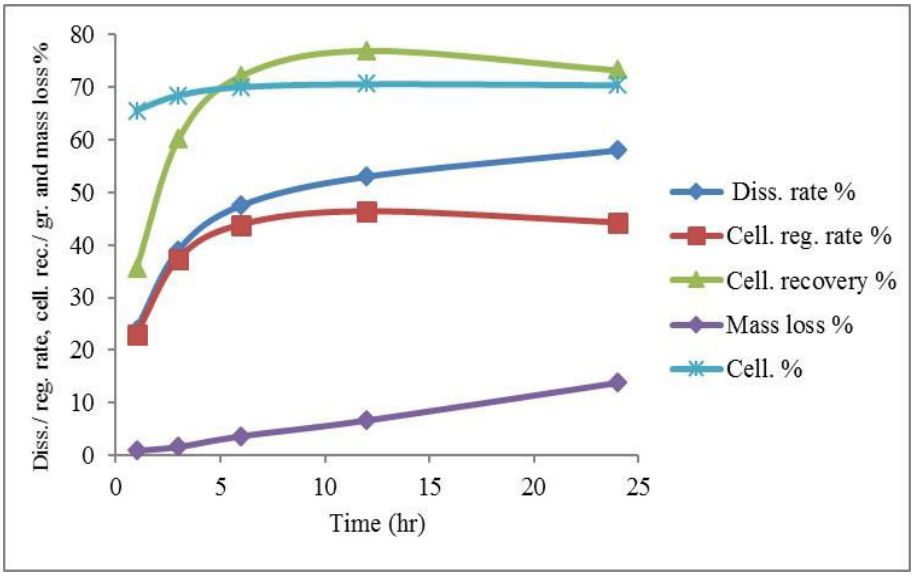

Figure IV.5. The effect of time (hr) on the extraction process

IV.3.2.6. Effect of miscanthus concentration

Table IV.7 shows the effect of miscanthus mass fraction on the extraction process in DMIMMPh at temperature 373 K and time 6 hr. Low concentration results in higher molecules dispersion in the solution and leads to high dissolution and regeneration rates. Increasing the miscanthus concentration from 2 wt% to 6 wt%, the dissolution rate decreased from 65.4% to 24.1%. High miscanthus concentrations may result in filtration and separation difficulties due to the high molecular weight of the miscanthus components.

Table IV.7. Effect of miscanthus mass fraction on the extraction process

Miscanthus mass fraction (%)	Dissolution rate %	Cell. regeneration rate %
2	65.4	48.64
3	47.5	43.79
4	35.6	29.42
5	28.5	24.80
6	24.1	18.55

IV.3.2.7. Applying Box-Behnken Design for the Miscanthus-DMIMMPh mixture

An experimental design technique, Box-Behnken Design, is used to optimize miscanthus solubility and extraction results in DMIMMPh ionic liquid and to evaluate the interaction between different parameters. Such an experiment allows the study of the effect of each factor temperature, time and miscanthus mass fraction, as well as the effects of interactions between factors on the cellulose solubility and extraction from miscanthus.

According to this design, the optimal conditions were estimated using a second order polynomial function by which a correlation between studied factors and response (mean diameter) was generated. The general form of this equation is:

$$Y = \beta_o + \beta_1 X_1 + \beta_2 X_2 + \beta_3 X_3 + \beta_{12}X_1X_2 + \beta_{13}X_1X_3 + \beta_{23}X_2X_3 + \beta_{11} X_1^2 + \beta_{22} X_2^2 + \beta_{33} X_3^2 \quad \text{(IV.9)}$$

Where: Y is the predicted response; dissolution rate, cellulose grade and cellulose recovery %, X_1, X_2 and X_3 are studied variables; temperature, time and miscanthus mass fraction; β_i are equation constant and coefficients. Software package, Design-Expert 6.0.5, Stat-Ease, Inc., Minneapolis, USA, was used for regression analysis of experimental data and to plot response surface. Analysis of variance (ANOVA) was used to estimate the statistical parameters. The extent of fitting the experimental results to the polynomial model equation was expressed by the determination coefficient, R^2. F-test was used to estimate the significance of all terms in the polynomial equation within 95% confidence interval. "Adeq Precision" measures the signal to noise ratio, a ratio greater than 4 is desirable and indicates an adequate signal.[62] ANOVA data of the system indicates the well fitting of the experimental results to the polynomial model equation and hence accuracy of this model, table IV.8. The Model F-values of 126.75, 144.18 and 126.40 imply the model is significant. The "Adeq Precision" ratios of 38.086, 35.868 and 32.401 indicate an adequate signal. The equation constants and coefficients values for the different responses are given in table IV.9.

Figure IV.6 (a,b, and c) shows the response surface plots of the miscanthus dissolution rate %, cellulose grade % and cellulose recovery % resulting from the main effects of different variables. It is noticed that the dissolution rate % and recovery increase with increasing the temperature and time and with decreasing the miscanthus mass fraction with a slight decrease of the recovery at high time. Cellulose grade is mainly dependent on the temperature, temperature higher than 380 K leads to lower cellulose grade. It is obvious that no important interaction between the different factors was observed, while temperature is the most effective variable on the extraction process.

Table IV.8. Analysis of variance (ANOVA) data for the miscanthus-DMIMMPh mixture

The stastical parameters	Dissolution rate %	Cell. Grade %	Cell. Recovery %
The standard deviation	2.67	0.85	1.86
R-squared	0.9939	0.9946	0.9939
Adequate precision	38.086	35.868	32.401
The Model F-value	126.75	144.18	126.40

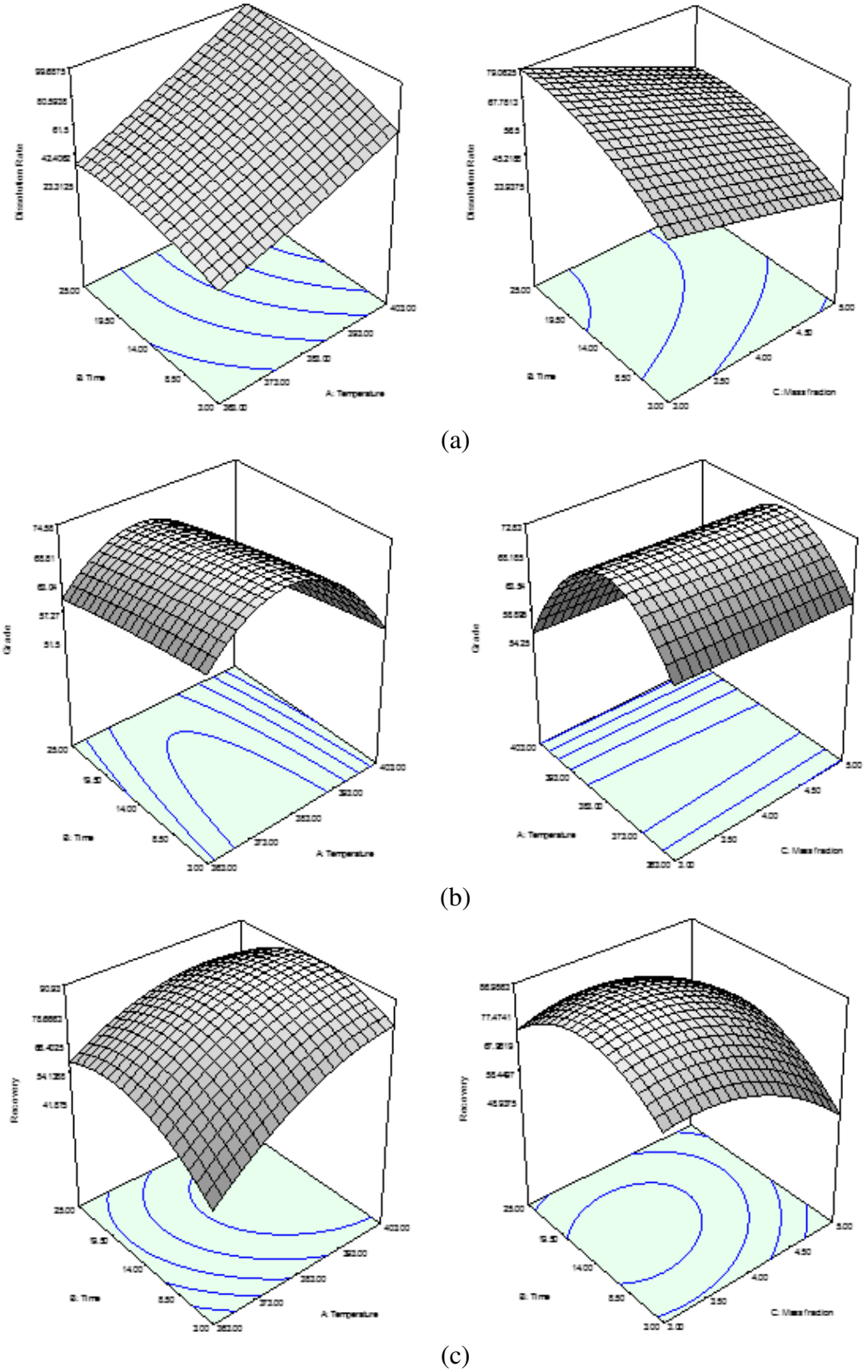

(a)

(b)

(c)

Figure IV.6 (a,b and c). The response surface plots of the miscanthus dissolution rate %, cellulose grade % and cellulose recovery % respectively resulting from the main effects of different variables, temperature, time and miscanthus mass fraction % for Miscanthus-DMIMMPh mixture

Table IV.9. Equation constants and coefficients for the different responses

The stastical parameters	Dissolution rate %	Cell. Grade %	Cell. Recovery %
β_o	210.49	-4609.32	-2933.73
β_1	-1.87	24.683	15.55
β_2	-5.15	-0.134	10.78
β_3	1.59	-0.500	-77.25
β_{12}	0.02	-0.000001	-0.02
β_{13}	-0.02	0.000005	0.35
β_{23}	-0.16	0.000001	0.32
β_{11}	3.91	-0.033	-0.02
β_{22}	-0.05	-0.0004	-0.10
β_{33}	-0.44	0.00002	-8.65

The best optimum parameters of the Box-Behnken design for the dissolution and extraction of miscanthus in DMIMMPh IL mixture are: temperature 379.8 K, time 6.30 hr and 3.2% miscanthus mass fraction. Applying these optimum parameters on miscanthus-DMIMMPh and BMIMCl mixtures, we could obtain cellulose grade of 74.4% and 71.75% with cellulose recovery of 77.55% and 73.78 respectively, table IV.10.

In conclusion, the treatment of miscanthus with ionic liquids using one-stage extraction process produces an amorphus cellulose-rich extract but it still has a lignin content about 9%, which might affect the hydrolysis efficiency. Therefore, a delignification process prior to the miscanthus dissolution and cellulose extraction with ionic liquids, two-stage extraction process, might give better results concerning the lignin content in the cellulose-rich extract.

Table IV.10. Applying the optimum parameters of Box-Behnken design for the miscanthus-DMIMMPh and BMIMCl mixtures

Solvent	Cellulose grade %	Cellulose recovery %	Hemicellulose grade %	Hemicellulose recovery %	Lignin grade %	Lignin recovery %	Others (ash & unknown products) %
DMIMMPh	74.406	77.552	13.703	22.905	9.099	14.395	2.793
BMIMCl	71.757	73.978	14.870	24.587	10.499	16.429	2.874

IV.3.2.8. Enhancement of miscanthus delignification

To enhance the delignification of miscanthus, a two-stage extraction process was performed. Firstly, alkaline solvent mixtures were used to enhance miscanthus delignification. Then, the lignin-free extract was treated with DMIMMPh and BMIMCl ionic liquids. Miscanthus was dissolved in different alkaline solvent mixtures, ethylene di-amine (EDA), ethylene di-amine/ethylene glycol (1:1) ratio by weight (EDA/EG) and ethylene di-amine/dimethyl

sulfoxide (1:1) ratio by weight (EDA/DMSO), at temperature = 448 K, time = 3 hr, and solvent/miscanthus mass ratio equal to 10. Although these three solvent mixtures do not dissolve miscanthus, they swell miscanthus sufficiently for significant lignin removal. This behavior is in a good agreement with the work of S. Padmanabhan et al., 2011.[31] Results presented in table IV.11 indicate that EDA/DMSO mixture gives better delignification efficiency compared to other mixtures. The delignification efficiency of EDA/DMSO mixture reaches up to 75% and it has no effect on the cellulose structure as discussed after. However, EDA/DMSO mixture has high polarity and hydrogen bond acceptor capacity, facilitating better interaction and solubilization of hemicellulose.[31] Hence, the recovery of hemicellulose in the produced solid extract is lower than 30%.

In the second-stage, the lignin-mostly free extract was treated with DMIMMPh or BMIMCl using the optimum parameters obtained from the Box-Behnken design. An amorphous cellulose-rich extract was obtained with cellulose grade of 88.64% and 86.5% and the total recovery of 70.30% and 69.40 respectively while the lignin content is only 4%, table IV.12.

A comparison between the cellulose-rich extract from the two extraction procedures, one-and two-stage extraction processes, shows that the two-stage process increases the cellulose grade with 14% while the cellulose recovery decreased with 7%. Also the lignin content is decreased with 5%.

Table IV.11. Miscanthus delignification process using different EDA mixtures

Solvent	Cellulose grade %	Cellulose recovery %	Hemicellulose grade %	Hemicellulose recovery %	Lignin grade %	Lignin recovery %	Others (ash & unknown products) %
EDA	53.4	59.98	23.96	43.16	19.64	33.48	2.99
EDA/EG	62.25	83.06	17.69	37.87	17.12	34.68	2.93
EDA/DMSO	67.94	80.22	15.46	29.29	13.60	24.37	2.97

Table IV.12. Treatment of the produced cellulose-rich material with DMIMMPh and BMIMCl ionic liquids

Solvent	Cell. grade %	Cell. recovery %	Total Cell. recovery	Hemicell. grade %	Hemicell. recovery %	Total Hemicell. recovery %	Lig. grade %	Lig. recovery %	Total Lig. recovery %	Others (ash & unknown products) %
DMIMMPh	88.64	87.64	70.30	5.6	24.32	7.12	3.99	19.72	4.81	1.767
BMIMCl	86.80	86.52	69.40	6.8	29.77	8.72	4.18	20.83	5.08	2.22

IV.3.2.9. Ionic liquids recycling

The IL-rich solution contains DMSO, water, lignin, and other sugars as a result of degradation occurrence. The solution was dried under vacuum to evaporate water and DMSO. Ethanol was added to precipitate lignin and other sugars. Our previous work[63, 64] show that ethanol could be used as an antisolvent to separate carbohydrates from ionic liquids. The solution was filtered, dried and the recycled ionic liquid was characterized with H^1NMR and Karl-fisher techniques. The results of H^1NMR and Karl-fisher presented in figure IV.7 and table IV.13 prove that DMIMMPh could be successfully recycled. Applying the optimum parameters obtained from Box-Behnken design on the system {miscanthus- recycled DMIMMPh}, good results are obtained when compared with those of pure DMIMMPh, table IV.14.

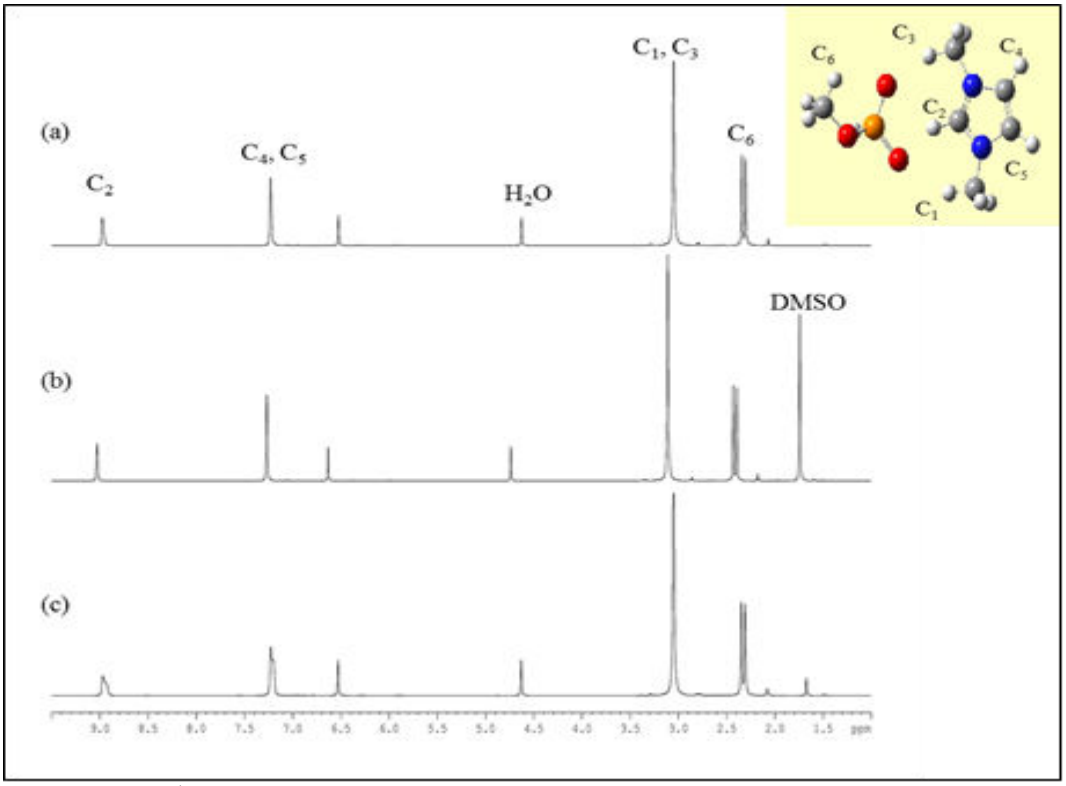

Figure IV.7. H^1 NMR of (a) pure DMIMMPh, (b) DMIMMPh/DMSO (80:20) and (c) recycled DMIMMPh

Table IV.13. Water content (ppm) in DMIMMPh solutions using Karl-fisher technique

IL- solution	Water content (ppm)
Pure DMIMMPh	450.50
DMSO	890.40
DMIMMPh-DMSO (80%:20%)	731.80
Recycled DMIMMPh	946.20

Table IV.14. Applying the optimum parameters of Box-Behnken design for the miscanthus-with pure DMIMMPh and recycled DMIMMPh mixtures

Solvent	Cellulose grade %	Cellulose recovery %
Pure DMIMMPh	74.406	77.55
Recycled DMIMMPh	72.254	73.54

IV.3.2.10. Cellulose, lignin and hemicellulose recovery

A quantification analysis of the mass and composition of recovered lignin and carbohydrates from miscanthus has been carried out when using 100 g of miscanthus in one and two-stage treatment processes in order to develop a proper mass balance and to evaluate the efficiency of the both treatment procedures.

In one-stage process, using DMIMMPh ionic liquid, it was found that 44.3 g was recovered as regenerated cellulose-rich material with a cellulose, lignin and hemicellulose content of 74.4, 9.0 and 13.7% respectively, see table IV.10. A 31 g lignin-rich material was obtained after ionic liquid recycling using ethanol as an antisolvent, with a cellulose, lignin and hemicellulose content of 9.7, 49.77 and 29.85 % respectively, table IV.15. Using one-stage treatment process, 55.10 % of the native lignin present in the original miscanthus was regenerated as lignin-rich extract, while 14.4% is still in the cellulose-rich material. For hemicellulose, 34.92% is recovered in the lignin-rich extract while 22.9 % is recovered in the cellulose rich extract. 77.6% of cellulose is regenerated in the cellulose-rich extract while only 7% is recovered in the lignin-rich phase.

On the other hand, in two-stage process, the recovery of lignin and carbohydrates is as follows: in the miscanthus delignification using EDA-DMSO solution mixture, it was found that 50.18 g was recovered as a cellulose-rich material with a cellulose, lignin and hemicellulose content of 67.9, 13.6 and 15.5% respectively, see table IV.11. The lignin-rich solution, filtrate, was acidified to a pH 2.0 with a 1 M HCl in order to precipitate the lignin-rich material. A 33 g lignin-rich extract obtained with a lignin and hemicellulose content of 45 and 31% respectively. Then, the 50.18 g cellulose-rich material was treated with DMIMMPh ionic liquid and a mass of 33.7 g cellulose-rich extract was recovered with a cellulose, lignin and hemicellulose content of 88.6, 4 and 5.6% respectively see table IV.12. A mass of 8.48 g lignin-rich extract was obtained after ionic liquid recycling using ethanol, with lignin and hemicellulose content of 55.6 and 26 % respectively, table IV.15.

Using two-stage treatment process, 67.74 % of lignin present in miscanthus is regenerated as lignin-rich extract, while 4.8 % is still in the cellulose-rich material. 46.95 % of hemicellulose is recovered in the lignin-rich extract while 7.12 % of the native is still in the cellulose-rich extract. Finally, 70.3 % of cellulose is regenerated in the cellulose-rich extract and 11.28% is recovered in the lignin-rich extract. The overall recovery of lignin and hemicellulose in lignin-rich extract is 12 % higher than in one stage process, while the overall recovery of cellulose in cellulose-rich extract is 7% lower than in one-stage process.

Table IV.15. Lignin-rich extract in one and two-stage treatment processes

Treatment Process	Treatment solvent	Cell. grade %	Cell. Rec. %	Total cell. Rec.%	Hemicell. grade %	Hemicell. rec. %	Total hemicell. rec. %	Lignin grade %	Lignin rec. %	Total lignin rec.%	Others
One-Stage process	DMIMMPh	9.70	7.08	7.08	29.85	34.92	34.92	49.77	55.10	55.10	10.68
Two-Stage process	EDA/DMSO	12.5	9.68	-	31.11	38.36	-	45.02	52.91	-	11.37
	DMIMMPh	8.01	1.99	11.28	26.00	28.39	46.95	55.60	69.06	69.74	10.39

IV.3.3. Charecterization of the regenerated cellulose-rich extract

IV.3.3.1. XRD analysis results

Figure IV.8 shows XRD spectra of original miscanthus and miscanthus pretreated with water for ash and extractables removal. The similarity in spectra indicate that water treatment at 373 K for 5 min has no effect on cellulose structure.

The X-ray spectra presented in figure IV.9 prove that amorphous cellulose is obtained from the regeneration of miscanthus with ionic liquids. The untreated miscanthus sample shows two prominent peaks near 2θ of 15° and 22°, indicating the characteristic diffraction pattern of crystalline cellulose. The cellulose-rich extracts display a slightly broad amorphous diffraction peak near 2θ of 21° which is the characteristic diffraction pattern of amorphus cellulose.[65,66] Compared with the diffraction pattern of the original miscanthus, the intensities of the diffraction peaks in the cellulose-rich extracts are smaller, revealing that ILs destroy the inter and intramolecular hydrogen bonds among lignocelluloses, leading to lower crystallinity in the cellulose-rich extract.[67]

Figure IV.10 indicates that the pretreatment of miscanthus with {EDA+DMSO} mixture has no effect on the cellulose structure. There is an increase of the degree of crystallinity of about 3 after the pretreatment and this is probably due to the increase in cellulose content and the decrease of lignin content.

The crystallinity index was calculated according to Segal's method, [47,48] equation IV.5. A strong decrease of the crystallinity degree (below 30) was observed for the produced amorphous cellulosic samples, table IV.16. This observation could be explained by a reduction in the intra- and intermolecular hydrogen bonds, occurring during the continuous transformation of miscanthus into amorphous cellulose. Figure IV.11 shows the crystallinity difference between microcrystalline cellulose, Cr. I. is 77, and the produced amorphous cellulose. A strong decrease in the degree of crystallinity was observed. CrI could be also calculated from Newman's method, [48,49] equation IV.6. In this method, the area at C_4 peak of the solid-state ^{13}C NMR spectrum of samples, figures IV.12 and IV.13, was used to evaluate the CrI. The values of CrI calculated with Newman's method are lower than those of Segal's method. This is in a good agreement with the observation of S. Park et al.,[48] 2010, who investigated that the most popular method for estimating cellulose CrI, the XRD height method or Segal's method, produces values that are significantly higher than the NMR C_4 peak separation method or Newman's method.

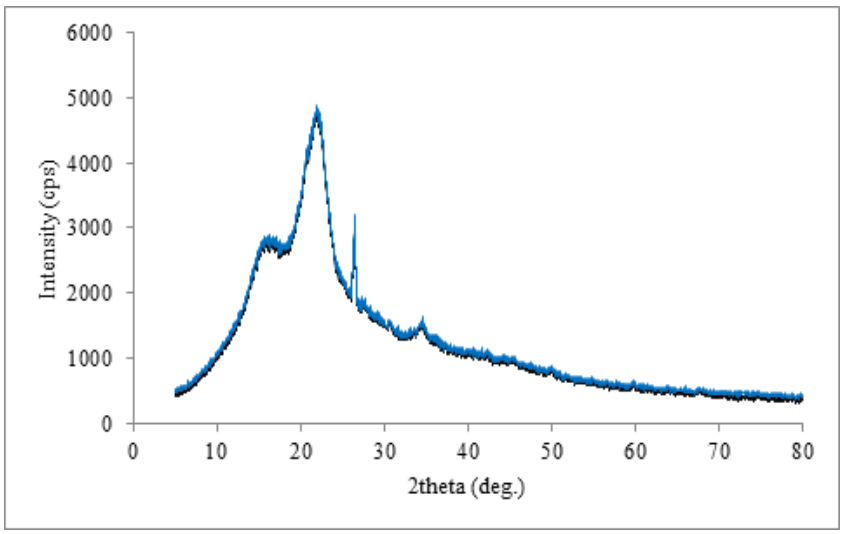

Figure IV.8. XRD of miscanthus ■) before and ■) after preatreatment with water for ash

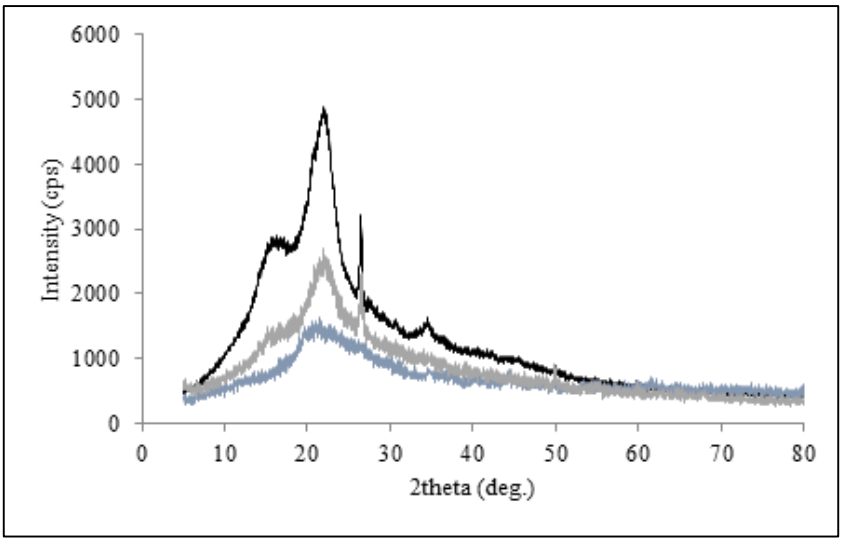

Figure IV.9. XRD of ■) miscanthus, ■) miscanthus residue and ■) cellulose-rich extract

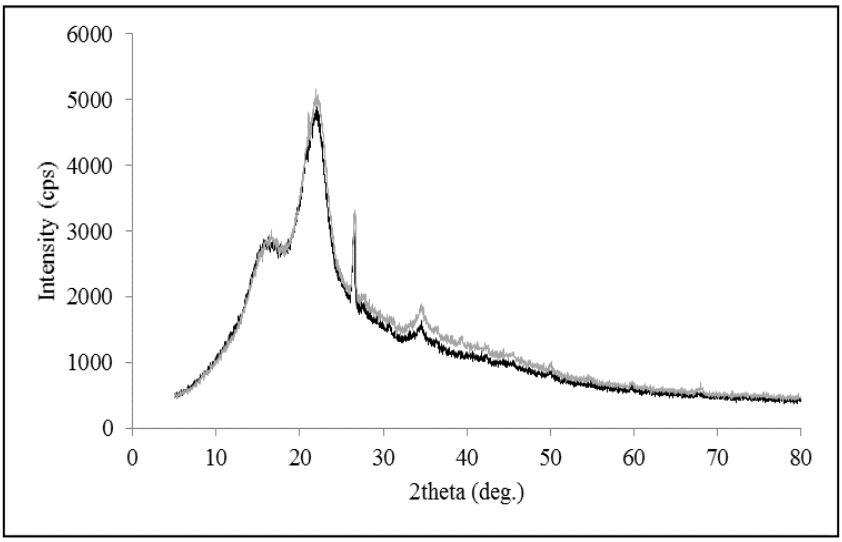

Figure IV.10. XRD of ■) miscanthus and ■) Miscanthus treated with EDA/DMSO

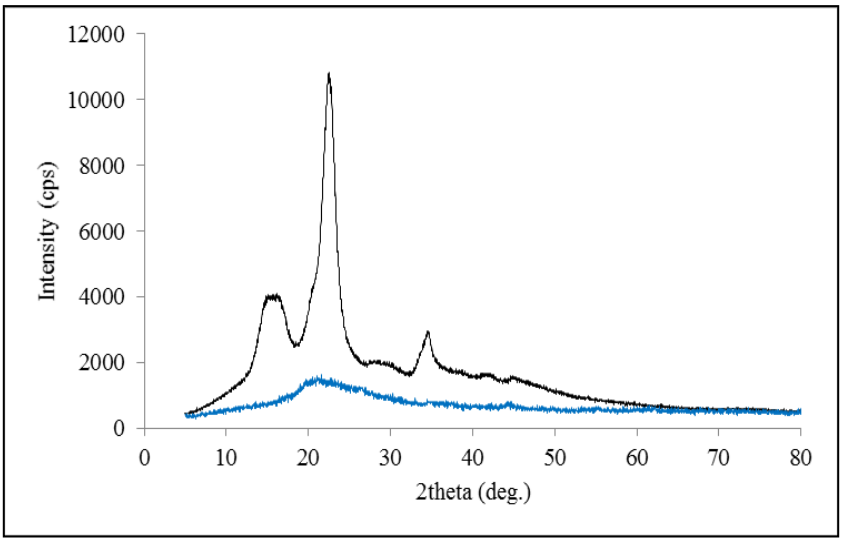

Figure IV.11. XRD of ■) microcrystalline cellulose and ■) cellulose-rich extract

Table IV.16. Crystallinity index calculation

CrI calculation method	Analytical technique used	Ionic liquids used	One-stage treatment process		Two-stage treatment process			
			Cr. I. of miscanthus treated with ionic liquids		Cr. I. of miscanthus pre-treated with EDA/DMSO		Cr. I. of cellulose-rich extracts treated with ionic liquids	
			Before	After	Before	After	Before	After
Segal's method	XRD	DMIMMPh	49	24	49	52	52	28
		BMIMCl	49	26	49	52	52	31
Newman's method	NMR	DMIMMPh	36	19	36	42	42	25

IV.3.3.2. NMR Analysis results

Solid-state CP/ MAS ^{13}C experiments were carried out on untreated and treated miscanthus samples. The spectra are shown in Figure IV.12. The NMR resonances were assigned according to data from the literature.[11,48,68,69] In the spectrum of untreated miscanthus, figure IV.12A, the peak (a) at 168-178 ppm is due to carbonyl groups of hemicelluloses and lignin. The peak (b) at 130-155 ppm is associated with the aromatic carbons of lignin. The peak (c) at 105 ppm assigned to the anomeric carbon C_1 of cellulose and hemicelluloses. The peaks (d) and (e) at 89 and 83 ppm correspond to crystalline and amorphus cellulose at C_4. The intense peaks (f) and (g) at 75 and 73 ppm are overlapping signals due to the C_2, C_3 and C_5 carbons of all polysaccharides. The peaks (h) and (i) at peaks 65 and 62 ppm correspond to crystalline and amorphous cellulose at C_6. The peak (j) at 56 ppm associated with the methoxyl group of lignin and hemicelluloses and finally, the peak (k) at 20 ppm is due to the acetyl groups of hemicelluloses.

In the NMR spectrum of miscanthus treated with EDA-DMSO solution mixture, figure IV.12B, the presence of small quantities of lignin and hemicellulose in the sample is revealed, with signals of very low intensity at 20, 55 and 130-190 ppm. Cellulose characteristic peaks have no significant change when compared with those in untereated miscanthus spectrum. This confirms that the preatreatment of miscanthus with EDA-DMSO mixture decreases the lignin content without affecting the cellulose structure.

The NMR spectrum of miscanthus treated with ionic liquids, figure IV.12C, shows very low intensity peaks for lignin and hemicellulose. Cellulose peaks confirm the high cellulose content of the regenerated cellulose, which can be compared with microcrystalline cellulose.

Figure IV.13 shows a comparison between the NMR spectrum of microcrystalline cellulose and the regenerated cellulose. Results showed the spectrum of microcrystalline cellulose had

characteristic peaks at 105 (C_1), 89 (C_4, crystalline), 83 (C_4, amorphous), 72 and 75 (C_2, C_3 and C_5), 65 (C_6, crystalline) and 62 ppm (C_6, amorphous).[56,58] The spectrum of microcrystalline cellulose, contains all the characteristic peaks above, although the chemical shifts (ı) had ±1 ppm deviation. The peak of regenerated cellulose from IL solution disappeared at 65 ppm, highly weakened at 89 ppm, while enlarged at 62 ppm, which could be an evidence that crystallinity decreases. The spectra for both microcrystalline and regenerated cellulose were similar to each other, except for the characteristic peaks of crystallinity. The CrI values calculated with the NMR C_4 peak separation method or Newman's method presented in table IV.16. As observed previously, both technique of CrI calculation lead to crystallinity differenence between untreated and treated miscanthus.

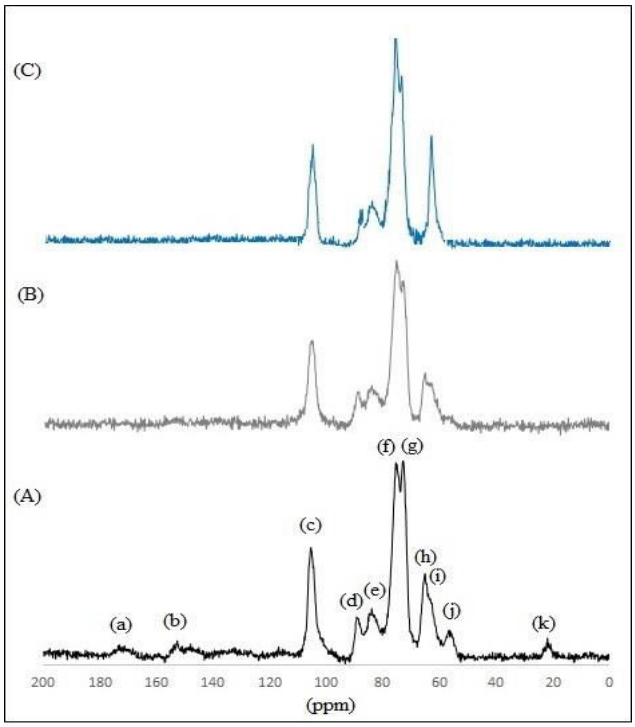

Figure IV.12. ^{13}C CP/MAS NMR spectra of miscanthus: (A) untreated, (B) pretreated with EDA-DMSO solution and (C) treated with DMIMMPh ionic liquid

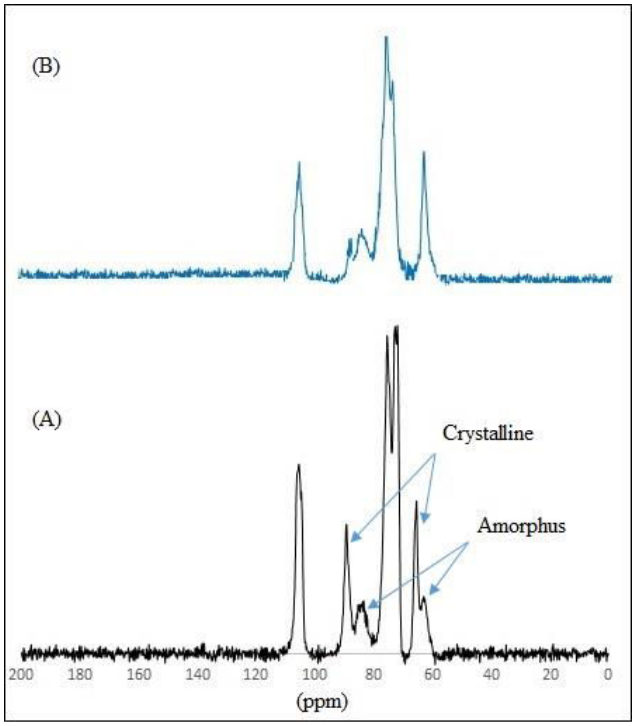

Figure IV.13. ^{13}C CP/MAS NMR spectra of (A) Microcrystalline cellulose and (B) regenerated cellulose

IV.3.3.3. FTIR analysis results

The similarity of FTIR spectra of original miscanthus and miscanthus pretreated with water for ash and extractables removal shown in figure IV.14 indicate that water treatment has no effect on miscanthus structure.

FTIR spectroscopic investigations evidenced the capacity of different absorption bands to characterize the ordering degree of the cellulosic polymers (Figs. IV.15, IV.16 and IV.17). An alteration of the crystalline organization leads to a significant simplification of the spectral contour through reduction in intensity or even disappearance of the bands characteristic of the crystalline domains.

The broad band in the 3600-3100 cm^{-1} region, which is due to the OH-stretching vibration, gives considerable information concerning the hydrogen bonds.[65] The intensity of peaks characteristic of hydrogen bonds from the spectra of amorphous celluloses is lower than those obtained from the orignial miscanthus samples. It could be correlated with the scission of the intra- and intermolecular hydrogen bonds. Also, in the case of amorphous samples, the peak shifted to higher wave number values, figures IV.15, IV.17.

The presence of amorphous cellulosic samples could be also confirmed by the shift of the band from 2900 cm^{-1}, corresponding to the C–H stretching vibration, to higher wave number values and by the strong decrease in the intensity of this band[65], figures IV.15, IV.17.

The adsorption bands from the 1500-899 cm^{-1} region are strongly reduced in intensity, or even absent. In addition, the FTIR absorption band at 1430 cm^{-1}, assigned to a symmetric CH_2 bending vibration decreases. This band is also known as the "crystallinity band"[65], indicating that a decrease in its intensity reflects reduction in the degree of crystallinity of the samples, figures IV.15, IV.17. The FTIR absorption band at 898 cm^{-1}, assigned to C–O–C stretching at β-(1→4)-glycosidic linkages, is designed as an "amorphous" absorption band.[58,65] An increase in its intensity is occurring in the amorphous samples, compared to the initial ones – as actually plotted in figures IV.15, IV.17.

On the other hand, the absence or the great decrease of the intensity of characteristic lignin bands at 1519, 1430 and 1262 cm^{-1} in the produced cellulose rich extracts indicate the performance of ionic liquids for the delignification process,[42,58] figures IV.15, IV.16. FTIR analysis results show that the preatreatment of miscanthus with EDA-DMSO mixture decreases the lignin content without affecting the cellulose structure, Figure 16. Indeed, FTIR spectroscopic investigations evidenced the production of amorphous cellulose almost free of lignin, which is suitable for enzymatic hydrolysis processes.

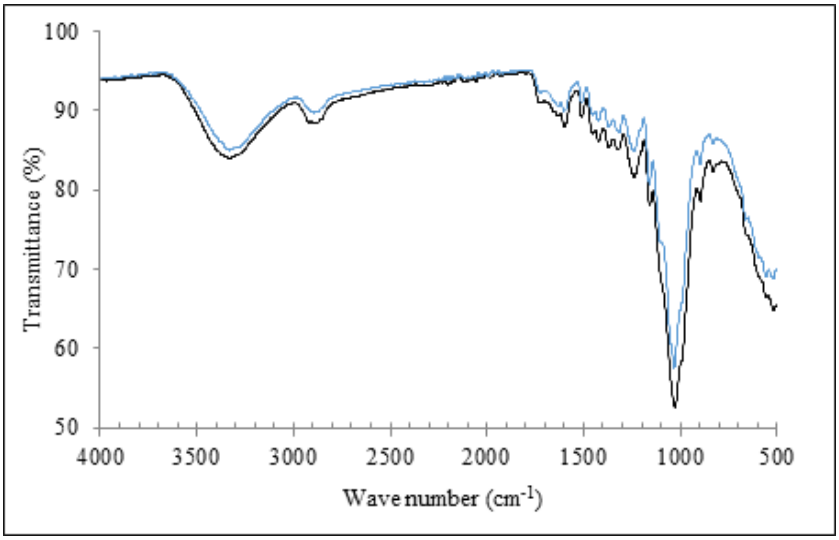

Figure IV.14. IR of miscanthus ■) before and ■) after preatreatment with water for ash removal

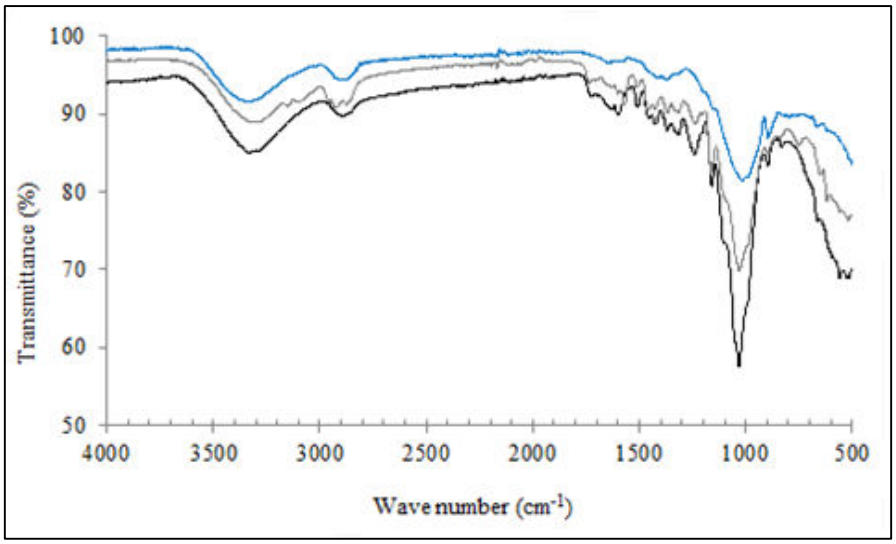

Figure IV.15. IR of ■) miscanthus, ■) miscanthus residue and ■) cellulose-rich extract

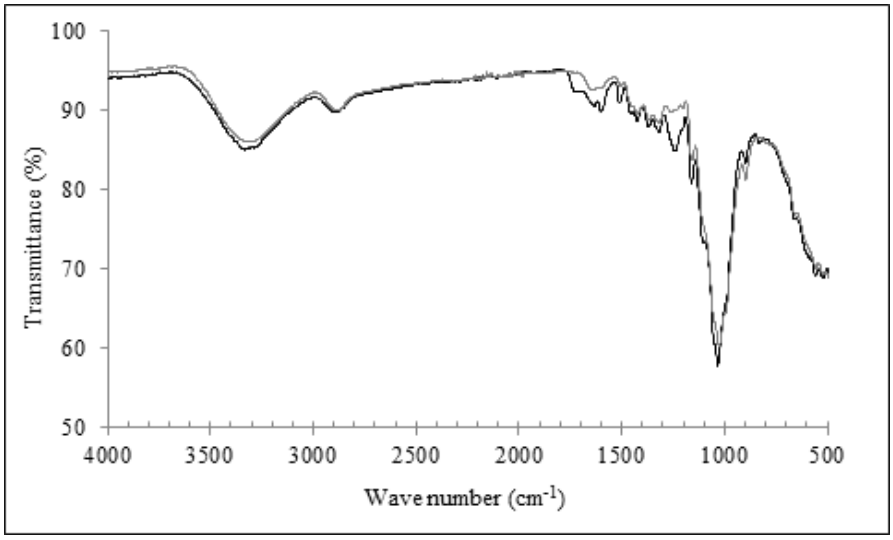

Figure IV.16. FTIR of ■) miscanthus and ■) Miscanthus treated with EDA-DMSO

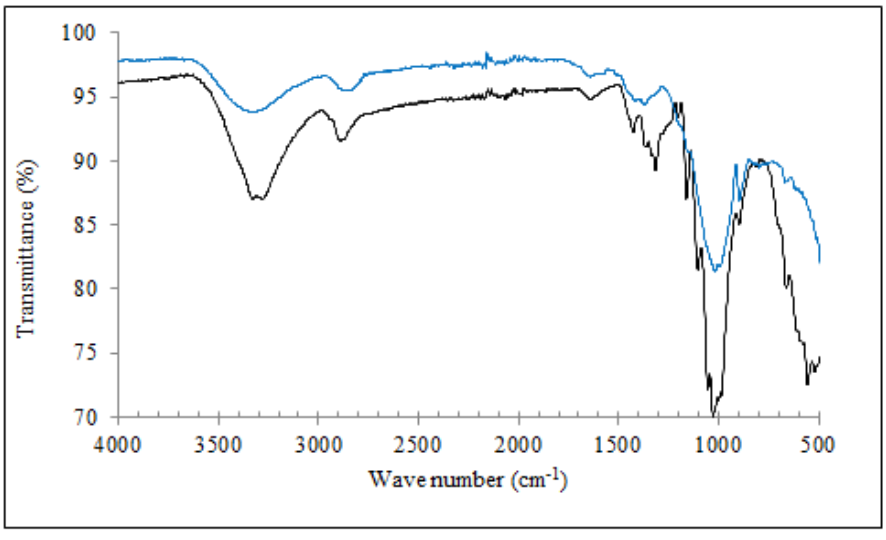

Figure IV.17. FTIR of ■) Microcrystalline celluose and ■) cellulose-rich extract

IV.3.3.4. Morphological investigation

Figure IV.18 shows SEM images of original miscanthus, the cellulose-rich extract, and miscanthus residue. Compared with the original miscanthus, which has a fascicular texture, the miscanthus residue shows a highly porous structure; this indicates that ILs effectively disrupts the intricate network of non-covalent interactions within lignocelluloses, leading to the dissolution of miscanthus. The regenerated cellulose- rich extract is homogeneous, dense, has a higher surface area and presents uniform macrostructures. A comparison between microcrystalline cellulose and the regenerated cellulose-rich extracts in figure IV.19 put in evidence the great difference between the highly intensive crystalline structure in microcrystalline cellulose (MCC) and the porous structure of the regenerated cellulose. The surface morphology of the two-stage regenerated cellulose is similar to that of the one-stage, except for some more porosity observed. This porosity is probably due to the delignification process using alkaline EDA-DMSO solution. In addition, the surface area of the IL pretreated cellulose rich-extracts was significantly increases. SEM images indicate that the regenerated cellulose is amorphous, porous, which is highly responsive to enzymatic saccharification.

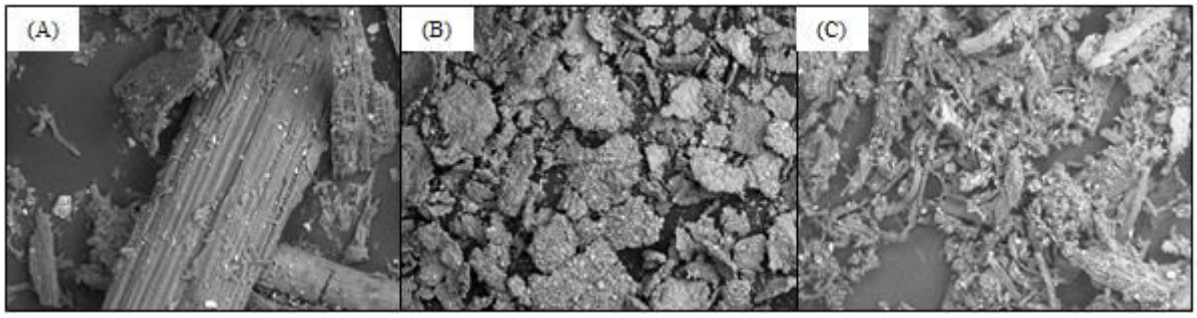

Figure IV.18. SEM images of (a) original miscanthus, (b) the cellulose-rich extract, and (c) miscanthus residue

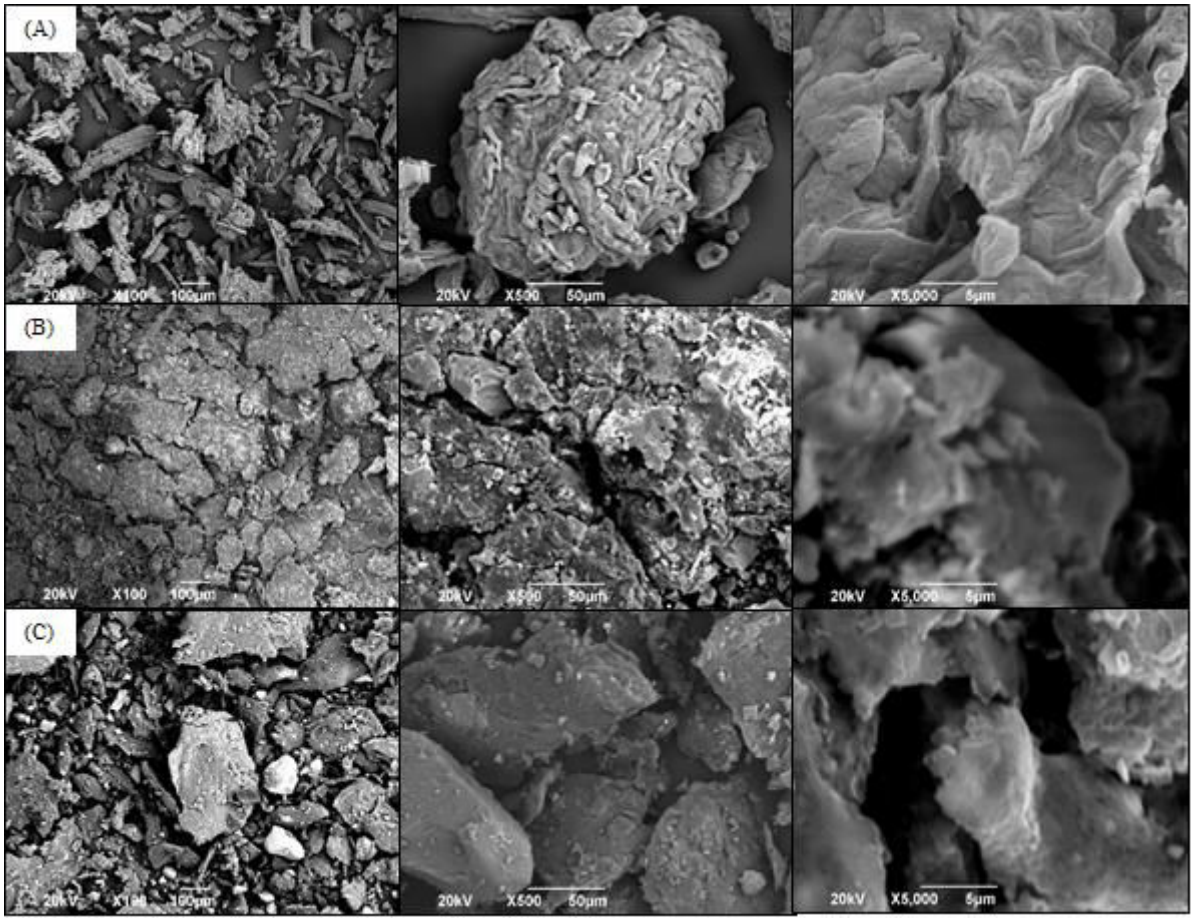

Figure IV.19. SEM images of A) microcrystalline cellulose and the cellulose-rich extract from B) one-stage and C) two-stage extraction processes

IV.3.4. Bioethanol production

The regenerated cellulose-rich extracts go through hydrolysis and fermentation processes in order to generate ethanol, which is used as a fuel in place of or in addition to conventional petroleum products. Hydrolysis is accomplished by the use of cellulose enzymes. In this process the complex carbohydrate chains are broken down to simple sugars. Then, these sugars are fermented by S. cerevisaie yeast which produces ethanol in a dilute form. In order to concentrate the ethanol, distillation techniques are used. If pure ethanol is required, the product is subjected to further separation techniques.

IV.3.4.1. Enzymatic hydrolysis

Enzymatic hydrolysis was carried out at temperature 323.15 K, time 72 hr, shaking at 200 rpm and adding cellulse enzyme at loading 20 FBU/g of cellulose with 1:1 volume of β-glucosidase. Figure IV.20 shows the hydrolysis rate for the untereated miscanthus and the cellulose

regenerated with DMIMMPh in one- and two-stage extraction processes. The rate of enzymatic hydrolysis of the cellulosic materials always decreases rapidly. Generally, enzymatic cellulose degradation is characterized by a rapid initial phase followed by a slow secondary phase that continues until all substrate is consumed. This could be explained by the rapid hydrolysis of the readily accessible fraction of cellulose.[39] The obtained glucose hydrolysis efficiency of the regenerated cellulose from one- and two-stage extraction procedures are 93.98 and 97.74% respectively.

Table IV.17, summarizes the results of different hydrolysis processes for untreated miscanthus and regenerated cellulose samples. In this table, A is the untreated miscanthus. B, C and D are the cellulose rich extracts from miscanthus treatment with DMIMMPh, recycled DMIMMPh and BMIMCl respectively in one-stage extraction process. E is the miscanthus treated with EDA/DMSO solvent mixture. F and G are the cellulose rich extracts from treatment with DMIMMPh and BMIMCl respectively, in two-stage extraction process.

It could be observed that the glucose hydrolysis efficiency of the untreated miscanthus is 11.89% compared to a value of 7% in the literature.[31] This difference may be resulted from the miscanthus ash removal with water. The hydrolysis efficiency of cellulose regenerated from the preatreatment with DMIMMPh ionic liquid is higher than the pretreatement with BMIMCl. This can be explained due to that chloride ions has an inhibition effect on the cellulase enzyme and hence on the hydrolysis efficiency. The regenerated cellulose from two-stage extraction process has glucose hydrolysis effeciency higher than that of the one-stage extraction process and this is maybe due to its lower lignin content.

On the other hand, the low hemicellulose content inside the cellulose rich extracts is converted into xylose during the hydrolysis process. It is obvious that the xylose conversion efficiency is lower than that of glucose and it does not exceed 70%. Xylose content in B, C and D samples obtained from the one-stage extraction process is higher than that of F and G samples obtained from the two-stage extraction process.

The one-stage process extract has 6% lignin content higher than that produced from two-stage extraction process. Nevertheless, the total sugar yield, glucose and xylose, produced from the hydrolysis process is higher than that produced from two-stage extraction processes. This is probably due to the low cellulose recovery obtained during two-stage extraction process. Furthermore, the lignin content of biomass is only one of the factors that could contribute to the biomass recalcitrance. Other factors including crystallinity index and surface area of cellulose could also influence the cellulose digestibility.[70,71] Such factors are closely associated to each other and sometimes give overlapping effects on the cellulose digestibility, depending on the

type of biomass. Besides, Zheng et al.[71] reported that when one of the barrier to cellulose digestion is reduced or eliminated, another barrier may become limiting. In principle, pretreatment efficiency is determined by its ability to improve cellulose accessibility and increase overall sugars yield rather than only concentrating on removing lignin content. This will further confirmed with the overall ethanol yield produced from the fermentation of the hydrolysates.

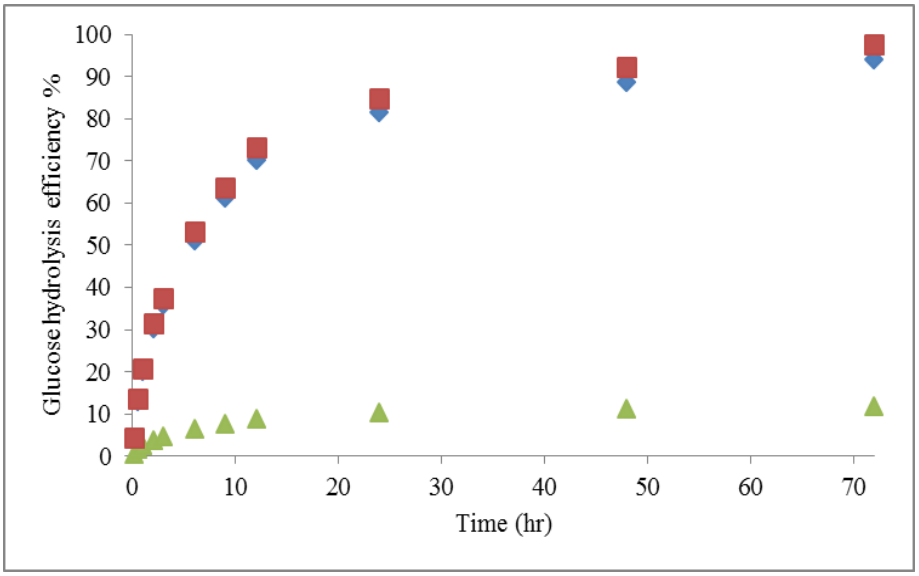

Figure IV.20. Glucose hydrolysis efficiency as a function of time for: ▲ untreated miscanthus, ♦ cellulose regenerated with DMIMMPh and ■ cellulose regenerated with (EDA/DMSO)/DMIMMPh

Table IV.17. Results for different hydrolysis processes for, untreated miscanthus and regenerated cellulose samples

Sample	Glucose (g/l)	Glucose hyd. efficiency (%)	Xylose (g/l)	Xylose hyd. efficiency (%)
A	1.39	11.89	0.5	6.80
B	41.88	93.98	5.02	61.18
C	37.92	87.77	3.35	43.58
D	32.53	84.72	3.1	45.52
E	10.08	55.66	1.01	23.81
F	42.35	97.74	1.88	68.95
G	38.54	88.94	1.54	56.48

IV.3.4.2. Fermentation of hydrolysates

The hydrolysate solutions, of the untreated miscanthus and the cellulose-rich extract samples, A, B, C, D, E, F and G were fermented using yeast from S cerevisaie and the results were compared with that of 40 g/l pure glucose hydrolysate. The fermentation results including cell growth, sugars consumption and ethanol formation for the fermentation of 40 g/l pure glucose, hydrolysate B and hydrolysate F are presented in figure IV.21 (a, b and c) respectively. A typical batch growth phase could be observed, including the following phases: lag phase (0 - 6 hr), exponential growth phase (6 - 36 hr), deceleration phase (36 - 48 hr) and stationary phase (48 - 72 hr). In the first 6 hours of fermentation, the yeasts adapted themselves to growth conditions. During the exponential phase, cell growth and substrate consumption are increasing exponentially with time After 36 hours of fermentation, the growth rate was found to slow down as a result of glucose depletion. Based on figure IV.21 (a, b and c), the concentration of glucose is shown to remain almost constant for the first 6 hours. The concentration of glucose was then decreased as expected during the fermentation, coinciding with an increase in the production of cell and ethanol. This is due to the cells consuming the glucose in the system to increase the growth of cell and the production of ethanol. It could also be observed that the glucose was depleted after 36 hours. The concentration of ethanol was found to increase rapidly during the first 36 hours of fermentation. It started to decrease only after achieving a maximum concentration of 19.15, 20.35 and 20.4 gL^{-1} for pure glucose, hydrolysate B and hydrolysate F respectively at 72 hours of fermentation. The ethanol is probably used as a carbon source by the yeast for its growth when the concentration of glucose started to deplete.[72,73] By comparing the cell and the concentrations of ethanol, it can be classified as a growth-associated product in which the product is produced simultaneously with the cell growth. The cell growth rates (u), for pure glucose, hydrolysate B and hydrolysate F were 0.0655, 0.0677 and 0.0668 h^{-1} respectively. These values are in a good agreement with values published by N. G. Cheng et al., 2009.[74]

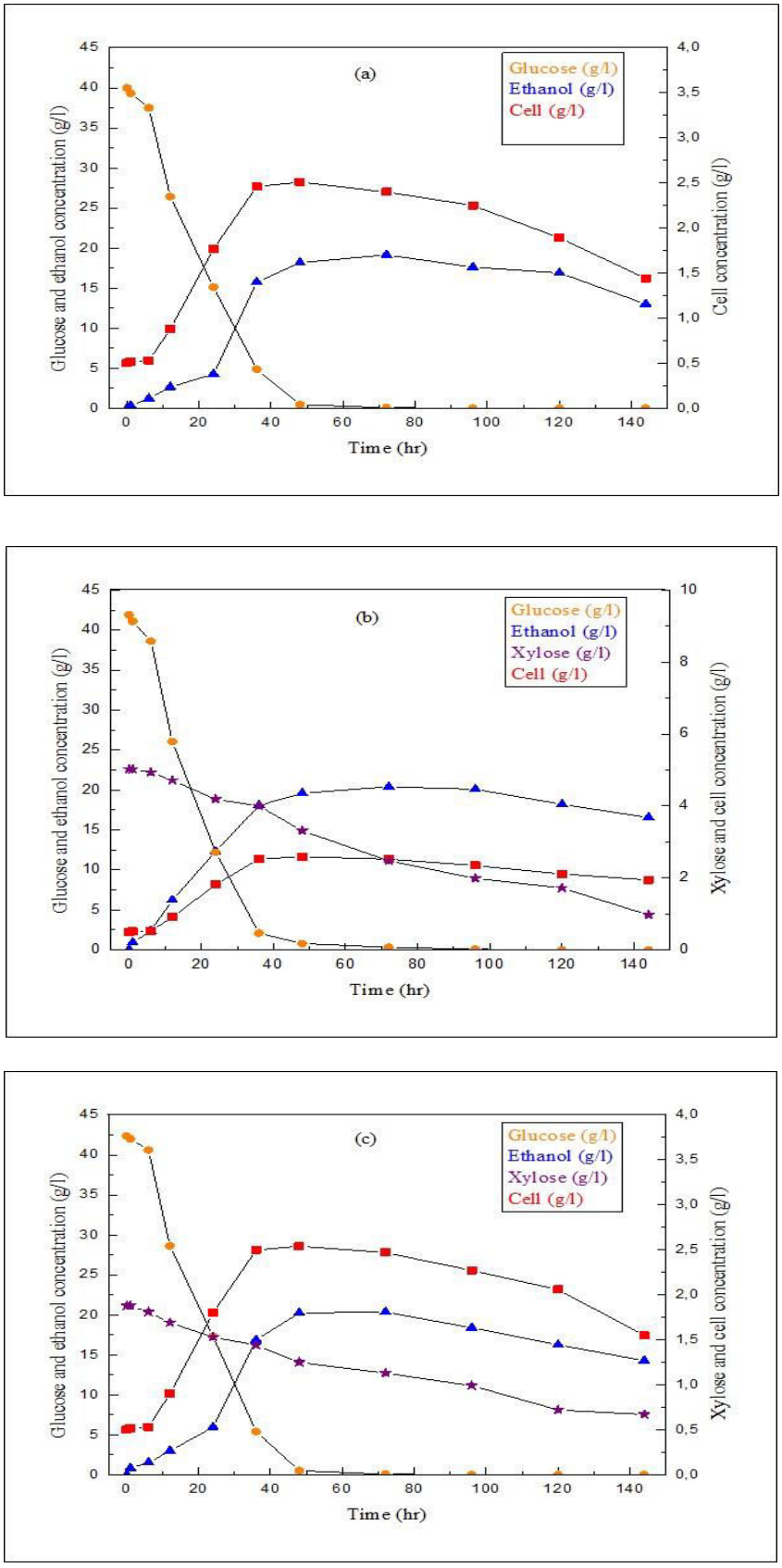

Figure IV.21. Fermentation results of (a) 40 g/l glucose, (b) hydrolysate B and (c) hydrolysate F

IV.3.4.3. Evaluation of fermentation results

Ethanol conversion percentage: According to the reactions, the maximum theoretical ethanol concentration from glucose and xylose was calculated according to the following stoichiometric relationships:[51]

$$C_6H_{12}O_6 \rightarrow 2C_2H_5OH + 2CO_2 \quad \text{(IV.10)}$$

$$3C_5H_{10}O_5 \rightarrow 5C_2H_5OH + 5CO_2 \quad \text{(IV.11)}$$

This means that 100 g of glucose or xylose can produce 51.1 g of ethanol. Therefore:

$$\text{The ethanol conversion rate} = C_e / [Cc(0) \times 0.511] \times 100\% \quad \text{(IV.12)}$$

Where: C_e is the terminal ethanol concentration of the fermentation liquid, $g{\cdot}L^{-1}$, and Cc(0) is the concentration of sugar, glucose and xylose, which was loaded into the system at the beginning of the fermentation, $g{\cdot}L^{-1}$. The conversion rate results for the fermentation of various hydrolysate solutions are shown in table IV.18. It is observed that the conversion rate is high in the hydrolysate solutions B, C,D, F and G which correspond to the cellulose rich extracts from one and two-stage extraction processes. The maximum ethanol conversion value of hydrolysates reaches up to 90% of the theoretical value, which is lower than the value obtained with pure glucose hydrolsate (93.67 %). This decrease is maybe due to the fact that S. cerevisiae cannot metabolize xylose efficiently, and therefore xylose did not converted totally to ethanol and the fuel yield is decreased. It is determined that the higher the xylose concentration in the hydrolysate, the lower the ethanol conversion rate. Nevertheless, the concentration of xylose is very low if compared to glucose concentration in the hydrolysates and hence the ethanol conversion rate does not change greatly.

Furthermore, in order to evaluate the ethanol production from the hydrolysates of the extracted cellulose, ethanol production efficiency with respect to the cellulose and hemicellulose content in the cellulose-rich extracts, is calculated as following:

$$\text{Ethanol production efficiency} = \text{ethanol produced [g]} / \{0.511 \times (1.111 \times \text{cellulose content [g]} + 1.1363 \times \text{hemicellulose content [g]})\} \times 100\% \quad \text{(IV.13)}$$

Where: the value 1.111 is equivalent to [molecular weight of glucose unit (180.16)/molecular weight of cellulose unit (162.14)] while the value 1.1363 is equivalent to [molecular weight of xylose unit (150.13)/ molecular weight of hemicellulose unit, xylan, (132.11)].

Ethanol production efficiency of hydrolysates F, G and B were 78.71%, 67.33% and 66.75% respectively, table IV.18. These values could be compared with those published in the literature concerning the hydrolysates based on acid and alkali pretreatments.Where, the ethanol production efficiency values of the CSTR AD fiber, PFR AD fiber and corn stover hydrolysates are in the range from 65 to 75%.[51,75-77]

An overall evaluation process for the production of ethanol from miscanthus after IL-pretreatment, enzymatic hydrolysis and fermentation processes, is shown in table IV.18. The overall ethanol yield was calculated based on total amount of miscanthus considering the loss of carbohydrates during the pretreatment, enzymatic hydrolysis and fermentation processes. The overall ethanol yields for the miscanthus treated with DMIMMPh through one and two-stage extraction processes were 148 and 142 g ethanol per kg miscanthus respectively. These values could be compared with the values of the overall ethanol yield published in the literature for corn stover, CSTR AD fiber, PFR AD fiber which are 135, 105 and 85 g ethanol kg^{-1} biomass respectively.[75-77]

Table IV.18. Fermentation results for glucose and different hydrolysate solutions at 72hr

Hydrolysate solution	Ethanol (g/l)	Ethanol conversion rate (%)	Ethanol production efficiency (%)	Ethanol produced in g per Kg miscanthus
Glucose (40 g/l)	19.15	93.67	-	-
A	0.53	55.02	4.51	17.70
B	20.40	85.13	66.75	148.43
C	16.72	79.28	55.88	119.14
D	14.72	80.85	49.03	115.63
E	3.87	68.32	28.53	67.52
F	20.35	90.03	78.71	142.09
G	17.57	85.79	67.33	121.79

IV.4. Conclusion

The results presented in this study make the proposed technology highly promising for future applications. It is concluded that DMIMMPh has higher efficiency for dissolving miscanthus and extracting cellulose than other studied ionic liquids. Extraction results were evaluated using Box-Behnken Design. Results indicate that temperature is the most effective parameter on the extraction process. The cellulose-rich extract produced from the two-stage process has cellulose grade 14% higher and lignin content 5% lower than that from one-stage process, while the cellulose recovery decreased with 7%. Ionic liquids could be recycled successfully from lignin and sugars using ethanol as an antisolvent. XRD, FTIR, NMR and SEM analyses results evidenced the production of amorphous, porous cellulose almost free of lignin, which is suitable for enzymatic hydrolysis processes. The glucose hydrolysis efficiency of the regenerated cellulose from untreated miscanthus, one- and two-stage extraction procedures are 11.88, 93.98 and 97.74% respectively. Ethanol could be produced up to 20 gl^{-1} at 72 hr with an ethanol conversion rate of 90%. In fact, the preatreatment of miscanthus with ionic liquids, results in a successful ethanol production. The high overall ethanol yield of the one- and two-stage extraction processes, 148.43 and 142.09 g ethanol kg^{-1} miscanthus respectively, indicates the high performance of ionic liquids in converting biomass feedstocks into bioethanol.

References

[1] A. J. Ragauskas, C. K. Williams, B. H. Davison, G. Britovsek, J. Cairney, C. A. Eckert, W. J. Frederick, J. P. Hallett, D. J. Leak, C. L. Liotta, J. R. Mielenz, R. Murphy, R. Templer, T. Tschaplinski, The path forward for biofuels and biomaterials, Science, 311 (2006) 484-489.

[2] J. H. Clark, Green chemistry for the second generation biorefinerys Sustainable chemical manufacturing based on biomass, J. Chem. Technol. Biotechnol., 82 (2007) 603-609.

[3] H. Tadesse, R. Luque, Advances on biomass pretreatment using ionic liquids: An overview, Energy Environ. Sci., 4 (2011) 3913-3929.

[4] R. L. Howard, E. Abotsi, E. L. Rensburg, S. Howard, Lignocellulose biotechnology: Issues of bioconversion and enzyme production, African Journal of Biotechnology, 2 (2003) 602-619.

[5] P. Kang, W. Qin, Z-M. Zheng, C-Q. Dong, Y-P. Yang, Theoretical study on the mechanisms of cellulose dissolution and precipitation in the phosphoric acid–acetone process, Carbohydrate Polymers, 90 (2012) 1771-1778.

[6] R. Wooley, M. F. Ruth, D. Glassner, J. Sheehan, Process design and costing of bioethanol technology: A tool for determining the status and direction of research and development, Biotechnology Progress, 15 (1999) 794-803.

[7] T. Vancov, A-S. Alston, T. Brown, S. McIntosh, Use of ionic liquids in converting lignocellulosic material to biofuels Renewable Energy, 45 (2012) 1-6.

[8] M. Galbe, G. Zacchi, Pretreatment of lignocellulosic materials for efficient bioethanol production, Biofuels, 108 (2007) 41- 65.

[9] P. Kumar, D. M. Barrett, M. J. Delwiche, P. Stroeve, Methods for pretreatment of lignocellulosic biomass for efficient hydrolysis and biofuel production, Ind Eng Chem Res, 48 (2009) 3713-3729.

[10] Y-H. P. Zhang, S-Y. Ding, J. R. Mielenz, J-B. Cui, R. T. Elander, M. Laser, M. E. Himmel, J. R. McMillan, L. R. Lynd, Fractionating recalcitrant lignocellulose at modest reaction conditions, Biotechnol Bioeng, 97 (2007) 214 -223.

[11] N. Brosse, P. Sannigrahi, A. Ragauskas, Pretreatment of miscanthus x giganteus using the ethanol organosolv process for ethanol production, Ind. Eng. Chem. Res., 48 (2009) 8328-8334.

[12] N. Brosse, A. Dufour, X. Meng, Q. Sun, A. Ragauskas, Miscanthus: a fast- growing crop for biofuels and chemicals production, a review, Biofuels, Bioprod. Bioref., 6 (2012) 580-598.

[13] T. de Vrije, G. G. de Haas, G. B. Tan, E. R. P. Keijsers, P. A. M. Claassen, Pretreatment of miscanthus for hydrogen production by Thermotoga elfii, Int. J. Hydrogen Energy, 27 (2002) 1381-1390.

[14] H. K. Murnen, V. Balan, S. P. S. Chundawat, B. Bals, L. da Costa Sousa, B. E. Dale, Optimization of ammonia fiber expansion (AFEX) pretreatment and enzymatic hydrolysis of miscanthus x giganteus to fermentable sugars, Biotechnol. Prog., 23 (2007) 846-850.

[15] A. Sørensen, P. J. Teller, T. Hilstrom, B. K. Ahring, Hydrolysis of miscanthus for bioethanol production using dilute acid presoaking combined with wet explosion pretreatment and enzymatic treatment, Bioresour. Technol., 99 (2008) 6602-6607.

[16] M. Yoshida, Y. Liu, S. Uchida, K. Kawarada, Y. Ukagami, H. Ichinose, S. Kaneko, K. Fukuda, Effects of cellulose crystallinity, hemicellulose, and lignin on the enzymatic hydrolysis of miscanthus sinensis to monosaccharides, Biosci. Biotechnol. Biochem., 72 (2008) 805-810.

[17] J. J. Villaverde, J. Li, M. Ek, P. Ligero, A. Vega, Native lignin structure of miscanthus × giganteus and its changes during acetic acid and formic acid fractionation, J. Agric. Food Chem., 57 (2009) 6262-6270.

[18] T. Le Ngoc Huyen, C. Rémond, R.M. Dheilly, B. Chabbert, Effect of harvesting date on the composition and the saccharification of miscanthus×giganteus, Bioresour. Technol., 101 (2010) 8224-8231.

[19] C. Reichardt, Polarity of ionic liquids determined empirically by means of solvatochromic pyridinium N-phenolate betaine dyes, Green Chem., 7 (2005) 339-351.

[20] U. Domanska, R. Bogel-Lukasik, Physicochemical properties and solubility of alkyl-(2-hydroxyethyl)-dimethylammonium bromide, J. Phys. Chem. B, 109 (2005) 12124-12132.

[21] M. E. Zakrzewska, E. Bogel-Lukasik, R. Bogel-Lukasik, Solubility of carbohydrates in ionic liquids, Energy Fuels, 24 (2010) 737-745.

[22] H. Yoon, G. H. Lane, Y. Shekibi, P. C. Howlett, M. Forsyth, A. S. Best, D. R. MacFarlane, Lithium electrochemistry and cycling behaviour of ionic liquids using cyano based anions, Energy Environ. Sci., 6 (2013) 979-986.

[23] D. Fu, G. Mazza, Y. Tamaki, Lignin extraction from straw by ionic liquids and enzymatic hydrolysis of the cellulosic residues, J. Agric. Food Chem., 58 (2010) 2915-2922.

[24] T. A. D. Nguyen, K. R. Kim, S. J. Han, H. Y. Cho, J. W. Kim, S. M. Park, J. C. Park, S. J. Sim, Pretreatment of rice straw with ammonia and ionic liquid for lignocellulose conversion to fermentable sugars, Bioresour. Technol., 101 (2010) 7432-7438.

[25] S. S. Y. Tan, D. R. MacFarlane, J. Upfal, L. A. Edye, W. O. S. Doherty, A. F. Patti, J. M. Pringle, J. L. Scott, Extraction of lignin from lignocellulose at atmospheric pressure using alkylbenzenesulfonate ionic liquid, Green Chem., 11 (2009) 339-345.

[26] H. Wu, M. Mora-Pale, J. Miao, T. V. Doherty, R. J. Linhardt, J. S. Dordick, Facile pretreatment of lignocellulosic biomass at high loadings in room temperature ionic liquids, Biotechnol. Bioeng., 108 (2011) 2865-2875.

[27] R. C. Remsing, R. P. Swatloski, R. D. Rogers, G. Moyna, Mechanism of cellulose dissolution in the ionic liquid 1-n-butyl-3-methylimidazolium chloride: a ^{13}C and $^{35/37}Cl$ NMR relaxation study on model systems, Chem. Commun., (2006) 1271-1273.

[28] S. H. Lee, T. V. Doherty, R. J.; Linhardt, J. S. Dordick, Ionic liquid-mediated selective extraction of lignin from wood leading to enhanced enzymatic cellulose hydrolysis, Biotechnol. Bioeng., 102 (2009) 1368-1376.

[29] A. M. da Costa Lopes, K. Joao, D. Rubik, E. Bogel-Lukasik, L. C. Duarte, J. Andreaus, R. Bogel-Lukasik, Pre-treatment of lignocellulosic biomass using ionic liquids: wheat straw fractionation, Bioresour. Technol., 142 (2013) 198-208.

[30] S. P. Magalhaes da Silva, A. M. da Costa Lopes, L. B. Roseiro, R. Bogel-Lukasik, Novel pre-treatment and fractionation method for lignocellulosic biomass using ionic liquids, RSC Adv., 3 (2013) 16040-16050.

[31] K. Shill, S. Padmanabhan, Q. Xin, J. M. Prausnitz, D. S. Clark, H. W. Blanch, Ionic liquid pretreatment of cellulosic biomass: Enzymatic hydrolysis and ionic liquid recycle, Biotechnol Bioeng., 108 (2011) 511-520.

[32] H. Rodríguez, S. Padmanabhan, G. Poon, J. M. Prausnitz, Addition of ammonia and/or oxygen to an ionic liquid for delignification of miscanthus, Bioresource Technol., 102 (2011) 7946 7952.

[33] S. Padmanabhan, M. Kim, H. W. Blanch, J. M. Prausnitz, Solubility and rate of dissolution for Miscanthus in hydrophilic ionic liquids, Fluid Phase Equilibr., 309 (2011) 89-96.

[34] S. Padmanabhan, E. Zaia, K. Wu, H. W. Blanch, D. S. Clark, A. T. Bell, J. M. Prausnitz, Delignification of miscanthus by extraction, Separation Science and Technology, 47 (2012) 370-376.

[35] Ø. Vessia, Biofuels from lignocellulosic material: In the Norwegian context 2010-technology, potential and costs, department of electrical engineering, NTNU, Norwegian University of Science and Technology, Projectreport,Trondheim, Norway, December 20, 2005.

[36] Y. Sun, Enzymatic hydrolysis of rye straw and Bermudagrass for ethanol production. PhD thesis, Biological and Agricultural Engineering, North Carolina State University, 2002.

[37] C. N. Hamelinck, G. van Hooijdonk, A. P. C. Faaij, Ethanol from lignocellulosic biomass: techno-economic performance in short-, middle- and long-term, Biomass Bioenergy, 28 (2005) 384-410.

[38] X. Pan, C. Arato, N. Gilkes, D. Gregg, W. Mabee, K. Pye, Z. Xiao, X. Zhang, J. Saddler, Biorefining of softwoods using ethanol organosolv pulping: Preliminary evaluation of process streams for manufacture of fuelgrade ethanol and co-products, Biotechnol Bioeng., 90 (2005) 473-81.

[39] M. Balat, H. Balat, C. Oz, Progress in bioethanol processing, Progress in Energy and Combustion Science, 34 (2008) 551-573.

[40] A. A. DiIorio, "Ethanol Production by an Isogenic Series of Saccharomyces Cerevisiae." Worcester Polytechnic Institute, Biotechnology. Worcester: WPI, (1986).

[41] T. K. Ghose, Measurement of cellulase activities, Pure Appl Chem., 59 (1987) 257-268.

[42] D. A. Fort, R. C. Remsing, R. P. Swatloski, P. Moyna, G. Moyna, R. D. Rogers, Can ionic liquids dissolve wood? Processing and analysis of lignocellulosic materials with 1-n-butyl-3-methylimidazolium chloride, Green Chem., 9 (2007) 63-69.

[43] N. Sun, M. Rahman, Y. Qin, M. L. Maxim, H. Rodríguez, R.D. Rogers, Complete dissolution and partial delignification of wood in the ionic liquid 1-ethyl-3-methylimidazolium acetate, Green Chem., 11 (2009) 646-655.

[44] D. Templeton, T. Ehrman, LAP 003-Standard Method for the Determination of Acid-Insoluble Lignin in Biomass, 1995, Available from World Wide Web: http://cobweb.ecn.purdue.edu/ ~lorre/16/research/LAP-003.pdf (accessed 20.03.10).

[45] H. T. Tan, K. T. Lee, Understanding the impact of ionic liquid pretreatment on biomass and enzymatic hydrolysis, Chemical Engineering Journal, 183 (2012) 448- 458.

[46] J. X. Sun, X. F. Sun, H. Zhao, R.C. Sun, Isolation and characterization of cellulose from sugarcane bagasse, Polymer Degradation and Stability, 84 (2004) 331-339.

[47] Y. Teramoto, S. Lee, T. Endo, Cost reduction and feedstock diversity for sulfuric acid-free ethanol cooking of lignocellulosic biomass as a pretreatment to enzymatic saccharification, Bioresource Technology, 100 (2009) 4783-4789.

[48] L. Segal, J. J. Creely, A. E. Martin Jr., C. M. Conrad, An empirical method for estimating the degree of crystallinity of native cellulose using the X-ray diffractometer, Textile Research Journal, 29 (1959) 786-794.

[49] S. Park, J. O. Baker, M. E. Himmel, P. A. Parilla, D. K. Johnson. Cellulose crystallinity index: measurement techniques and their impact of interpreting cellulose performance, Biotechnology for Biofuels, 3 (2010) 10.

[50] R. H. Newman, Homogeneity in cellulose crystallinity between samples of Pinus radiata wood, Holzforschung, 58 (2004) 91-96.

[51] Y. Lin, W. Zhang, C. Li, K. Sakakibara, S. Tanaka, H. Kong, Factors affecting ethanol fermentation using Saccharomyces cerevisaie BY4742, Biomass and Bioenergy, 47 (2012) 395-401.

[52] C. D. Skory, Lactic acid production by Saccharomyces serevisiae expressing a Rhizopus oryzae lactate dehydrogenase gene, J Ind Microbiol Biotechnol., 30 (2003) 22-27.

[53] K. Kasemets, I. Nisamedtinov, Growth characteristics of Saccharomyces serevisiae S288C in changing environmental conditions: auxo-accelerostat study, Anton Leeuw., 92 (2007) 109-128.

[54] R. P. Swatloski, S. K. Spear, J. D. Holbrey, R. D. Rogers, Dissolution of cellulose with ionic liquids, J. Am. Chem. Soc., 124 (2002) 4974-4975.

[55] H. Xie, S. Li, S. Zhang, Ionic liquids as novel solvents for the dissolution and blending of wool keratin fibers, Green Chem., 7 (2005) 606-608.

[56] X. Wanga, H. Li, Y. Cao, Q. Tang, Cellulose extraction from wood chip in an ionic liquid 1-allyl-3-methylimidazolium chloride (AmimCl), Bioresource Tech., 102 (2011) 7959-7965.

[57] T-Q. Yuan, W. Wan, F. Xu, R-C. Sun, Synergistic benefits of ionic liquid and alkaline pretreatments of poplar wood. Part 1: Effect of integrated pretreatment on enzymatic hydrolysis, Bioresource Technology, 144 (2013) 429-434.

[58] W-Z. Li, M-T. Ju, Y-N. Wang, L. Liu, Y. Jiang, Separation and recovery of cellulose from Zoysia japonica by 1-allyl-3-methylimidazolium chloride, Carbohydrate Polymers, 92 (2013) 228-235.

[59] P. Mäki-Arvela, I. Anugwom, P. Virtanen, R. Sjöholm, J. P. Mikkola, Dissolution of lignocellulosic materials and its constituents using ionic liquids-a review, Industrial Crops

and Products, 32 (2010) 175-201.

[60] M. Zavrel, D. Bross, M. Funke, J. Büchs, A.C. Spiess, High-throughput screening for ionic liquids dissolving (lingo-)cellulose, Bioresource Technology, 100 (2009) 2580-2587.

[61] A. Brandt, J. P. Hallett, D. J. Leak, R. J. Murphy, T. Welton, The effect of the ionic liquid anion in the pretreatment of pine wood chips, Green Chem., 12 (2010) 672.

[62] G. E. P. Box, D. W. Behnken, Some new three level designs for the study of quantitative variables, Technometrics, 2 (1960) 455-475.

[63] El-Sayed R. E. Hassan, F. Mutelet, S. Pontvianne, J-C. Moise, Studies on the dissolution of glucose in ionic liquids and extraction using the antisolvent method, Environ. Sci. Technol., 47 (2013) 2809-2816.

[64] El-Sayed R. E. Hassan, F. Mutelet, J-C. Moise, From the dissolution to the extraction of carbohydrates using ionic liquids, RSC Adv., 3 (2013) 20219-20226.

[65] D. Ciolacu, F. Ciolacu and V. I. Popa. Amorphus cellulose-structure and Characterization, Cellulose Chem. Technol., 45 (2011) 13-21.

[66] P. Mansikkamaki, M. Lahtinen, K. Rissanen, Structural changes of cellulose crystallites induced by mercerisation in different solvent systems; determined by powder X-ray diffraction method, Cellulose, 12 (2005) 233-242.

[67] Z. G. Wang, T. Yokoyama, H. M. Chang, Y. Matsumoto, Dissolution of beech and spruce milled woods in LiCl/DMSO, J. Agric. Food Chem., 57 (2009) 6167-6170.

[68] M. Matulova, R. Nouaille, P. Cappek, M. Péan, E. Forano, A. M. Delort, Degradation of wheat straw by Fibrobacter succinogenes S85: A liquid- and solid-state nuclear magnetic resonance study, Appl. EnViron. Microbiol., 71 (2005) 1247-1253.

[69] E. Locci, S. Laconi, R. Pompei, P. Scano, A. Lai, F. C. Marincola, Wheat bran biodegradation by Pleurotus ostreatus: A solid-state carbon-13 NMR study, Bioresour. Technol., 99 (2006) 4279-4284.

[70] G. Cheng, P. Varanasi, C. Li, H. Liu, Y. B. Melnichenko, B. A. Simmons, M. S. Kent, S. Singh, Transition of cellulose crystalline structure and surface morphology of biomass as a function of ionic liquid pretreatment and its relation to enzymatic hydrolysis, Biomacromolecules, 12 (2011) 933-941.

[71] Y. Zheng, Z. Pan, R. Zhang, Overview of biomass pretreatment for cellulosic ethanol production, International Journal of Agricultural and Biological Engineering, 2 (2009) 51-68.

[72] T. Bauchop, S. R. Elsden, The growth of micro-organism in relation to their energy supply, Journal of General Microbiology, 23 (1960) 457-469.

[73] S. J. Coppella, P. Dhurjati, A detailed analysis of saccharomyces cerevisiae growth kinetics in batch, fed-batch and hollow-fiber bioreactors, The Chemical Engineering Journal, 41 (1989) B27 – B35.

[74] N. G. Cheng, M. Hasan, A. C. Kumoro, C. F. Ling, M. Tham, Production of ethanol by fed-batch fermentation, Pertanika J. Sci. & Technol., 17 (2009) 399-408.

[75] Z. Yue, C. Teater, J. MacLellan, Y. Liu, W. Liao, Development of a new bioethanol feedstock-Anaerobically digested fiber from confined dairy operations using different digestion configurations, biomass and bioenergy, 35 (2011) 1946-1953.

[76] Z. Yue, C. Teater, Y. Liu, J. MacLellan, W. Liao, A sustainable Pathway of Cellulosic Ethanol production integrating anaerobic digestion with biorefining, Biotechnology and Bioengineering, 105 (2010) 1031-1039.

[77] L. Tan, Y-Q. Tang, H. Nishimura, S.Takei, S. Morimura, K. Kida, Eficcient production of bioethanol from corn stover by pretreatment with a combination of sulfuric acid and sodium hydroxide, Preparative Biochemistry & Biotechnology, 43 (2013) 682-695

Conclusion and Perspectives

The solubility of glucose, fructose, sucrose and lactose in ionic liquids was measured within a temperature range from 283 K to 383 K. It is observed that the solubility of di-saccharides, sucrose and lactose, exhibits a noticeably lower solubility than mono-saccharides, glucose and fructose. Solubility data were successfully correlated with local composition thermodynamic models such as NRTL and UNIQUAC. The possibility of extracting sugars from ionic liquids using the antisolvent method has been evaluated. A successful extraction process requires high ethanol/ IL ratio, low temperature and low water content. The considerable decrease of the solubility of sugars in the binary mixtures proves the ability of ethanol to be an excellent antisolvent for separating sugars from various types of ionic liquids.

Ab initio calculations were used as a tool to investigate the fundamental natures of the interaction between carbohydrates and ionic liquids. The most stable geometries of DMIMMPh, BMIMCl, EtOHMIMCl and EMIMSCN ionic liquids have been studied. It is shown that the most stable ionic liquid ion pairs have the anion positioned in front of the C2-H of the imidazolium ring of cation. It was concluded that the anion plays the main role in the dissolution process of carbohydrates, in which the H-bonding forces are the major interactions. The obtained results proved that DMIMMPh is more efficient than other ionic liquids. The effect of water on the IL-cellulose system was studied. It is investigated that water could be used as an antisolvent for the regeneration of cellulose. The analyses results indicate that the regenerated cellulose is quite similar to the original one with a great decrease in its crystallinity. This proves that the process of dissolution and regeneration of cellulose in ionic liquids is accompanied only with a physical change.

The use of ionic liquids in the pretreatment of miscanthus and the extraction of cellulose have been studied. Extraction results were evaluated using Box-Behnken Design. Analyses results evidenced the production of amorphous, porous cellulose almost free of lignin, thereby facilitating its enzymatic hydrolysis and fermentation for biofuel production. The glucose hydrolysis efficiency of the regenerated cellulose reached up to 97.74%. The pretreatment efficiency is determined by its ability to improve cellulose accessibility and increase overall sugars yield rather than only concentrating on removing lignin content. This could be confirmed with the high overall ethanol yield, up to 150 g ethanol kg^{-1} miscanthus, produced from the

fermentation of the hydrolysates. We proposed alkylphosphonate anion based ionic liquids as excellent candidates for Biomass treatment.

In this thesis, we studied the interaction between carbohydrates and ionic liquids using ab initio calculations. The obtained results are promising but further studies on the interaction between ionic liquids and other carbohydrates could be performed. Moreover, the interaction between two or more solute molecules with ionic liquids should be taken into consideration. Also, for the cellulose-IL systems more complicated cellulose structure, with more than two glucose units, could be tested. As a final step, a molecular dynamic study could be carried out to predict the thermodynamic properties of such mixtures.

We were also capable of producing bioethanol from biomass feedstocks using ionic liquids. This approach makes the proposed technology highly promising for industrial applications. Nevertheless, an extended work on the extraction performance, the efficient recovery and the characterization of lignin and hemicellulose components should be taken into consideration for the industrial feasibility. In addition, to concentrate the produced ethanol after fermentation, distillation techniques could be used. If pure ethanol is required, the product should be subjected to further separation techniques.

On the other hand, the toxicity of ionic liquids should be evaluated for their application as solvents in cellulose industry. A careful selection of both cations and anions as well as pretreatment conditions make the optimised Ils systems with unique physico-chemical properties, which could be more suitable for such processes. The deep eutectic solvents (DES) could be tested as solvents for biomass. Indeed, most DESs share the promising solvent characteristics of ILs. They often show low volatility, wide liquid range, water-compatibility, non-flammability, nontoxicity, biocompatibility and biodegradability. Furthermore, they show the ability to customize their physical properties by choosing the right DES constituents in terms of chemical nature, relative compositions or water content. In addition, they can be easily prepared from readily available materials at high purities and low cost compared to ILs, and they can be considered as environmentally benign solvents. Because of keeping most of the advantages of ILs but overcoming some of their limitations, DESs open room to research in multiple applications.

Finally, an economic study is required in order to evaluate the bioethanol production process as well as to compare the obtained results with those obtained from other conventional methods.

Abstract

The replacement of conventional organic solvents by a new generation of solvents less toxic, less flammable and less polluting is a major challenge for the chemical industry. Ionic liquids have been widely promoted as interesting substitutes for traditional solvents. The purpose of this work is to study the solubility of carbohydrates or biomass based materials in ionic liquids in order to overcome the lack of experimental data on phase equilibria of {biomass or carbohydrate-ILs} mixtures. Solubility data were successfully correlated using NRTL and UNIQUAC thermodynamic models. It was found that the antisolvent method is a good technique for the extraction of carbohydrates from ILs. Ionic liquids could be then recycled successfully for reuse. The fundamental natures of the interaction between carbohydrates and ionic liquids were investigated using ab initio calculations. The theoretical results are in good agreement with experimental data. It was concluded that ionic liquids mainly interact with carbohydrates via hydrogen bonding formation. This confirms that the process of dissolution and regeneration of cellulose in ionic liquids is accompanied only with a physical change. The preatreatment of miscanthus with ionic liquids resulted in the regeneration of amorphous, porous cellulose almost free of lignin, which is suitable for enzymatic hydrolysis and fermentation processes. A successful ethanol production was obtained with an overall ethanol yield reached up to 150 g ethanol kg^{-1} miscanthus. This indicates the high performance of ionic liquids in converting biomass feedstocks into biofuel. Indeed, applying the cellulose extraction processes on the industrial scale could be of great interest.

Résumé

Le remplacement des solvants organiques classiques par une nouvelle génération de solvants moins toxiques et moins polluants est un défi majeur pour l'industrie chimique. Les liquides ioniques (LIs) ont été largement identifiés comme substituts intéressants aux solvants traditionnels. Le but de ce travail est d'étudier la solubilité des sucres ou des constituants issus de la biomasse dans les liquides ioniques afin de pallier au manque de données expérimentales sur les équilibres de phases de systèmes {sucres + LIs} ou {biomasse + LIs}. Les données de solubilité ont été corrélées avec succès en utilisant les modèles thermodynamiques NRTL et UNIQUAC. Cette étude démontre que la méthode de l'antisolvant est une bonne technique pour l'extraction des sucres des LIs. Par conséquent, les liquides ioniques peuvent être facilement recyclés pour être réutilisés. Les natures fondamentales des interactions entre les sucres et les liquides ioniques ont été définies en utilisant le calcul ab initio. Les résultats obtenus par simulation sont en accord avec les données expérimentales et indiquent que les liquides ioniques interagissent avec les sucres par liaisons hydrogène. La seconde partie de ce travail met en évidence que le prétraitement du miscanthus avec les liquides ioniques permet d'obtenir une bonne production d'éthanol (jusqu'à 150 g d'éthanol par kg de miscanthus). Les résultats montrent que les liquides ioniques sont des solvants performants dans le domaine de la conversion des matières premières issues de la biomasse en biocarburant. Ainsi, l'application à l'échelle industrielle de ces procédés d'extraction de la cellulose pourrait être d'un grand intérêt.